POLYMERIZATION OF BRAIN MAP2 INTO STRUCTURES RESEMBLING ALZHEIMER FILAMENTS

By

MICHAEL ANTHONY DETURE

A DISSERTATION PRESENTED TO THE GRADUATE SCHOOL
OF THE UNIVERSITY OF FLORIDA IN PARTIAL FULFILLMENT
OF THE REQUIREMENTS FOR THE DEGREE OF
DOCTOR OF PHILOSOPHY

UNIVERSITY OF FLORIDA

1998

ACKNOWLEDGMENTS

I would like to thank Dan Purich for his support during my tenure in his lab. He has given his time and knowledge freely and patiently, and I consider him to be a model scientist and person. He is a good friend and I appreciate the opportunity to have worked with him. His lab has provided an excellent atmosphere for practicing science, and the members of the lab have been both friends and collaborators. I also would like to thank the members of my committee and the department. Many have provided advice and repeated assistance on problems I have encountered, and all have done so generously. My stay here has been enjoyable, because the people here have been so nice.

Additionally, I would like to thank my family. I could not have finished this without their support. My parents, Linda and Francis DeTure, and brother, Nick DeTure, have provided constant encouragement. Monica, my wife, has put in a tremendous amount of time and effort at home, and this has allowed me to do the same at lab. She accepted my life of science and loved me during the process, and I thank her now for all she has given. Finally, I would like to thank my children, Skylar and Haley. You rascals are the best, and I love you both for it.

TABLE OF CONTENTS

page

ACKNOWLEDGMENTS ii

ABBREVIATIONS v

ABSTRACT vii

CHAPTERS

1 INTRODUCTION 1

Overview of the Neuronal Cytoskeleton 1
Microfilaments 2
Intermediate Filaments 3
Microtubules 4
Tubulin 6
Microtubule-associated Proteins 7
Motor Proteins 11
Tau 13
MAP2 16
Abnormal Pathology in Alzheimer Disease 18
Senile β–Amyloid Plaques 19
Neurofibrillary Tangles 22
Tau in Alzheimer Disease 23
In Vitro Assembly of Tau 25
Assays for Measuring Tau Assembly 26
Anionic Agents that Promote Tau Assembly 28
Other Neurodegenerative Diseases Exhibiting NFTs 30
Aims of This Research Project 32

2 *IN VITRO* ASSEMBLY OF FRAGMENTS OF THE MAP2 MICROTUBULE-BINDING REGION INTO STRUCTURES RESEMBLING ALZHEIMER FILAMENTS 35

Introduction 35
Materials and Methods 37
Materials 37
Bacterial Expression and Purification of MAP2 and Tau Fragments 40
In Vitro Assembly of Filaments 42
Electron Microscopy 42
Fluorescence Spectroscopy 43
Results 43
Assembly Properties of MAP2-123 44
Assembly Properties of MAP2-N123C 48
Assembly Properties of MAP2-NN123C 51

Assembly Properties of MAP2c....51
Solution Conditions that Permit MAP2-123 Assembly....54
Interactions of MAP2 Filaments with Thioflavin S....62
Elongation of MAP2 Fragments from Alzheimer Paired Helical Filaments....62
Assembly of Tau-123, Tau-K12 and Tau-N123C....69
Discussion....69

3 FORMATION OF AN OXIDIZED DIMER AS A REQUIRED STEP IN THE *IN VITRO* ASSEMBLY OF MAP2C AND MAP2 FRAGMENTS INTO FILAMENTS....75

Introduction....75
Materials and Methods....78
Materials....78
Dimerization of MAP2 Fragments Visualized by SDS-PAGE....80
Sedimentation Equilibrium Analysis of MAP2....80
Results....80
Demonstration of Disulfide Cross-linked Dimer Formation....81
Assembly of the MAP2-N123C (C1709A) Mutant....85
Assembly of the MAP2-N133C andMAP2-N233C Mutants....85
Assembly of the MAP2-123 (C1709A) and MAP2-133 Mutants....88
Discussion....91

4 IDENTIFICATION OF AMINO ACID MUTATIONS PERMITTING FORMATION OF PAIRED HELICAL FILAMENTS FROM MAP2-123....93

Introduction....93
Materials and Methods....95
Materials....95
In Vitro Assembly of Filaments with tRNA or Heparin....99
Results....99
Assembly of MAP2-123 in the Presence of Heparin or Heparan Sulfate....100
Assembly of MAP2-123 in the Presence of tRNA....100
Assembly of MAP2-123 [Module-A] Mutants....103
Assembly of MAP2-123 [Module-B] Mutants....106
Assembly of MAP2-123 [Module-B] Point Mutants R1723Q, K1725E and E1727K....106
Assembly of MAP2-123 [Module-B] Point Mutant V1729E
Discussion....111

5 CONCLUSIONS AND FUTURE DIRECTIONS....126

Conclusions....126
Future Directions....132

LIST OF REFERENCES....141

BIOGRAPHICAL SKETCH....157

ABBREVIATIONS

AD	Alzheimer Disease
APP	amyloid precursor protein
ATP	adenosine triphosphate
C	centigrade
cDNA	complementary deoxyribonucleic acid
CK	casein kinase
DNA	deoxyribonucleic acid
DNase	deoxyribonuclease
DTT	dithiothreitol
EGTA	ethyleneglycol-bis-(b-amino-ethyl ether) N, N'- tetraacetic acid
FPLC	fast protein liquid chromotography
GDP	guanosine diphosphate
GTP	guanosine triphosphate
GSK	glycogen synthase kinase
IPTG	isopropyl thiogalactopyranoside
kDa	kilodalton
KIF	kinesin superfamily
M	molar
M#	repeat # in MAP2
MAP	microtubule-associated protein
MAPK	mitogen-activated kinase
MBP	Module-B point mutation

MES	morpholino ethanesulfonic acid
MOPS	morpholino propanesulfonic acid
MT	microtubule
MTBR	microtubule-binding region
NCLK	neuronal cyclin-dependent-like kinase
NFT	neurofibrillary tangle
PAGE	polyacrylamide gel electrophorysis
PCR	polymerase chain reaction
PHF	paired helical filament
PKA	cAMP-dependent kinase
PKC	protein kinase C
PMSF	phenylmethylsulfonyl fluoride
RNA	ribonucleic acid
SDS	sodium dodecyl sulfate
T#	repeat # in Tau
Tris	tris (hydroxymethyl) aminomethane
tRNA	transfer ribonucleic acid

Abstract of Dissertation Presented to the Graduate School
of the University of Florida in Partial Fulfillment of the
Requirements for the Degree of Doctor of Philosophy

POLYMERIZATION OF BRAIN MAP2 INTO STRUCTURES RESEMBLING ALZHEIMER FILAMENTS

By

Michael Anthony DeTure

December, 1998

Chairman: Daniel L Purich
Major Department: Biochemistry and Molecular Biology

The neuronal microtubule-associated proteins, MAP2 and Tau, modulate microtubule assembly and help insure proper neuronal performance is maintained. Microtubules not only provide structural support for neurons, but they also operate as tracks for transport of materials throughout the neuron. Many neurodegenerative diseases are characterized by the accumulation of neurofibrillary tangles and exhibit abnormal cytoskeletal behavior . These diseases include Alzheimer Disease (AD) which is confirmed by the postmortem identification of amyloid plaques and neurofibrillary tangles. The primary components of these neurofibrillary tangles are paired helical filaments (PHFs) and straight filaments formed by the polymerization of Tau within the cell body. Recombinant full length Tau and the microtubule-binding region (MTBR) of Tau can polymerize *in vitro* into structures resembling these Alzheimer filaments, but no one has investigated the assembly properties of related MAP2 polypeptides.

Because Tau and MAP2 share a homologous MTBR and because MAP2 is found in the cell bodies of neurons where neurofibrillary tangles form, these experiments explored the polymerization characteristics of recombinant MAP2 fragments. Full length MAP2c and smaller fragments of MAP2 containing the MTBR each assembled when incubated at neutral pH under oxidizng conditions at physiological relevant concentrations. Straight filaments of MAP2 bound the AD histologic marker thioflavin S and polymerized from AD paired helical filaments. Analogous to Tau assembly, polymerization of MAP 2

polypeptides proceeded by forming a disulfide cross-linked dimer. The importance of the disulfide cross-linked dimer was addressed by creating cysteine-to-alanine mutants which did not assemble well. Certain polyanions, like heparin or tRNA, are known to facilitate PHF formation from Tau, but they did not induce PHF formation with MAP 2. Accordingly, mutations were generated in MAP 2 to create a protein that exhibited assembly properties similar to Tau. Four amino acid residues after the second repeat in MAP2 were identified that prevented paired helical filament formation. Of these, a valine-to-glutamic acid mutation at position 1729 in MAP2 was made, and this MAP2 mutant assembled into structures resembling paired helical filaments. These experiments demonstrate that MAP2 and Tau share certain assembly properties, and the results suggest that MAP2 may be found in the neurofibrillary tangles of certain neurodegenerative disorders.

CHAPTER 1
INTRODUCTION

Overview of the Neuronal Cytoskeleton

The eukaryotic cytoskeleton maintains structural integrity for the cell and provides special mechanical properties that a cell uses in its resting and dividing states. The components of this framework are several types of filamentous protein subunits and various associated proteins that interact with the polymerized and unpolymerized forms to maintain, utilize and regulate these structures. The most prominent members of the cytoskeleton are microtubules, microfilaments and intermediate filaments, and all three function within the cell to maintain cell shape, form the spindle apparatus during mitosis, transport organelles and provide cell motility (Alberts et al., 1994; Hall, 1994; Purich and Kristofferson, 1984). Many of these tasks are performed with the assistance of associated proteins which can mediate signal transduction events and modulate cytoskeletal behavior.

In terms of cellular anisometry, there is no better case known than neurons which are highly differentiated cells. They typically function by receiving signals post-synaptically from many sources, integrating these signals and transmitting an appropriate response signal (Hall, 1994). Neurons are asymmetric cells which have large dendritic trees for receiving chemical signals from thousands of presynaptic cells. The response to these signals is determined by the time, magnitude and location of the input stimuli. The chemical signals act by binding receptors in the synaptic junctions which results in the opening of ion channels which in turn generates electrical signals. The integration of these electrical signals is controlled by the shape of the neuron, the location of the synapse and the duration of the input. If the membrane potential is reduced below a threshold value, an

action potential results which travels down the axon resulting in the flow of information at the next synapse or neuromuscular junction.

During neuritogenesis, the cytoskeleton first plays a role in determining neuronal structure. As these cellular extensions project from the cell body, they are guided and moved by ameba-like structures called growth cones. These growth cones send out actin-rich filopodia and lamellipodia that are responsible for movement. Some of the neurites become dendrites and one becomes the axon. Those that are not needed degenerate which requires plasticity of the cytoskeleton. Those that remain are rich in parallel arrays of cross-linked microtubules and intermediate filaments called neurofilaments. These arrays stabilize the neuritic structure and contribute to the caliber, or diameter, of the axon which ultimately determines the passive electrical properties of the neuron. Additionally, the axonal and dendritic microtubule cytoskeletons act as tracks for transport of materials needed outside the cell body. After neuronal morphogenesis, the cytoskeleton maintains the structural anisometry of the neuron. In fact if neurons cannot maintain their proper shape, then their ability to integrate incoming signals and respond correctly may be lost or impaired.

Actin Filaments

Microfilaments are composed of 43 kDa actin subunits forming a dynamic supramolecular structure where ATP-bound actin modulates the kinetics of association and disassociation at each end. These microfilaments have a helical structure, and ADP-bound actin is released from the minus end (Alberts et al., 1994). These dynamic events give rise to actin treadmilling which results from the different critical concentrations for the plus and minus ends. This treadmilling is believed to generate mechanical energy from the hydrolysis of ATP. The filaments appear as a double-stranded helical polymer which varies in width from 5-9 nm. Within cells, they are found in bundles, two-dimensional arrays and three-dimensional gels. Obviously, the function the actin network performs

depends on the components it interacts with and its location within the cell. To date, over fifty different actin regulatory proteins have been identified, and they function to sequester monomeric actin, bind actin filaments, sever actin filaments, cap actin filaments, cross-link actin filaments to one another and to other cytoskeletal elements, stimulate nucleotide exchange and generate motile forces. This leads to actin filaments being found as the thin filaments in the contractile apparatus of muscle cells, in the cortical region of motile and nonmuscle cells and in focal contacts. The microfilaments function to generate motility or establish cellular polarity with the help of other cytoskeletal components. In neurons, actin filaments are found in the cortex of the cell body and the filopodia and lamellipodia of growth cones. Generally, their appearance blocks the accessibility of a region to microtubules and neurofilaments.

Neurofilaments

Neurofilaments are the principal intermediate filaments in neurons, and they are composed of three different subunits each having its own unique mass (Shaw, 1998; Hall, 1994). The light subunit has a mass of 60 kDa. The medium subunit has a mass of 100 kDa, and the heavy subunit has a mass of 110 kDa. Each fibrous subunit consists of a nonhelical amino-terminal head domain, a central alpha helical rod domain capable of forming a coiled-coil dimer with another subunit and a carboxy-terminal tail which varies in length and composition and may determine neurofilaments function (Heins et al., 1993). The neurofilaments are primarily found in the cell bodies and projections of neurons where they provide protection from mechanical stresses. They are often observed in parallel arrays where they are heavily cross-linked with microtubules and other neurofilaments. Neurofilaments polymerize in a nucleotide -independent series of reactions where coiled-coil dimers form staggered, antiparallel tetramers which eventually pack into helical intermediate filaments. The resulting filament is 10 nm wide and exhibits no polarity meaning both ends are equal. Studies report that the light subunit must be a core

component of neurofilaments (Lee et al., 1993) and that the carboxy-terminal tails of the medium and heavy subunits project away from the filament and are involved in cross-linking the neurofilaments to other cytoskeletal elements. This arrangement makes neurofilaments very stable even in the presence of high salt or mild detergents, and it provides protection for the axons and dendrites from mechanical stresses.

Microtubules

Microtubules (MT) constitute the third class of proteins in the cytoskeletal. These three polymer systems share many of the same binding partners and work in conjunction to determine the composition of the cytosol. Microtubules are highly dynamic cytoskeletal elements and polymerize in a GTP-dependent process (Kobayashi, 1975; MacNeil and Purich, 1978). In a manner akin to actin assembly, GTP-bound tubulin subunits add preferentially to the growing end of a microtubule if the end contains predominantly tubulin dimers with unhydrolyzed GTP (Karr et al., 1979; Mitchison and Kirschner, 1984). This results in slow growth only at the plus end, since the other end is typically anchored in a stabilizing manner within the cell. If the tubulin heterodimers at the growing end hydrolyze their GTP before GTP-bound subunits add, the microtubule undergoes a catastrophic event where GDP-bound tubulin dimers quickly go into solution (Mitchison and Kirschner, 1984). This leads to a dynamic equilibrium where there is a one hundred fold excess of slow growing microtubules over rapidly depolymerizing microtubules. This arrangement allows for the creation of polarity within the neuron and expedient action when signaling events require reorganization of the cytoskeleton.

The steps of microtubule assembly involve nucleation, elongation, monomer/ polymer equilibrium and steady-state turnover of tubulin subunits. Microtubules are hollow structures with a 24 nm outer diameter and an inner diameter of 15 nm. They are made of protofilaments which are observed as linear strands of tubulin heterodimers, and there are typically 13 or 14 protofilaments in a cellular microtubule. Tubulin adds to the

plus ends of microtubules which elongate from a microtubule-organizing center *in vivo*. These centers serves to nucleate growth and stabilize their minus ends (Brinkley, 1985). In most cells, the centrioles provide this role. But neurons contain large numbers of microtubules, and there appears to be additional nucleation sites. Evidence for the existence of additional microtubule-organizing centers can be found in the axon where all the microtubules are oriented with their plus ends pointing away from the centriole and cell body. Since most microtubules are 100 μm in length (Bray and Bunge, 1981) and an axon can be one meter long, there must be more nucleating structures, and compelling evidence suggests the plus ends of stable microtubules act as nucleating centers (Baas and Ahmad, 1992). Similar evidence is found in the dendrites where microtubules are found oriented in both directions. Those microtubules with their minus ends at the nerve terminus must be growing from structures other than centrioles, but the identification of these organizing centers has not been determined.

Neuronal microtubules are classified as dynamic or stable structures depending on the frequency with which they undergo catastrophic depolymerization. This stability in part appears to depend on the particular tubulin isotype or covalently modified tubulin forms in the microtubule, but other components like the organizing centers attaching to the minus end and the stabilizing factors may play major roles as well (Scaife et al., 1992). The microtubules that form *in vitro* from purified, unmodified tubulin in the presence of GTP and magnesium ions assemble in an entropy driven reaction. Without an organizing center to nucleate and stabilize the minus end, critical concentration behavior is observed (Angelastro and Purich, 1994). This phenomenon is controlled by the on and off rates of free tubulin dimer to the plus end. Because most stabilizing factors bind microtubules not free tubulin, their function can be studied *in vitro* by looking at their effects on critical concentration behavior. In the cell where microtubules are anchored at their minus ends, microtubules are characterized by dynamic instability where many are elongating slowly and fewer are depolymerizing rapidly. The binding of stabilizing factors to the

microtubules acts to slow down the rate and duration of microtubule depolymerization (Kowalski and Williams, 1993).

Tubulin

Alpha and beta tubulin form heterodimers which assemble into microtubules. Tubulin is also expressed as many different isoforms, and each is characterized by primary sequence changes as well as covalent modifications. These isoforms are believed to participate in determining the functional role of microtubules. Nearly ten isoforms for each α– and β– tubulin polypeptides have been identified in mammals (Villasant et al., 1986; Wang et al., 1986; Lopata and Cleveland, 1987). Some cell types contain very few isoforms, leading to the speculation that the various isoforms may have special functions in certain cells (Villasant et al., 1986). The expressed proteins are 50 kDa, and they form a heterodimer . One half of this dimer, the α- tubulin, binds GTP at a nonexchangeable site that is created at the α-, β– tubulin interface within the heterodimer (Gaehlin and Haley, 1977; Gaehlin and Haley, 1979). The hydrolyzable GTP binds to the exchangeable site before incorporation into a microtubule (MacNeil and Purich, 1978; Zeeberg and Caplow, 1979). This site is located at the amino terminus of β - tubulin where heterodimer addition occurs (Shivanna et al., 1993; Jayaram and Halley, 1994). A cap of GTP tubulin is created at the growing end of a microtubule which accepts the addition of further GTP-bound tubulin dimers easily (Karr et al., 1979). Once a subunit is incorporated into a microtubule, the nucleotide bound at the exchangeable site becomes nonexchangeable, and it becomes part of the microtubule lattice accepting addition of more GTP-bound dimers. Eventually, the nucleotide is hydrolyzed, and the subunit remains in the microtubules which have a half-life of ten minutes. When the microtubule depolymerizes, the GDP can be exchanged for GTP or dGTP to repeat the cycle (Angelastro and Purich, 1992). This occurs throughout the lifetime of tubulin in cells which on the order of 3 - 5 days (Spiegelman et al. 1977).

Microtubule-associated Proteins

The microtubule-associated proteins (MAPs) are a group of proteins defined by their ability to co-purify with microtubules in a stoichiometric manner. Neurons are a particularly rich source of MAPs, and proteins isolated from brain have been grouped according to their mobility on SDS-PAGE gels (Wiche, 1989). MAPs within the same group number are not always related with similar functionality, but several groups do arise from alternative splicing of a single mRNA transcript. These proteins function to nucleate MTs, promote assembly of MTs, stabilize MTs transport organelles along MTs and cross-link MTs to other filamentous and membranous structures in the cell (Hall, 1994). Several of the MAPs share homologous domains that perform similar functions in the cells. Among these are motor domains, proline-rich regions and phosphorylation consensus sites, but the most obvious microtubule-binding region (MTBR) containing the eighteen amino acid repeats found in the carboxy-terminal portion of the fibrous MAP2a, -2b, -2c, -2d, MAP-4 and the Tau family. MAPs are generally grouped according to their functional roles or properties, and most fall into the category of the fibrous MAPs or the motors. Others include those which bind and stabilize cold-stable microtubules, those which link microtubules to vesicles and organelles, those involved in forming the spindle apparatus during mitosis and those which may sever or nucleate microtubules.

Fibrous MAPs include the ubiquitous MAP4 and the neuronal MAPs, Tau and MAP2. These proteins bind to microtubules largely through strong electrostatic interactions between the highly anionic carboxy-tails of tubulin and the very basic microtubule-binding region of the MAPs (Littauer et al., 1986). Both axonal Tau and dendritic MAP2 have projection arms which are thought to space microtubules differently in the axons and dendrites. The projection arm is connected to the MTBR by a protease-accessible hinge region (Figure 1-1), and the projection arm may also function in cross-linking microtubules to other cytoskeletal elements. These interactions between MT and MAPs have been studied in detail, and specific sequences of the fibrous MAPs that bind

MTs have been revealed. These binding domains require not only basic amino acids but the proper spatial arrangement of them (Coffey et al., 1994; Coffey, 1994). The repeats of the MT-binding region are aligned for neuronal MAP2 and Tau and the ubiquitous MAP-4 (Figure 1-2). Strong homology is observed at particular amino acid residues, and many of these are known to be critical for MT binding. Many basic amino acid residues have been found to be important using cloned genes, mutagenesis, recombinant protein and *in vitro* assays to detect affects on binding, nucleation and the ability to promote MT assembly. These residues are observed to be preserved in the MT-binding repeats among most mammals and represent a common functional motif found in fibrous MAPs. Additionally, several aliphatic amino acids are also preserved as are what appears to be consensus phosphorylation sites and several cysteines. Although the exact roles of the conserved aliphatic residues are not fully understood, it is possible they form tight hydrophobic interactions or keep the required basic residues in the correct spatial arrangement to bind MTs. As for the roles of the phosphorylation sites and cysteine residues, these are being studied closely as they surely are involved in mediating MAP function (Ainzstein and Purich, 1994).

MAPs may also play a role in the intracellular transport of materials throughout the cell. In more symmetric cells, microtubules are observed to emanate from the perinuclear centrioles and radiate to the cell periphery. These microtubules can be used as tracks to transport materials to different regions, and motors are believed to be involved in separating chromosomes in dividing cells and moving vesicles through the golgi in quiescent cells (Angelastro and Purich, 1994). In neurons, many components are needed at distal sites in axons and dendrites, and they must be transported to these sites from their point of origin in the cell body. Likewise, materials produced or those taken up at the nerve termini must be transported to the cell body. In particular, materials for neurotransmitter synthesis and secretion must be transported to the synaptic junction in axons; cytoskeletal elements must be transported to axons and dendrites; vesicles are cycled to and from the nerve terminal

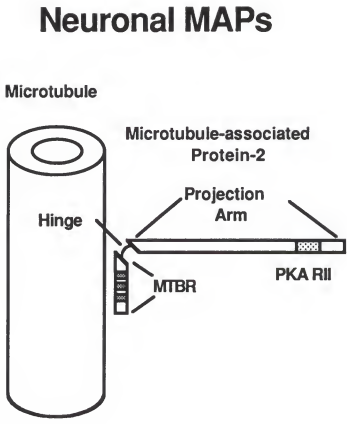

Figure 1-1. Schematic Representation of MAP2 Binding to a Microtubule. The MTBR and repeat-region can be observed in close association with the MT while the projection arm extends away from the microtubule allowing it to act as a spacer or possible cross-linker. These domains are connected by a hinge region that is susceptible to protease activity.

TAU	VKSKIGSTENLKHQPGGG	
MAP2	VKSKIGSTDNIKYQPKGG	**First Repeat**
MAP4	VRSKVGSTENIKHQPGGG	
TAU	VQSKCGSKDNIKHVPGGG	
MAP2	VQSRCGSKDNIKHSAGGG	**Second Repeat**
MAP4	VTKAAGPIGNAQKPPTG-	
TAU	VTSKCGSLGNIHHKPGGG	
MAP2	VTSKCGSLKNIRHRPGGG	**Third Repeat**
MAP4	VSSKCGSKANIKHKPGGG	
TAU	VQSKIGSLDNITHVPGGG	
MAP2	AQAKVGSLDNAHHVPGGG	**Fourth Repeat**
MAP4	AQAKVGSLDNVGHLPAGG	

Figure 1-2. Sequence Alignment of the 18 Amino Acid Repeats Found in the Microtubule-binding Region for the Different Fibrous, Heat-stable Microtubule -associated Proteins. Note the conserved cysteine residues found in the second and third repeat of MAP2 and Tau. The sequences for Tau and MAP2 are from human sources. The MAP4 sequence is from bovine. [Note: The MAP2 sequence is identical in the repeats for bovine and human.]

membrane; and growth factors must be transported to the cell body when they are taken up in the periphery of the cell (Hall, 1994). These functions are usually carried out by motor proteins which bind to and move along microtubules in an ATP-dependent mechanism. These motors may bind specifically to different components to be moved, or they may bind adapters which bind specific components for travel. For movement in axons, most membrane bound vesicles and organelles are moved along microtubules at the fast rate of 200-400 mm per day while cytoskeletal components are transported along microtubules in an unknown mechanism at the slow rate of 0.2-8.0 mm per day.

Motor Proteins

Historically, motor proteins have been classified according to the direction that they travel along microtubules. As homologous motor domains have been identified that can move in different directions along the microtubule, the dintinctions between motors are less clear, and perhaps they should be classified based on the homology of the motor domains and not the directions they travel. The motors that travel from the minus to the plus ends of microtubules typically belong to the kinesin family while those that travel along microtubules in the other direction mostly belong to the cytoplasmic dynein family. In axons where the microtubules are all growing with their plus ends towards the synapse, conventional kinesins are responsible for anterograde movement of membranous vesicles and organelles. Movement in the opposite direction is termed anterograde transport, and in the axon cytoplasmic dynein usually provides this function although the kinesin-like motor NCD also travels to the minus end of microtubules (McDonald et al., 1990). Kinesins and dyneins are known to compete with MAP2 and Tau for binding sites on the microtubules, and MAP2 and Tau both inhibit *in vitro* microtubule gliding by kinesin or cytoplasmic dynein in a dose dependent manner (Paschal et al., 1989; Hagiwara et al., 1994).

The members of the conventional plus-end-directed kinesin family of microtubule motors are typically considered to be tetramers composed of two heavy chains of 120 kDa and two light chains of 60 kDa (Bloom et al., 1988), but it is believed that monomeric

kinesin and combinations of kinesin-like motors and adapters exist also (Vale, 1992). The globular heavy chains each contain a microtubule binding site and an ATP binding site. Attached to the two heavy chains are the light chains which function in connecting the motor to the object to be transported. Translocation is an ATP-dependent process that drives the kinesin along the 8 nm tubulin dimer steps of a microtubule protofilament (Malik et al., 1994), and although 16 nm steps have been recorded for single kinesin molecules, 8 nm is the most likely step distance. Presumably, different kinesins can be used to transport different components, and the initial observation that supported this was the detection of varying rates of transport for different components traveling to the end of an axon. Several of these kinesin superfamily (KIF) have been cloned including the mitochondria-specific KIF1B and the synaptic vesicle-specific KIF1A (Nangaku et al., 1994). More kinesin-like genes are constantly being found and sequenced including some that travel towards the minus end of a microtubule. NCD is an example of a minus-end-directed kinesin-like motor, and recently it has been shown that chimeras with the stalk and neck of NCD fused to the motor domain of kinesin move towards the minus ends of microtubules (Endow and Waligora, 1998).

The dynein family is composed of several well known members including axonemal ATPases responsible for flagellar and cilliary movement and motors responsible for fast retrograde transport of materials in axons. Like the kinesins, the complete set of dynein-like molecules is still being discovered and contains members that are atypical (Vale, 1992). Cytoplasmic dyneins are connected to microtubules by two or three large globular heads of 500 kDa which each contain up to four ATP-binding sites. These globular domains are connected to a smaller common base by a variety of stalk molecules, and presumably different combinations of dynein isoforms determine transport activity. Another important multimeric protein complex known as dynactin appears to be required for proper retrograde dynein activity (Waterman-Storer et al., 1997). These additional complexes can bind microtubules, membranous organelles and dynein in a manner believed

to link and activate the components for transport. In addition to fast retrograde transport, cytoplasmic dyneins have also been implicated in slow anterograde transport of cytoskeletal components (Dillman et al., 1996). With the orientation of cytoplasmic dynein stabilized within the axon, its microtubule-binding site is exposed during slow transport to the synapse. This allows microtubules sliding along the dynein complex to be pushed towards the synapse. This mechanism allows the dynein to work while it is being transported to the synapse where it presumably picks up materials for retrograde transport, but the exact mechanism has not been determined. The importance of the motor proteins is clearly evident as is the need for stable microtubule tracks in the neuron. In fact, motor proteins and fibrous MAPs must work in unison for materials to be transported along microtubules. They bind overlapping regions of tubulin, and the fibrous MAP2 and Tau could interfere with motor movement along the microtubule.

Tau

The roles of specific regions and amino acids in the microtubule-binding region of the neuronal, fibrous MAP2 and Tau proteins have received considerable attention, and the current state of knowledge reflects this. The six known Tau isoforms have three or four of the 31 amino acid repeats for adults and juveniles respectively, and they arise from alternative splicing of a single transcript (Goedert et al., 1991). The repeats traditionally have been divided into the first 18 amino acids which constitute the originally described repeated regions of Tau (T1-T4) and the following 13 or 14 amino acids which were termed the inter-repeats. These highly phosphorylated proteins have been shown to promote MT assembly and to stabilize MT in the axons with the four-repeat adult forms having a larger effect (Lee et al., 1989). Synthetic octadecapeptides corresponding to T1 and T2 have been shown to promote the assembly of MTs while synthetic peptides of T3, T4 and randomized T1 did not (Ennulat et al., 1989). In addition, the inter-repeat between T1 and T2 of adult Tau was found to bind MTs in a strong electrostatic interaction that required three lysines (Goode and Feinstein. 1994). Synthetic polypeptides of this inter-

repeat containing the basic residues were shown to promote MT assembly, but when the sequence was randomized, the ability to promote MT assembly was lost. This tightly binding region has been hypothesized to confer extra stability to MTs in the axons of adults by providing an additional MT binding site that reduces microtubule depolymerization.

The Tau repeat region has many potential phosphorylation sites, and many kinases have been shown to phosphorylate Tau within and around the microtubule-binding region. Similar to MAP2, this phosphorylation is believed to alter microtubule binding, proteolysis of Tau and intracellular trafficking of Tau (Mandelkow et al., 1995; Billingsley and Kincaid, 1997). Since Tau has been implicated as a core component of neurofibrillary tangles in Alzheimer disease (AD), a significant effort has materialized to identify the kinases which normally phosphorylate Tau and those which may be acting abnormally. This effort has led to the identification of over a dozen kinases which can phosphorylate Tau *in vitro* (Mandelkow et al., 1995; Billingsley and Kincaid, 1997), and from these candidates may emerge some that could be altered in various neurodegenerative diseases. These candidates presumably would block binding of Tau to microtubules and should show a decreased electrophoretic mobility on SDS-PAGE gel as is observed in AD-Tau.

Protein kinase C (PKC), cAMP-dependent kinase (PKA) and calcium/calmodulin-dependent kinase II (CAMK II) are all activated by signal transduction pathways involving second messengers, and any chronic or poorly timed activation of these pathways could lead to altered Tau function. PKA, PKC and CAMK II all phosphorylate Tau *in vitro*, but only PKA and CAMK II phosphorylation results in the decreased electrophoretic mobility of Tau (Baudier and Cole, 1987; Littersky and Johnson, 1993) with phosphorylation of Tau at serine-262 and serine-356 (Littersky and Johnson, 1996). PKC also phosphorylates Tau *in vitro* which causes reduced microtubule assembly activity (Hoshi et al., 1987), but PKC phosphorylation does not slow the electrophoretic mobility of Tau. Decreased mobility may still be related to PKC action as microinjection of PKC into neuroblastoma cells leads to the formation of PHF-1 and ALZ-50 epitopes (Cressman and

Shea, 1995). Each of these kinases may be involved in abnormal Tau behavior in Alzheimer disease, but none of them alone are capable of perturbing Tau function to the degree observed in this disorder.

Other kinases thought to be involved during Tau phosphorylation in Alzheimer disease are the proline-directed kinases, and this enzymatic activity is known to purify with certain Tau preparation from brain. These include mitogen-activated kinases (MAPK), glycogen synthase kinase 3 (GSK3) and the neuronal cdc2-like kinases (NCLK). The MAPK family contains certain members like p42-MAPK, p44-MAPK, p40-ERK2 and p49-3F12 which are known to phosphorylate Tau (Billingsley and Kincaid, 1997). The MAPKs are interesting, because some associate with the neuronal cytoskeleton and generate Alzheimer antibody epitopes like PHF-1 (Mandelkow et al., 1995) while others are activated by β-amyloid precursor protein (Greenberg et al., 1994). Perhaps the most interesting is the novel p49-3F12 which colocalizes with the ALZ-50 epitope and has a genetic locus on chromosome 21 which is implicated in paired helical filament formation in Down syndrome. In addition to the MAPK family, GSK3 β is known to associate with microtubules and can phosphorylate Tau inhibiting its ability to promote microtubule assembly (Utton et al., 1997). Phosphorylation by GSK3 is increased by phosphorylation by other kinases as the consensus site is -S (P)-X-X-S- where the first serine is phosphorylated. Many of these sites are found in and around the repeat region of Tau. This type of phosphorylation is known to inhibit the binding of Tau to microtubules, and it phosphorylates serine-235 and serine-404 which produces the mobility shift associated with abnormal Tau in Alzheimer disease (Yang et al., 1993). Still, the signals which regulate GSK3 are not fully understood. The neuronal cdc2-like kinase phosphorylates five sites on Tau *in vitro* that are phosphorylated in AD-Tau, and phosphorylation of recombinant Tau by NCLK promotes Tau dimerization *in vitro* (Paudel, 1997). Additionally, other kinases like p110-MAPK, CK I, CK II and DNA-dependent kinases have all been shown to phosphorylate Tau *in vitro*. Plus, phosphatases like phosphatase

2A are also known to regulate the binding of Tau to microtubules (Sontag et al., 1996), and their effects are likely to be disturbing the system during cellular dysfunction. The elucidation of which kinases and phosphatases are activated during normal activities and neurodegeneration should lead to a better understanding of the ways these diseases can be attacked (Billingsley and Kincaid, 1997).

MAP2

MAP2 exists both as adult and juvenile forms whose biosynthesis appears to be developmentally controlled. Alternative splicing of a single transcript into 6 kb and 9 kb transcripts is known to occur from a single gene on chromosome 2 (Neve et al., 1986). MAP2a and MAP2b are the high-molecular-weight, three-repeat forms, and another high-molecular-weight four-repeat isoform has also been found (Kalcheva et al., 1995). MAP2a, the larger isoform, is found only in adults while MAP2b is present throughout life. The low-molecular-weight forms are MAP2c and MAP2d, and they contain three (M1 - M3) and four (M1 - M3 & MG) repeats respectively (Garner et al., 1988; Doll et al., 1993). The juvenile three-repeat MAP2c and adult four-repeat MAP2d each are missing 1372 amino acids of the projection arm. This leaves only the 150 amino acids at the amino-terminal portion of the projection arm and the MTBR which are common to all MAP2 isoforms in these low molecular weight forms. The juvenile MAP2c appears to be replaced by MAP2a as the transition from juvenile to adult occurs, but some of the previous MAP2c results require clarification as MAP2d is novel and similar to MAP2c in size and composition (Tucker et al., 1988). To date all known MAP2 proteins are highly phosphorylated with an amino terminal PKA RII binding site on the projection arm, a carboxy-terminal MTBR and a protease accessible hinge connecting the two domains (Rubino et al., 1989; Vallee, 1980).

The microtubule-binding region of MAP2 was originally identified as a 28-36 kDa protease cleavage product of the carboxy-terminal tail which promoted MT assembly (Vallee, 1980; Flynn et al., 1987a; 1987b). This region was subsequently cloned from rat,

mouse, bovine and human and led to the elucidation of the repeats and residues responsible for MT binding. Work in the Purich lab using cassette and site-directed point mutagenesis of MAP2 in an E. coli expression system demonstrated that the second octadecapeptide repeat M2 is the major binding repeat of MAP2 (Coffey, 1994; Zhang, 1997). This was confirmed using synthetic polypeptides corresponding to M1, M2, M3 and MG to displace MAP2 from MTs. Experiments with recombinant protein in which the M2 sequence was replaced with M3 exhibited reduced binding affinity for MTs and a reduced ability to promote MT assembly; but if the M2 sequence was reintroduced at the M1 position, this effect was nullified (Coffey et al., 1994). Additionally, experiments showed that synthetic octadecapeptides corresponding to M2 and not M1, M3 or MG blocked MAP2 binding to MTs and promoted MT assembly (Joly et al., 1989; Joly and Purich, 1990; Zhang, 1997). Further investigations subsequently showed that mutating the second lysine or two arginines in M2 of the MTBR to aliphatic or acidic amino acid residues gave the same result as when the entire M2 was replaced (Coffey et al., 1994).

There are nearly 200 serine and threonine residues which are potential phosphorylation sites in high molecular weight MAP2 with consensus sequences for cAMP-dependent kinase, calcium/phospholipid-dependent kinase, calcium/calmodulin-dependent kinase, glycogen synthase kinase and several proline-directed kinases. At least two of these kinases, PKA and MAPK-2, purify with cycled microtubules and are known to phosphorylate the protein *in vitro* (Theurkauf and Vallee, 1982; Lopez and Sheets, 1995). Of these, more is known about PKA. The regulatory dimer of this kinase binds the projection arm near the amino-terminus with a low nanomolar dissociation constant, and it has been determined that approximately one in 40 MAP2 molecules is associated with PKA *in vivo* (Rubino et al., 1989). In neurons, MAP2 is found to be extremely phosphorylated when purified using focused microwave irradiation to denature kinases and phosphatases *in situ*. It has been determined that there are 46 moles of phosphoryls incorporated per mole of MAP2 *in vivo* (Tsuyama et al., 1987), but only one actual site has been identified as

being phosphorylated *in vivo*. This is serine 136, and it is believed to be phosphorylated by a proline-directed kinase such as MAPK or GSK-3 (Berling et al., 1994). Unfortunately no other *in vivo* sites have been identified. This remains a major challenge demanding future work, because *in vitro* the action of phosphorylated MAP2 has been investigated and shown to affect the dynamics of microtubule assembly and disassembly. In particular, binding of MAP2 to MT is slightly reduced when either the serine immediately preceding M2 or the second serine in M2 was phosphorylated by PKC, and this decreases MT nucleation. A more dramatic effect was observed when the serine immediately after M2 is phosphorylated by PKC in addition to one of the aforementioned serines (Ainzstein and Purich, 1994). These recombinant MAP2 molecules were shown to bind poorly to MTs and lacked the ability to promote MT assembly. This PKC study along with the mutagenesis and synthetic polypeptide work clearly indicates that the second repeat M2 is critical for proper interactions with MTs, and more work is being done to uncover the roles of other conserved amino acids and regions in the MTBR of MAP2.

Abnormal Pathology in Alzheimer Disease

Alzheimer disease (AD) is a neurodegenerative condition which affects one half of Americans over the age of 85. The disease is characterized by progressively more profound cognitive dysfunction eventually culminating in death. Dementia is the result of insoluble amyloid plaques and neurofibrillary tangles (NFTs) developing and killing the neurons in the limbic and cerebral cortices of affected individuals (Selkoe, 1994). These inclusions eventually cause a breakdown in normal neural activity that is similar to that observed in normal aging and numerous other neurodegenerative diseases. The formation of β-amyloid plaques from soluble fragments of amyloid precursor protein outside the cell precedes the accumulation of neurofibrillary tangles. These senile plaques are dense, spherical deposits of 8 nm amyloid filaments commonly found in the hippocampus, amygdala, entorhinal cortex and cerebral cortex of AD brains (Wisniewski et al., 1989).

These plaques surround dystrophic axons and dendrites as well as activated microglia and reactive, fibrous astrocytes. Additionally, accumulations of amorphous, diffuse amyloid deposits are observed in Alzheimer and normal brain tissue, but these do not contain dilated, dystrophic neurites or activated microglia (Tagliavini et al., 1988). The relationship of these accumulations to senile plaques is not well defined, but these diffuse plaques do not seem to be as detrimental. This is thought to be true as normal individuals exhibit many diffuse amyloid plaques, and Alzheimer patients do not exhibit symptoms associated with neuronal dysfunction of the areas containing these plaques.

Senile β-amyloid Plaques

Amyloid precursor protein (APP) is normally found in a variety of isoforms resulting from alternative splicing. The longest of these isoforms is 770 amino acids long, and the portion that ultimately forms senile plaques is from 671-711 (Glenner and Wong, 1984). These type I transmembrane proteins have a seventeen amino acid signal peptide that directs them to the endoplasmic reticulum (Kang et al., 1987), single N- and O- linked glycosylation sites (Kang et al., 1987), and they undergo other posttranslational modifications including phosphorylation, sulfation and perhaps the addition of glycosaminoglycan side groups (Weidmann et al., 1989; Oltersdorf et al., 1990; Shioi et al., 1992). The APP has a transmembrane domain from position 700-723, and is quite often cleaved at position 687. This constitutive cleavage affects less than one third of nascent proteins and releases the large amino terminus into the extracellular space. This soluble form of APP contains a 56 amino acid insert with 50% homology to the Kunitz family of serine protease inhibitors and contains the amino third of the β-amyloid peptide found in senile plaques (Ponte et al., 1988; Tanzi et al., 1988). The other two thirds of the β-amyloid peptide remain partially buried in the transmembrane domain.

This type of cleavage presumably blocks the release of the type of β-amyloid peptides found in senile plaques, but truncated forms of APP are also produced by cleavage at 671 which leave the smaller membrane bound fragment with the β-amyloid peptide

region intact. Since APP contains a putative consensus motif for clatherin-mediated internalization (Chen et al., 1990), this type of cleavage can produce fragments with the β-amyloid peptides sequence intact. Other cleavage sites for APP also generate β-amyloid peptides that are released from the cell under normal conditions, and the exact roles of these different soluble APP fragments and whole APP are not completely understood. However, it is known that APP accumulates in the axon and growth cone where it may function in cell adhesion or inhibiting nonneuronal growth (Selkoe, 1994). The soluble forms appear to be important mediators in normal APP function, and soluble APP is released after electrical stimulation of the neuron, not injury to the membrane, where it may function in modulating neurite proliferation, synaptogenesis and neuronal survival.

The causes of the aberrant cleavage of APP by unknown proteases termed α–, β– and γ– secretases are not known, but several factors which result in the accumulation of the 40-42 amino acid β-amyloid peptide have been identified. These include the identification of several genes linked to familial, early-onset AD. The genes include the APP gene (Citron et al., 1992; Hardy, 1992, Cai et al., 1993), the Apo E gene (Strittmatter et al., 1993) and a family of genes known as the presenilins (Campion et al., 1995). In cell culture experiments and transgenic animal studies, these gene products have all been shown to increase the release and accumulation of β-amyloid fibrils when altered, but it is not known how generation of the β-amyloid peptide which forms fibrils is related to normal APP processing and the generation of soluble APP fragments (Selkoe, 1994).

The mutations related to early onset, familial AD account for less than 20 % of AD cases, and the causes of other spontaneous forms of AD have not been identified. Currently a number of events which are observed in AD have been linked in a speculative model based on autopsies and experiments in model systems. A putative timeline of events is being assembled which highlights when certain changes take place and which cellular components are candidates for being agents of degeneration. In all of the published results, one hindrance is the lack of an appropriate animal model and the other is the late

examination of human material which does not occur until many years after the disease course began. That amyloid plaque formation precedes neurofibrillary tangle accumulation is established, but why this occurs is not. This an extremely important detail as the number of NTFs correlates with the severity of dementia in AD patients (Wilcock and Esiri, 1992), and NFTs do not necessarily occur in the same neurons or brain regions where plaques are found. In Alzheimer disease, the senile plaques or their causative agents must eventually lead to the abnormality which initiates neurofibrillary tangle formation. Neurofibrillary tangles though are found in many diseases and apparently normal aging, so it appears possible that plaques and tangles could arise independently in AD, but this probably is not typical. Research in the field covers all aspects of the disease, but finding the source of senile plaque formation would presumably provide the best target for preventative or curative strategies.

This search for the source of increased β-amyloid peptide production is perhaps the greatest quest at the moment, but it is only one component in understanding how senile plaques affect normal neuronal behavior. Other work has been done establishing the effects of β-amyloid peptides and β-amyloid fibrils on neurons. The β-amyloid fibrils which form β-amyloid plaques are 8 nm filaments composed of 40-42 amino acid long polypeptides. These filaments have been purified from patients where they are found as extracellular spheres of dense fibrils surrounding dilated neurites. In addition to the biochemical analysis identifying β-amyloid peptide as the major component in plaques, purified AD fibrils and those assembled *in vitro* have been used to study their toxic effects in animal and cell culture systems. Impaired membrane transport, changing calcium concentrations, increased oxidative stress and the activation of numerous signal transduction cascades leads to a neuron where there are many possible agents capable of killing the neuron or generating the formation and accumulation neurofibrillary tangles which could harm cells.

Neurofibrillary Tangles

Neurofibrillary tangles are most prevalent in the hippocampal formation, the transentorhinal region and the entorhinal region. They are observed as accumulations which fill the cell bodies of neurons and as neuropil threads in the distal portions of dendrites (Kidd, 1963; Terry, 1963). They seem to contain many different components when examined by electron microscopy and gold-labeled antibodies, and some of the components identified in NFTs include neurofilaments (Anderton et al., 1982; Miller et al., 1986; Cork et al., 1986), ubiquitin (Shaw and Chau, 1988; Manetto et al., 1988), β-amyloid (Spillantini et al., 1990; Perry et al., 1993), polyglycosaminoglycans (Perry et al., 1991; Snow et al., 1992) and microtubule-associated proteins Tau (Brion et al., 1985; Kosik et al., 1986; Grundke-Iqbal et al., 1986) and MAP2 (Nukina and Ihara, 1983; Kosik et al., 1984; Neve et al., 1986; Yen et al., 1987; Kosik et al., 1988; Mulvihill and Perry, 1989; Dammerman et al., 1989). The most prominent structural features of the NFTs are paired helical filaments. These filaments have been shown to contain all six isoforms of Tau as their core component (Goedert et al., 1989) and are easily identified by their periodic modulations in diameter which varies from 10-20 nm with a crossover distance of 75-80 nm. As observed when purified based on their extremely insoluble nature and viewed by electron microscopy with negative staining, the filaments are surrounded by a fuzzy coat of material which can be removed by pronase treatment. This action leaves a core filament which contains the repeat sequences from Tau (Goedert et al., 1988; Wischik et al., 1988). Proteolytic fragments of Tau are also found in NFTs, and their presence has been correlated with DNA fragmentation in AD neurons (Ugolini et al., 1997).

In addition to paired helical filaments, straight filaments are also found in the neurofibrillary tangles of AD brains. The number of straight filaments is much less than the number of paired helical filaments, but stain exclusion density maps of cross-sections of the two filaments demonstrate they have the same amount of polymeric material in a given length (Crowther, 1991). In fact, intact filaments from AD tangles have been found

where a paired helical filament turns directly into a straight filaments with no break. The straight filaments are also believed to contain Tau, but no rigorous work has demonstrated this sufficiently. They vary from 12-15 nm in diameter with a crossover length of 150 nm, and like paired helical filaments, they are found in other neurodegenerative diseases. These straight filaments are not the same as 10 nm filaments which arise from the longitudinal splitting of PHFs, but often it is difficult to differentiate between straight filaments and split filaments (Wischik et al, 1985).

Tau in Alzheimer Disease

Many of the studies on neurofibrillary tangle formation have investigated the post-translational modifications which Tau undergoes during AD development or the assembly properties of purified and recombinant Tau. To date, no adequate animal or cell culture model has been generated to study neurofibrillary tangle formation *in vivo* although several exist where amyloid plaques form. The Tau found in NFTs has been found in various ubiquitinated, phosphorylated, glycosylated and glycated forms. Of these modifications, phosphorylation patterns of Tau have been intensely investigated as they presumably would indicate which signal transduction pathways are acting abnormally, and this presumably would shed light on how plaque formation generates tangle formation as is suspected in AD. Currently there are a number of components which may act in plaque formation and are known to affect Tau assembly into tangles. These include glycosaminoglycans which are observed in plaques and facilitate Tau assembly *in vitro* (Goedert et al., 1996; Perez et al., 1996), ApoE which elevates β-amyloid peptide accumulation in familial AD (Selkoe, 1994) and is known to bind Tau (Strittmatter et al., 1993) and others like free fatty acids which are affected by oxidative stress and promote Tau assembly (Wilson and Binder, 1997).

The first indication that Tau might be adversely affected in AD brains, came from studies where microtubule protein purified from AD brain showed poor microtubule assembly. These preparations typically contain 80 % tubulin and 20 % associated proteins

which include mostly Tau and MAP2. The tubulin from these brains was further isolated from the binding proteins and assembled in the presence of polycations which mimic MAP function (Iqbal et al., 1986). The AD-Tau was shown to be greatly inhibited in its ability to promotes the assembly of tubulin from bovine brain (Alonso et al., 1994). This microtubule-assembly-promoting activity could be restored if the Tau was dephosphorylated using alkaline phosphatase. This AD-Tau was also shown to bind normal Tau and MAP2 inhibiting MAP-stimulated microtubule assembly (Alonso et al., 1996), and it formed filaments with the normal Tau but not the MAP2 (Alonso et al., 1997). From there, the search for sites of Tau phosphorylation in AD tissue has lead to the identification of several kinases and phosphatases which are believed to alter the normal function of Tau. This is believed to cause the Tau to not bind microtubules and to enhance the formation of straight and paired helical filaments.

Tau isolated from AD patients runs on an SDS-PAGE gel as three major bands of 60, 64 and 68 kDa with a minor band at 72 kDa. Since Tau isolated from AD brain has reduced mobility on SDS-PAGE gels that can be restored by phosphatase treatment of the Tau, researches have tried to identify kinases that can produce a similar retardation of Tau mobility in gels. The first antibody evidence that AD-Tau was phosphorylated came from studies with the mouse monoclonal Tau-1. This antibody reacts with Tau from normal brain tissue, but did not react with the most common AD-Tau isoform, A68, unless the sample was first phosphatase treated. More recently, it was found that AD-Tau has 3-4 times more phosphoryl groups than are typically incorporated into Tau of normal subjects. Several kinases which phosphorylate normal Tau at the same sites that are phosphorylated in AD-Tau have been found, and phosphopeptide mapping of phosphorylation sites in AD-Tau fragments has permitted the identification of several candidate kinases that may play a role in Alzheimer disease. These include the proline-directed kinases p34-cdc2 and GSK-3 which are known to phosphorylate Tau and to produce retarded mobility on SDS-PAGE gels. Whether these kinases affect Tau polymerization into paired helical filaments or

whether they are phosphorylated after filament assembly remains to be determined. Although several early AD epitopes are phosphorylation-sensitive, more work is clearly needed to determine how phosphorylation is altered during the course of Alzheimer filament assembly.

In Vitro Assembly of Tau

Additionally, work on the polymerization properties of Tau from recombinant and animal sources has lead to a greater understanding of how this assembly occurs. Full-length recombinant three and four-repeat Tau are the benchmark standards as they are all found in the neurofibrillary tangles (Goedert et al., 1992). Full length Tau can polymerize in a number of settings (Montejo de Garcini et al., 1986; Montejo de Garcini and Avila, 1987; Montejo de Garcini et al., 1988; Dudek and Johnson, 1993; Troncoso et al., 1993; Crowther et al., 1994; Wilson and Binder, 1995; Perez et al., 1996; Goedert et al., 1996; Kampers et al., 1996; Wilson and Binder, 1997), but they do not assemble as well as small fragments containing only the microtubule-binding region containing the repeat region (Crowther et al., 1992; Wille et al., 1992; Schweers et al., 1995). Assembly of recombinant material has the advantage that all the proteins are in the same nonphosphorylated state, and they tend to assemble best under oxidizing conditions at high salt and a variety of pHs (Crowther et al., 1992, 1994; Wille et al., 1992; Schweers et al., 1995). Typically, these results show that paired helical filaments form most easily as the Tau gets trimmed away leaving only the repeats (Wille et al., 1992; Schweers et al., 1995). The original experiments using recombinant Tau showed that 10 mg/mL of the material polymerized into paired helical filaments within 3 - 4 weeks in buffers ranging from 500 mM Tris at pH 5.0-5.5 to 200 mM Tris/ 200 mM acetate at pH 6.8 and temperatures from RT to 37 ° C (Crowther et al., 1992; Wille et al., 1992; Crowther et al. 1994; Schweers et al., 1995).

When the three-repeat fragments containing only one cysteine were used, homodimers were shown to form that could be reverted to monomers by treatment with

reducing agents (Schweers et al., 1995). Additionally, these polypeptides showed a greatly reduced ability to form filaments if reducing agents were added to the assembly buffer or if the cysteine was mutated to an alanine (Schweers et al., 1995). Dimerization with the four-repeat Tau polypeptides was slightly different, because they contained two cysteines which could form intramolecular or intermolecular disulfide linkages. When intramolecular disulfide bonds formed, the protein remained monomeric, had an altered mobility on a native gel, and was poorly incorporated into filaments (Schweers et al., 1995). The material that did form intermolecular disulfide linkages appeared to form filaments, but there was no way to selectively drive more material into the dimeric form without mutating one of the cysteines. This was done so that the cysteine in the extra repeat was mutated into an alanine, and this appeared to restore the ability to form paired helical filaments efficiently (Schweers et al., 1995). Homodimers form homopolymers in *in vitro* studies, and presumably the filaments should have no polarity. In Alzheimer disease, the filaments in NFTs may contain heterodimers, and there is the possibility that the PHFs are polar structures like microfilaments and microtubules.

Assays for Measuring Tau Assembly

A major obstacle to filament assembly research has been the lack of an accurate, quantitative measure of polymer assembly. In the previous experiments, the Mandelkow lab demonstrated that a cysteine-to-alanine mutant polymerized poorly, but they did not state that this Tau fragment never formed filaments. They only claimed the assembly was greatly inhibited under these conditions. Their observations indicate that some filaments did form, and data subsequently obtained supports this conjecture. The various techniques for measuring polymer assembly have inherent advantages and limitations on their potential applicability. Centrifugation assays represent one of the simplest techniques, but even here, there are inherent problems. In the *in vitro* experiments using recombinant Tau and MAP2 fragments, polymerization times range from 1 - 4 weeks. During this extended period of time, even a heat stable MAP may denature, aggregate or undergo proteolysis.

This implies an accurate measure of the fraction of polymer and aggregated protein in the pellet must be determined. The development of such an assay is a daunting task, because correlative electron microscopy data is required to differentiate between aggregates, straight filaments and paired helical filaments. Additionally, many assembly systems being studied now contain polyanionic agents which are believed to enhance filament assembly, but they work by aggregating Tau on their own scaffolding. These systems cannot be studied using centrifugation because of the aggregation factor. In fact, centrifugation does hold some promise but only on clean systems that polymerize quickly and are stable in their native state.

Other popular methods currently include quantitation of polymerization from electron micrographs. Quantitation from electron micrographs holds some promise, but the technique is full of potential problems. First, very little material is needed to be observed on electron micrographs. A 10 μL solution containing 10,000 1 μm long filaments should be readily observed on the microscope with negative staining, but the amount of polymerized material may be very small. Microfilaments contain 370 subunits per micrometer and microtubules contain 1600 subunits per micron, thus it is a fair estimate that PHFs contain 1000 subunits with an average molecular weight of 50 kDa. That means only one million subunits are in the polymerized state per μL which is a concentration of less than 2 picomolar. This is six orders of magnitude lower than the lowest concentrations of Tau or MAP2 which polymerize *in vitro* so this makes it very difficult to quantitate the mass of polymer formed using the assay. For example, if one tenth of a ten micromolar solution polymerizes, this material would need to be diluted a million fold. This is not normally difficult, but the polymer solutions may not be homogeneous. Any clumping or aggregation of filaments can skew the results. Additionally, special care must be taken to ensure that the adsorption rate is constant for all the different constructs and conditions tested. This again is not always feasible especially when polyanions are present, but certain systems may be amenable to quantitation and comparison this way. These would

include systems where the solution variables are the same and the molecules forming the filaments are similar. It may not work to compare systems where the expressed constructs are different sizes; but if proteins vary only by several mutations, perhaps this technique could provide some useful information.

Finally, there are several spectrophotometric methods which may be feasible for studying certain systems. These include measuring polymerization by following thioflavin S binding to filaments, using light scattering as an assay for polymer mass formed and looking at spectrophotometric changes as subunits are incorporated into filaments. None of these techniques is adequate presently, but work is being done to develop a practical methodology. The thioflavin S binding is easy to follow as it becomes mores fluorescent when binding to AD paired helical filaments. This characteristic fluorescence has also been observed with thioflavin S binding to filaments of recombinant Tau or MAP2 fragments, but no one has demonstrated that it is quantifiable. In fact, dimeric Tau also binds thioflavin S so that it fluoresces while monomeric Tau does not produce this effect. Still, this method is promising as Alzheimer PHFs and amyloid fibrils are marked by this dye.

Anionic Agents that Promote Tau Assembly

Investigation of Tau polymerization in the presence of certain agents has lead to the identification of several compounds which facilitate *in vitro* Tau filaments assembly. Certain glycosaminoglycans like heparin, heparan sulfate, dermatan sulfate and chondroitan sulfate have been found to facilitate the polymerization of recombinant Tau into paired helical filament-like structures (Perez et al. 1996; Goedert et al., 1996). This work was strictly qualitative with the observation that they promoted assembly of Tau. Incubation times in the presence of either heparin or tRNA was reduced from 3 weeks to one day for filament assembly. The concentration of three-repeat Tau required for assembly was lowered ten-fold, and four-repeat full-length gave similar results. Polyglycosaminoglycans with a higher linear charge density gave the best results, and these agents have been shown to invade neurons with neurofibrillary tangles (Goedert et al., 1996). Early work had

suggested that the regions flanking the repeats interfered with the assembly of recombinant Tau as did the presence of two cysteines in four-repeat Tau (Wille et al., 1992; Schweers et al., 1995). Presumably these flanking regions folded over and masked part of the repeat sequences resulting in lowered filament assembly. The four-repeat fragments also polymerized poorly, and this was due to intramolecular disulfide linkage of the cysteines which prevented dimer and polymer assembly (Schweers et al., 1995; Kampers et al., 1996). The gylcosaminoglycans supposedly act in two ways to facilitate assembly (Kampers et al., 1996). First, they may bind the MAPs so that the repeat region is exposed and the fragments assemble readily. Second, at low MAP concentrations, they act in concentrating Tau molecules and aiding in nucleation as the Tau as aggregates along the polyanion.

A central issue in AD filament assembly is whether glycosaminoglycans are present during Tau polymerization and if so whether they are specific in their interaction. In fact, numerous reports indicate that glycosaminoglycans are present in some neurons of Alzheimer brain (Perry et al., 1991; Snow et al., 1992). Other polyanions, such as polyglutamate and RNA, may have a similar physical, chemical pathway for promoting assembly, but their importance in the AD polymerization pathway for Tau is less certain. (Perez et al., 1996; Kampers et al., 1996). In these experiments, investigators employed recombinant Tau material as the polymerizing material, and all of cases paired helical filaments were capable of forming. These experiments also demonstrated that Tau can form straight filaments, coiled filaments, ribbons and paired helical filaments with crossover distances ranging from 50 -120 nm. It is this structural versatility of Tau that characterizes its behavior. This is further illustrated by experiments using Tau from porcine cycled microtubule preparations where only straight 10 nm wide filaments formed (Wilson and Binder, 1995). Other anions, such as fatty acids, are known to promote polymerization as determined by electron microscopy (Wilson and Binder, 1997), and the

authors propose a model where abnormal fatty acids generated by amyloid plaques facilitate neurofibrillary tangle formation elsewhere.

The identification of various anions that promote assembly should not be viewed as proof of their physiologic importance, and this underscores the need to develop model cellular systems where neurofibrillary tangles can form over a period of time. Only then can rival mechanisms be studied under comparable conditions, and such model systems would also allow for the study of brain tissue throughout the course of disease. In Alzheimer disease, the period of time from onset to debilitation is often decades, and this precludes an effective study especially when one must have access to human brain tissue during the course of the disease progression. Animal models would allow one to quantify filament formation and factors as the assembly process proceeds. Moreover, because the phosphorylation of Tau has been observed in brain tissue from AD patients and because the AD-Tau does not bind microtubules well, model systems could prove valuable in understanding how phosphorylation of Tau and MAP2 controls their interactions with microtubules *in vivo*.

Other Neurodegenerative Diseases Exhibiting Neurofibrillary Tangles

There are well over ten other neurodegenerative disorders known to cause dementia that also are characterized by the presence of neurofibrillary tangles (Wisniewski et al., 1978; Jellinger, 1996; Dickson et al., 1996). These include Down syndrome (Olson et al., 1969; Wisniewski et al., 1976a; Cork, 1990), Parkinson-dementia of Gaum (Hirano et al., 1961, 1968), diffuse Lewy body disease (Gibb et al., 1987; Pollanen et al., 1992), Gerstmann-Straussler-Scheinker disease (Tagliavini et al., 1993; Ghetti et al., 1994), prion protein amyloid angiopathy (Hsiao et al., 1997; Tranchant et al., 1997), familial presenile dementia (Sumi et al., 1992; Spillantini et al., 1992), dementia pugilistica (Wisniewski et al., 1976b), Pick's disease ((Murayama et al., 1990; Love et al., 1995), corticobasal degeneration (Paulus and Selim, 1990; Ksiezak et al., 1994; Feany and Dickson, 1995),

progressive supranuclear palsy (Flament et al., 1991; Vermersch et al., 1994) and familial multiple system Tauopathy (Spillantini et al., 1997). These disorders are similar in that they all exhibit accumulations of neurofibrillary tangles, but they differ in their locations of deposit, the type of structures that they form, the dementia they cause and the isoforms of Tau they contain. In these neurodegenerative disorders, studies with anti-Tau antibodies indicated the presence of hyperphosphorylated Tau in the neurofibrillary tangles. It should also be stressed that one does not know whether phosphorylation plays a causative role in the formation and accumulation of these neurofibrillary tangles. It has simply been observed that the Tau is hyperphosphorylated.

Although Tau has been characterized as a neuronal cytoskeletal component, this protein is also found in the glial fibrillary tangles and neurofibrillary tangles of progressive supranuclear palsy, Pick's disease, familial multiple system Tauopathy and corticobasal degeneration (Feany and Dickson, 1996; Chin and Goldman, 1996; Spillantini et al., 1997). These disorders are all accompanied by the formation of filaments that do not morphologically resemble the paired helical filaments from Alzheimer brain. This suggests that other cellular abnormalities may alter the pathways for filament assembly. In fact, familial multiple system Tauopathy has recently been shown to be linked to mutations in the Tau gene on chromosome 17 (Poorkaj et al., 1998; Spillantini et al., 1998; Hutton et al., 1998). These mutations are clustered around exon 10 which codes for the extra repeat that is found in four-repeat Tau, and several of these mutations are believed to increase the relative amounts of four-repeat Tau to three-repeat Tau. Moreover, these four diseases and Alzheimer disease do not share the same complement of hyperphosphorylated Tau bands (Spillantini et al., 1997). Tau from AD tangles has 60, 64 , 68 and a minor 72 kDa bands whereas familial multisystem Tauopathy does not exhibit the 60 kDa band. Progressive supranuclear palsy and corticobasal degeneration exhibit band only at 64 and 68 kDa while in Pick's disease bands are only observed at 60 and 64 kDa. It should also be noted that

while these disease are characterized by the presence of Tau-containing filaments, the location, composition and type of filaments can vary.

Aims of This Research Project

Because Tau and MAP2 share so many common features, the fact that Tau is the only component of filaments in neurodegeneration is a curious phenomenon. MAP2 has not been identified as a core component for any of these filaments, but this does not exclude a role for MAP2 in promoting Tau filament assembly or engaging in polymerization on its own. It is possible and probable to believe that normal MAP2 behavior does suffer during the course of these conditions such that it does not function properly with microtubules. It should be stressed that MAP2 and Tau share a functional 200 amino acid microtubule binding domain that is 65% identical in amino acid primary sequence. This microtubule binding region contains repeats that are very similar in sequence and spacing with many identical consensus phosphorylation sites thought to be important in regulating their binding to microtubules and other cytoskeletal components. Thus, it seems highly unlikely that any abnormal phosphorylation of sites in Tau would not affect MAP2 in a similar manner. In addition to conserved phosphorylation sites in MAP2 and Tau, they are both susceptible to proteases which are known to release the MTBR from these proteins. Finally, neurofibrillary tangles formation occurs in the cell bodies of affected neurons where MAP2 rather than Tau is normally present in this cellular region. This suggests that some factors interfere with the transport of Tau from its sites of synthesis in the cell body to its final destination in the axon. If this is true, MAP2 and the abnormal Tau are both present during filament assembly and accumulation.

Ultimately answering the questions concerning why Tau and not MAP2 becomes incorporated into Alzheimer neurofibrillary tangles will help us to understand more about the origin of neurofibrillary tangles and how they might be prevented. First, MAP2 may have nothing at all to do with neurofibrillary tangle formation. Polyclonal and monoclonal

antibodies to rat MAP2 are known to stain AD tangles; however, prior extraction of tangle preparations with SDS eliminates such staining (Nukina and Ihara, 1983; Kosik et al., 1984), leading to the widely held view that MAP2 may associate with NFTs without actually playing an integral structural role. Of course, most antibodies to MAP2 react in the projection-arm region (Kosik et al., 1984; Brion et al., 1985; Dammerman et al., 1989), and the well known proteolytic susceptibility of MAP2 (Vallee and Borisy, 1977; Vallee, 1980; Flynn et al., 1987a) may result in the removal of these projection-arm epitopes from AD NFTs, leaving behind the weakly immunogenic MAP2 MT-binding region. A second explanation for the failure to identify MAP2 thus far in NFTs is that while MAP2 may be present in NFTs, perhaps even as an essential component in their assembly, the concentrations of MAP2 may have been below the detection limits of previously employed methods. The work of the Wischik lab focused on two major polypeptides in pronase-treated PHFs lab (Wischik et al., 1988), but their approach would not have detected components amounting to 5-15% of the total polymer mass. Third, one cannot exclude the possibility that a small pool of MAP2-enriched NFTs in one or more regions of the brain may be obscured by whole brain tissue sampling. There is no proof that NFTs present at various sites in AD brain are of uniform composition. Finally, MAP2 may be selectively depleted or removed after initial NFT assembly *in vivo* or during the multi-step isolation and analysis of Alzheimer filaments.

Because there is no compelling reason why Tau and not MAP2 is involved in Alzheimer disease and because MAP2 is plentiful in cell bodies and dendrites, one must consider the possibility MAP2 can likewise polymerize into paired helical filaments or straight filaments. Moreover if MAP2 were to form straight filaments and if the straight filaments were more rapidly degraded than paired helical filaments, MAP2 may have a role in the early course of Alzheimer disease that is not in evidence at later times during neurodegeneration. MAP2 should be studied to determine if it is present in any of the dozen disorders characterized by neurofibrillary tangle formation, and if it is not, then it is

important to describe the mechanisms that prevent its incorporation into filaments. The purpose of this study was to learn what polymerizing properties MAP2 does have and to begin to understand what variables may control how MAP2 assembles into filaments. The project began by testing MAP2 under a variety of conditions known to promote the assembly of Tau *in vitro* and ends with a demonstration that MAP2 can assemble into paired helical filaments when slightly modified.

The polymerization properties of different recombinant MAP2 fragments and full-length MAP2c were first examined in this project. The structures of these MAP2 polymers were compared to those filaments found in Alzheimer disease and those that formed *in vitro* with purified and recombinant Tau. The ability of MAP2 filaments to extend from Alzheimer paired helical filaments and to bind the Alzheimer diagnostic marker thioflavin S was also demonstrated in a group of experiments that characterized several similarities between MAP2 and Tau filaments. Since recombinant Tau-123 had been shown to assemble in a process that was favored upon disulfide cross-linked dimer formation, the role of MAP2 disulfide cross-linked dimer formation in polymerization of MAP2 filaments was investigated using nonreducing SDS-PAGE, analytical ultracentrifugation and mutants of MAP2 where the lone cysteine was converted into an alanine. The ability of polyglycosaminoglycan and RNA to stimulate polymerization of recombinant Tau had been recorded; and if these agents do act in Alzheimer disease development, then it was important to know how MAP2 was affected by these polyanions. Finally, since MAP2 and Tau have 70 % preservation of primary sequence in the repeat region of the microtubule-binding region, experiments were done to identify the minimal number of mutations needed to convert MAP2-123 into a protein with the assembly properties of Tau-123. The results from these experiments indicated that certain amino acids in MAP2 may prevent it from forming paired helical filaments, and they also suggested that certain courses of action may be beneficial in understanding normal and pathological Tau behavior.

CHAPTER 2
IN VITRO POLYMERIZATION OF EMBRYONIC MAP2C AND FRAGMENTS OF THE MAP2 MICROTUBULE-BINDING REGION INTO STRUCTURES RESEMBLING ALZHEIMER FILAMENTS

Introduction

Neurofibrillary tangles, a histological feature characteristic of Alzheimer disease, are a dense accumulation of paired helical filaments and straight filaments with many associated proteins (Kidd, 1963). Although other cytoskeletal proteins are associated with the neurofibrillary tangles, the microtubule-associated protein Tau now is generally accepted to be the principal structural component of the paired helical filaments and straight filaments (Wischik et al., 1988). Tau and MAP2 are highly abundant in brain tissue where they stabilize microtubules and suppress dynamic tubulin dimer exchange resulting from catastrophic microtubule disassembly. In adults Tau is the predominant axonal MAP whereas MAP2a and MAP2b are found in the dendrites and perikaryal regions (Hall, 1994). MAP2 cross-links microtubules to one another as well as to microfilaments, intermediates filaments and vesicular components (Hirokawa et al., 1982; Hirokawa et al., 1988). A shared structural motif in these MAPs is a trio or quartet of non-identical 31-amino acid repeats in the microtubule binding region, and synthetic octadecapeptide repeat analogues to the repeats can directly promote tubulin polymerization and block MAP binding to microtubules (Joly et al., 1989; Ennulat et al., 1989; Joly and Purich, 1990).

Previously, it has been shown that recombinant fragments of Tau containing three not four repeats polymerized into a variety of structures including some that resemble Alzheimer paired helical filaments (Crowther et al., 1992; Wille et al., 1992; Schweers et al., 1995). The Mandelkow lab reported conditions where a purified Tau fragment of 122 amino acids from Q244 to Y394 termed Tau-K12, polymerized at concentrations from 500

μM to 2 mM of protein when incubated in 500 mM Tris (pH 5.0 - 5.5) for 4 weeks (Wille et al., 1992). For reasons presented in the introduction, they could not quantify the proportion of each type of filament they observed, but they reported that most of the filaments were smooth with a length from 200 to 1000 nm. In addition to these, some showed periodicity in width from 8 nm to 15 nm with a crossover distance of 70 - 75 nm, and they observed many short rod-like particles resembling bowties with a length of 80 - 150 nm. The filaments tended to aggregate, and they could not discern any fine axial structure. At the same time, the Crowther lab demonstrated that a shorter 99 amino acid long fragment of Tau from position M250 to R379 could polymerize in 600 mM Tris (pH4.5 - 5.0) in a vapor diffusion, hanging-drop apparatus (Crowther et al., 1992). They reported observing many types of filamentous structures including smooth filaments equal in diameter to a half of a paired helical filament, coiled ribbon-like structures, thin short filaments and some resembling Alzheimer paired helical filaments. This last group of structures varied in width from 5nm to 16 nm with a crossover distance of 70 - 90 nm, and they believed that some fine structure as observed in Alzheimer filaments, four longitudinal lines of stain exclusion, were observable in some filaments. Earlier, investigators had shown that Tau purified from cycled microtubules preparations could form filaments (Montejo de Garcini et al., 1986; Montejo de Garcini and Avila, 1987; Montejo de Garcini et al., 1988), but these experiments from the Crowther lab were the first to use recombinant Tau in filament assembly assays. This Tau is all in the unphosphorylated state. With no animal or cellular models available, this means solution conditions can be modified to test the ability of different agents in promoting filament assembly without having to deal with the heterogeneity of purified Tau.

Evidence for the association of MAP2 with neurofibrillary tangle formation in Alzheimer disease is less than convincing. While antibodies directed against MAP2-specific epitopes do bind to neurofibrillary tangles in autopsy brain tissue from Alzheimer patients (Nukina and Ihara, 1983; Kosik et al., 1984, 1988; Neve et al., 1986; Yen et al.,

1987; Mulvihill and Perry, 1989; Dammerman et al., 1989), no direct biochemical connection of MAP2 to paired helical filament formation has ever been reported. The striking conservation of primary structure within the microtubule-binding regions of MAP2 and Tau stimulated this investigation of the polymerization properties of the MAP2 microtubule-binding region of MAP2. There is greater than 65% primary sequence preservation in the microtubule-binding regions of MAP2 and Tau with over 70% preservation of sequence in the region containing the three repeats (Figure 2-1). This project began with the expectation that fragments of MAP2 would not polymerize, and the goal was to identify the minimal set of site-directed mutations needed for MAP2 to assemble into paired helical filaments. The work described here details the assembly properties of fragments of MAP2 corresponding to the microtubule-binding region and also embryonic MAP2c.

Materials and Methods

Materials

Synthetic single-stranded oligonucleotides for cloning and mutations were made by Genemed Synthesis Incorporated, and cDNA products were ligated into the pETh-3b vector for cloning and expression. This vector was a derivative of pBR-322 and was a gift from Dr. Donald McCarty at the University of Florida. Invitrogen One Shot competent cells or DM1 competent cells from Gibco-BRL were used for cloning, and E. coli BL21 (DE3) pLYS S competent cells from Novagen were used for protein expression. Agar, tryptone and yeast extract were obtained from DIFCO Laboratories. Tris base, sodium acetate, phenylmethylsulfonyl fluoride, dithiothreitol, sodium dodecylsulfate, ampicillin, magnesium chloride, 2- (N-morpholino) ethanesulfonic acid, DNase (#5025), sodium chloride, Folin reagent, thioflavin S and isopropyl-β-thiogalacto-pyranoside were from Sigma Chemical Company. DNA high melt agarose, Wizard Minipreps, dNTPs, Lambda DNA markers and certain restriction enzymes were obtained the bioproducts division of

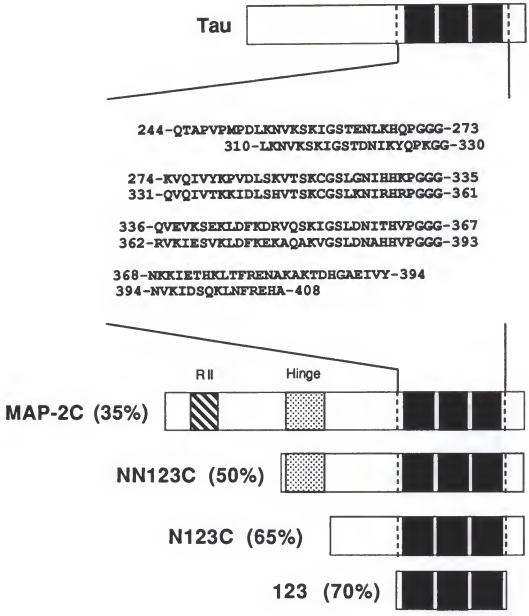

Figure 2-1. Sequence Alignment of Tau-K12 and MAP2-123 and Schematic Representation of the Different MAP2 Constructs. Note the conservation of primary sequence within these microtubule-binding regions.

Fisher Scientific. Most restriction enzymes were purchased from New England Biolabs while T4 DNA ligase, Taq DNA polymerase and chloramphenicol were purchased from Boehringer-Mannheim. FPLC materials including HiTrap SP disposable columns and Sephaglass Bandprep kits were obtained from Pharmacia. Microcon, Centricon and Centriprep devices for protein sample concentration were made by Amicon. Whatman Corporation provided the P11 phosphocellulose, and Coomassie Brilliant Blue R 250 was from Crescent Chemicals. Sitting bridge crystallization cells and ancillary material for polymerization experiments were obtained from Hampton Research. Purified paired helical filament preparations from Alzheimer brain tissue were a generous gift from Dr. Peter Davies at Albert Einstein University.

Clones for bacterial expression of recombinant proteins were obtained as followed. All the MAP2 fragments and embryonic MAP2c were cloned earlier by different members of the lab (Coffey et al., 1994; DeTure et al., 1996). The MAP2c was cloned from rat brain poly(A)-RNA using reverse transcription and the polymerase chain reaction. Amplified cDNA was cloned into the expression vector pETh-3b using the 5' NdeI site and the 3' HindIII site. The fragments of MAP2 coding for various portions of the microtubule-binding region were obtained from a bovine brain cDNA library clone that contained the sequence from positions 1508-1828 which is the carboxy-terminus of MAP2 that is common to all the three-repeat isoforms. This cDNA fragment, MAP2-NN123C, was cloned into pETh-3b using the 5' NdeI site and the 3' EcoRV site. In addition, clones corresponding to the microtubule-binding region starting after the thrombin cleavage site between positions 1628 and 1629 to the carboxy-terminus at position 1828, MAP2-N123C, and a fragment of the protein from positions 1671-1770 containing only the repeat region, MAP2-123, were subcloned into the pETh-3b vector. There are only several conservative amino acid differences in the microtubule-binding regions of bovine and human MAP2, and the sequences for bovine and human MAP2-123 which contain the three nonidentical repeats are identical.

The Tau-N123C, Tau-K12 and Tau-123 expressed for use as positive controls in the experiments presented in this dissertation were all subcloned from a cDNA isolated by reverse transcription and polymerase chain reaction from total RNA isolated from retinoic acid-differentiated human NT2 cells from Strategene. The original cDNA corresponded in sequence and identity to the longest Tau isoform that contains two amino-terminal inserts and a fourth repeat sequence inserted between the first and second repeat of three-repeat Tau found by the Goedert lab (Goedert et al., 1992). This DNA was amplified for cloning into the pETh-3b plasmid using a sequence-specific 5' primer which contains an NdeI site and a sequence-specific 3' primer which contains an EcoRI site. The PCR product was then introduced into the 5' NdeI site and the 3' EcoRI site of the pETh-3b plasmid which positioned it in frame for bacterial expression. From this full-length Tau clone, three-repeat Tau with the two amino terminal inserts was generated using a four primer PCR scheme with internal primers that contained sequence on both sides of the 93 base pair sequence to be removed. This allowed the front 5' portion of Tau to be amplified up to the deleted region, but the product contained some sequence on the other side of the deleted sequence. Concurrently, the rear 3' portion of Tau was amplified up to the deleted region, and it to contained sequence on the other side of the deleted sequence. The products from these two reactions were gel purified and used as template in a PCR reaction containing the 5' and 3' primers described above. The product from this reaction was a cDNA coding for full-length, three-repeat Tau which could be inserted into the NdeI and EcoRI sites of the pETh-3b plasmid. From this clone, constructs corresponding to MAP2-N123C, MAP2-123 and Tau-K12 were made by PCR with sequence-specific primers which allowed for cloning into the pETh-3b vector. Each of these was sequenced by the ICBR DNA sequencing core at the University of Florida.

Bacterial Expression and Purification of MAP2 and Tau Fragments

MAP2 and Tau fragments were expressed and purified using a modified version of the protocol based on the heat stability and cationic nature of the MAPs (Coffey et al.,

1994). For expressing proteins, cDNAs in the pETh-3b vector were transformed into E. coli BL21 (DE3) cells. Overnight cultures of 10 mL of these cells were used to inoculate one liter cultures of LB media containing 50 µg/mL of ampicillin and 34 µg/mL of chloramphenicol. The cells were grown at 37 °C until the cultures reached an OD-600 of 0.4 - 0.5 at which time they were induced by bringing the media to 0.5 mM IPTG. This agent allows the bacterial gene expression of T7 RNA polymerase which then binds the T7 promoter found upstream of the cloned cDNA. This resulted in massive transcription and translation of the cDNA of interest.

After 2 hours of protein expression the cells were harvested by centrifugation at 5,000 x g for 5 minutes. The cells were then washed by resuspending them with ice-cold 1 x MEM buffer (100 mM MES, 1 mM EGTA and 1 mM $MgCl_2$ at pH 6.8) and pelleting again at 5,000 x g for 5 minutes. Bacteria from one liter of culture were resuspended in 18 mL of cell lysis buffer (100 mM Tris, 50 mM NaCl, 1 mM $MgCl_2$, 1 mM PMSF, 20 units/mL DNase and 1 mM DTT) and sonicated with a Branson Model 450 Sonifier at 20 watts output at 80 % for two two-minute sessions on ice. This step lysed the cells and fragmented the DNA. This sample was then made to be 500 mM NaCl with the addition of two mL of 5 M NaCl and was heated at 80 °C for 10 minutes before being placed on ice for 20 minutes. The solution was then freed of denatured, aggregated proteins by centrifugation at 40,000 x g for 20 minutes. The supernatant from this spin contained mostly heat-stable MAP2 or Tau fragments in high salt. The sample was diluted with water to bring the salt concentration below 150 mM NaCl before loading it onto a 1mL phosphocellulose column equilibrated in 1 x MEM. The sample was loaded by gravity, and the column was washed extensively with 10 mL of 1 x MEM. The sample was eluted with 1 x MEM containing 1 M NaCl and 1 mL fractions were collected. The fractions with and OD-280 above 0.1 were pooled and then dialyzed into 3 x 200 volumes of 100 mM Tris at pH 6.8 for 16 hours. These samples were then processed directly in filament assembly reactions or aliquoted and frozen at - 20 °C. Sample purity was confirmed by

SDS-PAGE, and the molecular weights of the polypeptides was verified by matrix-assisted laser desorption mass spectroscopy. Some samples contained lower-molecular-weight bands, presumably formed by incomplete translation or proteolysis (Zhang, 1997). These samples were further purified on a FPLC using High Trap SP columns to collect the sample and a 0 - 400 mM NaCl gradient to elute the samples. This additional processing was only necessary for MAP2c.

In Vitro Assembly of Filaments

Samples in 100 mM Tris at pH 6.8 were approximately 1-2 mg/mL after the purification and dialysis steps. According to the Mandelkow lab, concentrated samples of Tau-K12 from 5-10 mg/mL polymerized best. Below 5 mg/mL, assembly did not occur reproducibly (Schweers et al., 1995). Samples were concentrated approximately 10 x in a Centricon apparatus with a molecular weight cutoff of 3 kDa. A modified Lowry was then done to determine the concentration of the MAP samples (Coffey and Purich, 1994). Buffers were then changed to 200 mM Tris-HCl and 200 mM sodium acetate (pH 6.8) by diluting with 0.6 M Tris-HCl and 1.0 M sodium acetate (pH 6.8). Aliquots of 20 µL were placed in a sitting-bridge crystallization cells, and the bridges were kept in sealed vapor equilibrium chamber containing 1 mL of 0.6 M Tris-HCL and 1.0 M sodium acetate (pH 6.8) at room temperature for 1-6 weeks.

Electron Microscopy

Carbon-coated grids were prepared by coating 400-mesh copper grids with grid glue (i.e. 1 inch Scotch tape washed into 10 mL chloroform) to ensure proper adhesion of carbon films onto the grids. Carbon films created by vapor adsorption of elemental carbon onto mica strips were floated on water and then picked up with copper grids. These carbon-coated grids were prepared freshly for each microscope session. Sample was adsorbed on to the grids by floating a grid on a drop of sample for 30 seconds. The nonadsorbed sample was then wicked off and the grid was negatively stained by floating it on a drop of 1 % uranyl acetate or 1 % phosphotungstic acid for 30 seconds. Grids were

examined after 15 minutes on a Hitachi H-7000 transmission electron microscope at 75 kV. For polymer length measurements, digitally scanned images were analyzed using Image-1 software (Universal Imaging Inc.).

Fluorescence Spectroscopy

Binding of thioflavin S to paired helical filaments in Alzheimer neurofibrillary tangles has traditionally been used as a diagnostic marker to confirm the disease on post mortem brain samples. The dye is known to exhibit a characteristic fluorescence at 480 - 490 nm when bound to Alzheimer paired helical filaments and filaments formed *in vitro* from recombinant Tau fragments (Schweers et al., 1995). Binding of thioflavin S to polymers of recombinant MAP2 fragments or MAP2c was monitored by the change of extrinsic fluorescence of the dye using a Photon Technology International model A1010 photon-counting spectrofluorimeter. Samples were prepared at concentrations from 1 - 27 μM with each containing 0.65 μM thioflavin S. The excitation wavelength was set at 440 nm, and the emission spectra was recorded from 460 - 550 nm. The spectrum of thioflavin S alone was used as a control in each experiment and gave no emission peak in the 460 - 500 nm range.

Results

In the absence of any report demonstrating the polymerization of MAP2 into structures resembling Tau polymers, researchers could readily dismiss the relevance of MAP2 in neurofibrillary tangle formation. To determine whether sequence differences in the microtubule binding regions of MAP2 and Tau prevented MAP2 from polymerizing into rod-like particles, ribbons, coils straight filaments and paired helical filaments found with recombinant Tau-K12 and Tau-123, recombinant MAP2-N123C and MAP2-123 were incubated under conditions permitting oxidation and known to promote Tau-K12 and Tau-123 assembly (Crowther et al., 1992; Schweers et al., 1995). Tau and MAP2 possess structurally related microtubule-binding regions that are similar but not identical (Figure 2-

1). Our 100-amino acid fragment MAP2-123 includes the first, second and third nonidentical repeats found in three-repeat MAP2. Like the 99-amino acid Tau-123 fragment used by the Crowther lab and the 122-amino acid Tau-K12 fragment used by the Mandelkow lab, MAP2-123 contains a single sulfhydryl group in the middle of the second repeat positioned analogously to that found in the Tau fragments. As reported by the Mandelkow lab, oxidation of this thiol promotes the polymerization process, and for this reason no reducing reagents were incorporated into the assembly buffers. Wells containing 20 μL aliquots of 1 mM MAP2-123 were prepared and allowed to incubate at room temperature. Each day, the samples were examined by electron microscopy to determine if polymerization had occurred. Upon incubation of the sample for a period of 5 days or longer, the MAP2-123 fragment formed a viscous gel, suggesting that aggregation and/or polymerization had occurred.

Assembly Properties of MAP2-123

Examination of this material by electron microscopy using uranyl acetate as a negative contrast stain for polymeric species revealed that massive assembly of the MAP2-123 fragment had occurred, and numerous, long filaments are observed in the electron micrographs (Figure 2-2 a-d). The measured polymer length distribution gives a mean length of 350 nm (Figure 2-3). This is probably an underestimate because filaments not completely contained in the micrograph and those broken by mechanical shearing during sample preparation would result in a lower reported length. These filaments appear to be uniform in diameter with very little, if any, modulations in width, and measurements from 40 sample filaments gave an average width of 8.7 nm $\pm$ 1.0 nm. The filaments do not seem to aggregate and are similar in diameter to pronase-treated straight filaments or longitudinally split paired helical filaments from Alzheimer patients which are known to have a diameter of 12-15 nm or 10-12 nm respectively. The differences between longitudinally split filaments which supposedly represent half of a paired helical filament and straight filaments which have the same mass per length as a paired helical filament are

Figure 2-2. Assembly of MAP2-123 into Straight Filaments. Panel a-d: Filaments assembled in sitting bridge wells for 5 days with 800 μM MAP2-123 in the absence of a reducing agent. They are uniform in diameter with an average width of 8.7 ± 1.0 nm. The bars are 100 nm.

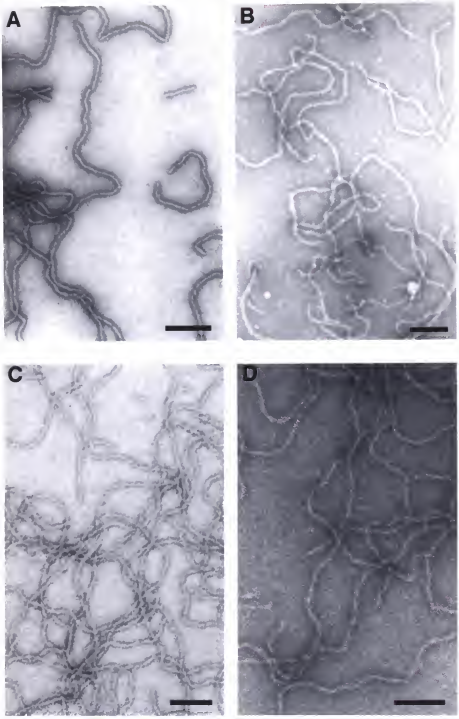
A
B
C
D

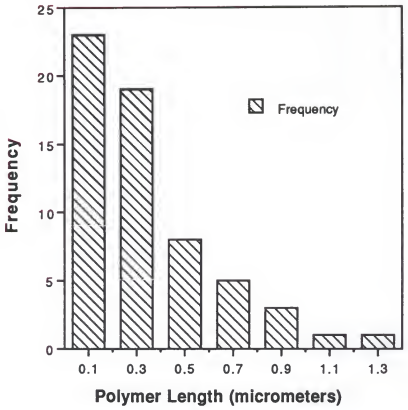

Figure 2-3. The polymer length distribution for MAP2-123 shows the average length to be 350 nm, but this may be an underestimate due to shearing during handling.

difficult to detect by electron micrographs alone, and often no attempt is made to differentiate between these two related filaments which have mostly uniform diameters. The formation of MAP2-123 filaments was quite unexpected, since they had not been isolated as a core component in Alzheimer filaments. Moreover, earlier experiments with MAP2-123 fragments had not generated filaments under conditions that should have promoted the assembly of recombinant Tau (Wille et al., 1992).

Assembly Properties of MAP2-N123C

The demonstration that the repeat region of MAP2 formed filaments resembling Alzheimer straight filaments led to the hypothesis that regions of MAP2 flanking the MAP2 repeat sequences might block the assembly of larger MAP2 fragments. To test this hypothesis, the 203-amino acid residue MAP2-N123C was expressed, purified and incubated in the sitting bridge cells at a concentration of 500 - 1000 μM. This MAP2 fragment has an amino acid sequence that is 65 % identical to the corresponding region of Tau, and MAP2-N123C as well as longer fragments of MAP2 promote microtubule assembly (Coffey et al., 1994). In addition, this piece of MAP2 is equivalent to the portion of MAP2 released upon thrombin digestion of MAP2 (Joly et al., 1989). This MAP2 fragment is 81 residues longer than the Tau-K12 which is the longest recombinant isoform that still polymerizes well. That is Tau-K12 polymerizes at lower concentrations, in less time than the full-length Tau proteins. After 5 days, the samples were neither viscous nor did they contain filaments when viewed by electron microscopy. These samples were examined every several days, and electron microscopy confirmed the formation of filamentous aggregates after day 17 (Figure 2-4 a-d). Like the filaments from MAP2-123, these polymers were very uniform in width although their diameter was slightly larger at 10.6 nm $\pm$ 1.0 nm. The appearance of individual filaments resembled those formed by MAP2-123, but as a whole they were not well dispersed.

Figure 2-4. Assembly of MAP2-N123C into Straight Filaments. Panels a-d: MAP2-N123C was incubated at 800 μM for 3 weeks in sitting bridge wells before these straight filaments were observed. They tended to form loose aggregates, and the filaments had an average diameter of 10.6 ± 1.0 nm. The bars are 100 nm.

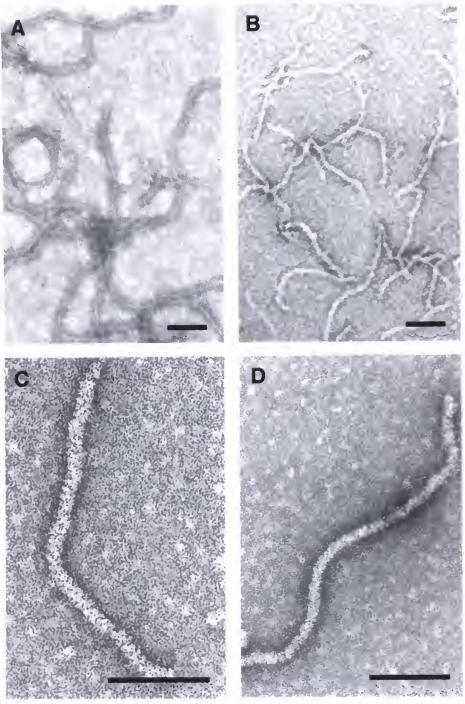
A
B
C
D

Assembly Properties of MAP2-NN123C

MAP2-NN123C is a 320-amino acid MAP2 fragment originating near the MAP2c splice site and containing the entire microtubule-binding region. It is nearly equivalent in length to the portion of MAP2 generated by chymotrypsin digestion of MAP2 (Vallee, 1980), and this polypeptide promotes microtubule assembly slightly better than MAP2-N123C (Coffey et al., 1994). Compared to the corresponding segment of Tau, this fragment of MAP2 shares only 50 % sequence identity meaning the projection arm extending away from the repeat region is very different from that observed in Tau, and perhaps it blocks MAP2 assembly into filaments. This portion of MAP2 was examined using the same protocol as before, and filaments were observed by electron microscopy after 3 weeks (Figure 2-5 a-b). Similar to those filaments formed by MAP2-N123C, these filaments tended to clump and resembled straight filaments, showing very little modulation in width. These filaments were slightly larger in diameter at 11.8 nm $\pm$ 1.4 nm. The striking difference between these filaments and those formed by MAP2-123 and MAP2-N123C was the occasional appearance of a short, straight filament with an apparent width nearly twice that of the plentiful straight filaments (Figure 2-5 c-d). These structures were not paired helical filaments, but their appearance did demonstrate for the first time the ability to form more than one type of polymeric species. Again, these experiments could not demonstrate that areas outside the repeat region blocked assembly, and really appeared to show that a naturally occurring proteolytic fragment of MAP2 could assemble into straight filamentous structures.

Assembly Properties of MAP2c

MAP2c is typically described as an embryonic form of MAP2, but it is expressed in the adult olfactory bulb and retina where stem cell differentiation into neurons continues into adulthood (Tucker et al., 1988; Viereck et al., 1989). This is important as the phosphorylation patterns of these cells are similar to those observed during neuronal development, and certain phosphorylated Tau epitopes are supposedly generated by these

Figure 2-5. Assembly of MAP2-N123C into Two Types of Straight Filaments. Panel a-b: MAP2-N123C assembled into straight filaments with a width of 11.8 $\pm$ 1.4 nm when incubated under the same conditions used for MAP2-N123C. Panel c-d: The majority of the filaments formed with MAP2-NN123C were of the type shown above, but some formed that were nearly twice the diameter. This is the only wildtype MAP2 fragment which form anything other than narrow straight filaments. The bars are 100 nm.

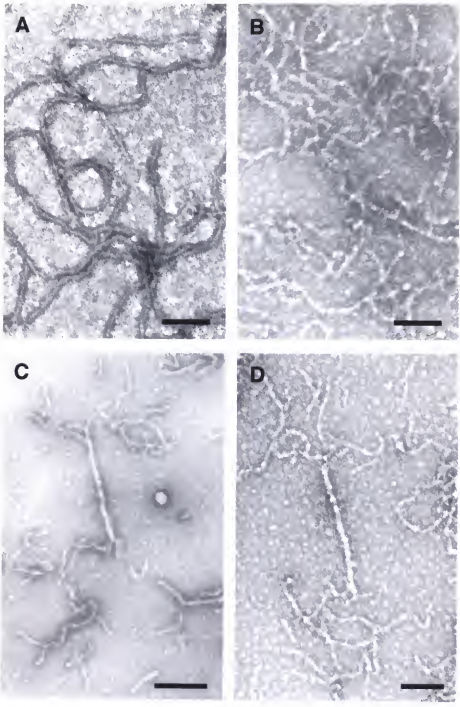
A
B
C
D

same kinases. Taken with observations that Alzheimer patients have abnormal olfactory function as an early symptom (Talamo et al., 1989) and the abnormally high neuronal loss in the retina (Blanks et al., 1996), this information indicates the importance of studying MAP2c assembly. At 150 amino acids longer than MAP2-NN123C, MAP2c only shares only a 35 % sequence preservation with Tau, and their projection arms are completely different. This MAP2 isoform polymerized in 3 weeks, and it represented the first demonstration that a naturally occurring, full-length form of MAP2 could assemble into filaments (Figure 2-6 a-d). All of MAP2c filaments examined were of the straight filament type with an average diameter of 12.4 nm $\pm$ 1.2 nm, and no filaments were observed to be of the twice width variety. These observations indicated that the projection arm of MAP2c does not prevent the assembly process.

Solution Conditions that Permit MAP2-123 Assembly

After demonstrating that MAP2c and fragments of MAP2 were assembly-competent, experiments were undertaken to determine which solution variables allowed polymerization of MAP2-123. This fragment was chosen as it polymerized the fastest and the filaments did not appear to aggregate. The filament dispersion of MAP2-123 was an advantage as aggregation tends to blow out the carbon films even when the samples are diluted, and it is easy to miss the clumps of filaments unless they are just small enough to leave the film intact. Still accurate quantitation of the extent of polymerization is risky as discussed in the introduction, and here only the simple observations that filaments assemble or do not is made. During the first several sets of experiments with MAP2-123, assembly solutions with various pHs were tested. The pH range examined varied from 6.0 to 7.5, and the filaments look identical to those presented earlier (Figure 2-7 a-b). Likewise, the addition of salt to the sample had little effect on the polymerization of MAP2-123, and NaCl concentrations as high as 500 mM did not block assembly (Figure 2-7 c-d). The formation of MAP2-123 filaments was not completely unexpected as the assembly buffer is

Figure 2-6. Assembly of MAP2c into Straight Filaments. Panels a-d: MAP2c was the first native MAP2 isoform shown to polymerize. It did not assemble as well as the shorter MAP2 isoforms containing the microtubule-binding region under the same conditions, but the filaments did resemble those found with the shorter MAP2 constructs. The average diameter of the filaments was 12.4 ± 1.2 nm and none were observed that were substantially wider. The bars are 100 nm.

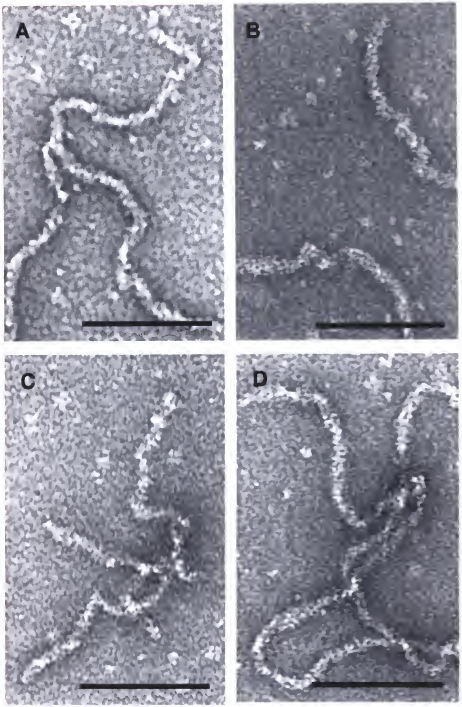
A
B
C
D

at relatively high ionic strength, and it becomes more concentrated as the incubation proceeds. Additionally, it was demonstrated that MAP2-123 polymerized in 100 mM Tris at pH 6.8 in a closed system at 37 ° C where the protein and salts did not become more concentrated (data not shown).

The most interesting variable was the protein concentration of MAP2 fragments needed for assembly. Several labs working on the polymerization of recombinant Tau had observed that incubations of at least 3 weeks and at concentrations greater than 500 μM were necessary for *in vitro* polymerization (Wille et al., 1992; Crowther et al., 1992; Crowther et al., 1994; Schweers et al., 1995) They had observed that the full-length three and four-repeat recombinant Tau polymerized poorly, suggesting that the additional sequences were suppressing polymerization. The experiments with MAP2 fragments had also suggested that sequences flanking the repeat region interfered with polymerization, and, like Tau, they appeared to retard filament assembly. Experiments in sitting-bridge crystallization cells were undertaken with protein concentrations of MAP2-123 ranging from 100 - 400 μM. All samples polymerized in less than 10 days, and more bridges were prepared with concentrations ranging from 5 - 50 μM. These samples also polymerized within two weeks (Figure 2-8 a-b), and the resulting filaments resemble those formed at higher concentrations. These results indicated that MAP2-123 polymerizes more readily than Tau-123, because lower concentrations of protein and shorter incubation times are required. These experiments were followed by looking at the concentration requirements for polymerization of MAP2-N123C and MAP2-NN123C. These samples had required 2-3 weeks to assemble at high concentrations; and at concentration as low as 10 μM, they assembled into straight filaments resembling those formed at higher concentrations (Figure 2-8 c-f). Apparently MAP2 fragments have the ability to polymerize at physiologically relevant concentration even though they have not been discovered in any of the diseases characterized with neurofibrillary tangles.

Figure 2-7. MAP-123 Assembles into Straight Filaments Under Varying Conditions. Panel a: At pH 6.0 MAP2-123 assembled. Panel b: At pH 7.5 MAP2-123 assembled. Panel c: With 250 mM NaCl added to the assembly buffer, MAP2-123 assembled. Panel d: With 500 mM NaCl Added to the assembly buffer, MAP2-123 assembled. The bars are 100 nm.

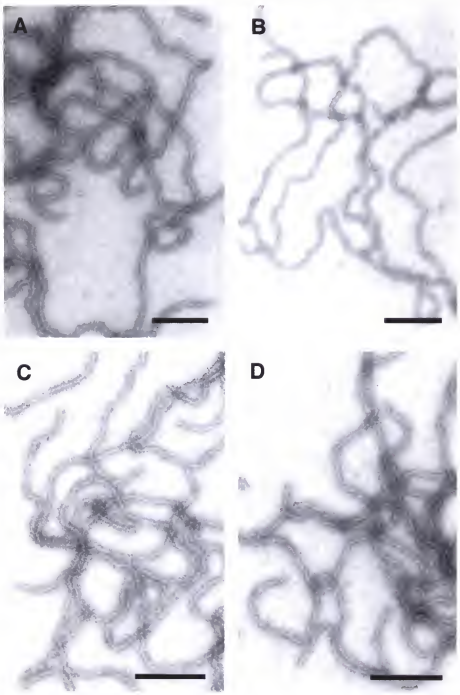
A
B
C
D

Figure 2-8. MAP2-123, MAP2-N123C and MAP2-NN123C Assembles at Concentrations below 50 μM. Panel a-b: MAP2-123 forms straight filaments in sitting bridges at concentrations of 20 μM. Panel c-d: MAP2-N123C also forms straight filaments at concentrations of 20 μM. Panel e-f: MAP2-NN123C forms straight filaments at concentrations of 20 μM too. The bars are 100 nm.

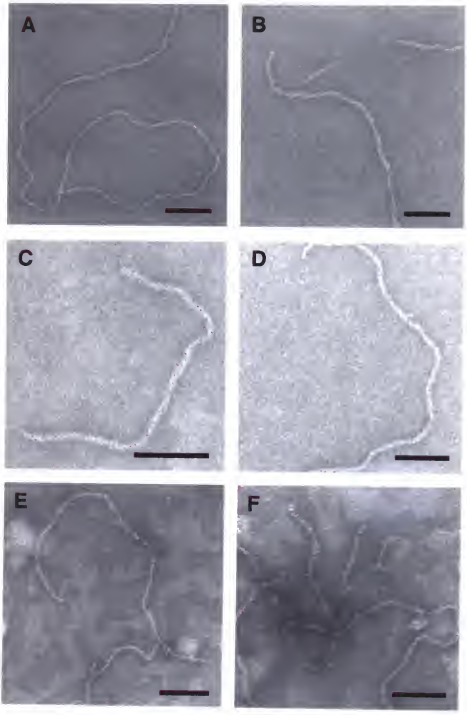
A
B
C
D
E
F

Interactions of MAP2 Filaments with Thioflavin S

Thioflavin S has routinely been used to stain the amyloid plaques and neurofibrillary tangles in the post-mortem confirmation of Alzheimer disease. The Mandelkow lab has reported that polymerized Tau-K12 exhibited dye-binding properties typical of Alzheimer plaques (Schweers et al., 1995), and they demonstrated that the addition of polymerized Tau-K12 to thioflavin S enhanced the fluorescence emission of the dye with a characteristic peak being observed at 480 - 490 nm. To determine if MAP2 polymers also bind thioflavin S, fluorescence measurements at 0, 4, 14 and 27 μM MAP2-123 in the presence of 0.65 μM thioflavin S were recorded. The highest concentration of MAP2-123 corresponds to the only concentration of Tau-K12 used by the Mandelkows. A similar interaction of thioflavin S with polymerized MAP2-123 filaments was observed to give the same characteristic fluorescence at 480 - 490 nm (Figure 2-9). This suggests that the binding interaction with polymers of MAP2-123 closely resembles that recorded for Alzheimer paired helical filaments and Tau-K12 polymers, and the structure of the binding site for thioflavin S on these three types of filaments is very similar. Additional experiments with MAP2-N123C and MAP2c filaments indicated that they also shared the same thioflavin S binding capabilities (DeTure et al., 1996; Zhang et al., 1996), and for all these experiments, examination of the samples after treatment with the dye by electron microscopy confirmed that the MAP2 polymers remained intact (data not shown).

Elongation of MAP2 Fragments from Alzheimer Paired Helical Filaments

Since MAP2c and fragments of MAP2 containing the microtubule-binding region polymerized at physiological concentrations and solution conditions, experiments were done to discover whether these MAP2 filaments were structurally similar enough to Alzheimer paired helical filaments to bind and elongate from these disease structures. The Alzheimer paired helical filaments were used alone as a positive control to ensure that twisting structures could be visualized in our hands (Figure 2-10 a-d), and they provided a means for determining whether the MAP2 filaments were true paired straight filaments or if

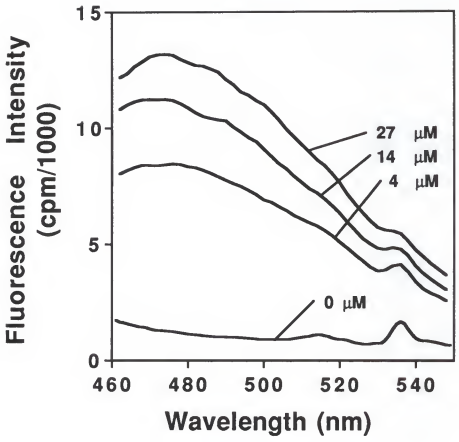

Figure 2-9. MAP2 Filaments Bind the Alzheimer Diagnostic Dye Thioflavin S. MAP2-123 at varying concentrations in the presence of 0.65 μM thioflavin S fluoresces at 480 - 490 nm when excited at 440 nm.

they were equivalent to longitudinally split paired helical filaments. These results confirm that the MAP2 filaments do not twist, and they suggest that they are structurally equivalent to half of a paired helical filament although ambiguous use of these terms in the literature implies it is accurate to still call them straight filaments.

The ability of MAP2 fragments to bind and assemble from Alzheimer paired helical filament seeds is potentially significant, because MAP2 is found in the neuronal cell body during the formation and elongation of Tau filaments in neurofibrillary accumulation. If MAP2 fragments assembled from Alzheimer filaments, then they must be structurally related and are likely to share common binding surfaces. In fact, purified Tau also assembles from Alzheimer paired helical filaments as 10 nm straight filaments that do not twist (Wilson and Binder. 1997). Nevertheless, these seeded assembly results cannot be regarded as evidence that MAP2 will be found as a component of the filament cores or that MAP2 is incorporated into Alzheimer filaments. This data suggested that MAP2 fragments were capable of modulating formation of Alzheimer filaments, but there probably are other factors that may control Alzheimer filament assembly. These molecules may competitively inhibit binding of Tau to an elongating filament, and may mediate filament growth if they must be removed before Tau can assemble from the end of a filament. MAP2-123 at a concentration of 40 μM was incubated in the presence of 0.4 μM Alzheimer filaments for 1 week as described before. Examination of the samples showed that all the wider Alzheimer seeds were associated with straight filaments when the filaments were present at high number concentration, but one cannot directly determine whether the seeds were resting on top of a straight filament mass or if the filaments grew from the seeds. However, when Alzheimer seeds were found in isolation, it was observed that MAP2 filaments grew from both ends of the seeds (Figure 2-11 a-d). This finding was confirmed for MAP2-N123C and MAP2-NN123C (Figure 2-11 e-g), and in no instances were filaments observed to cross the longitudinal axis of the seeds. When observed by electron microscopy, they

Figure 2-10. Electron Micrographs of True Alzheimer Paired Helical Filaments. Panel a-d: Paired Helical Filaments Purified from Alzheimer Tangles by Peter Davies at Albert Einstein University. This data suggest the MAP2-123 filaments are equivalent to half of an Alzheimer paired helical filament. The bars are 100 nm.

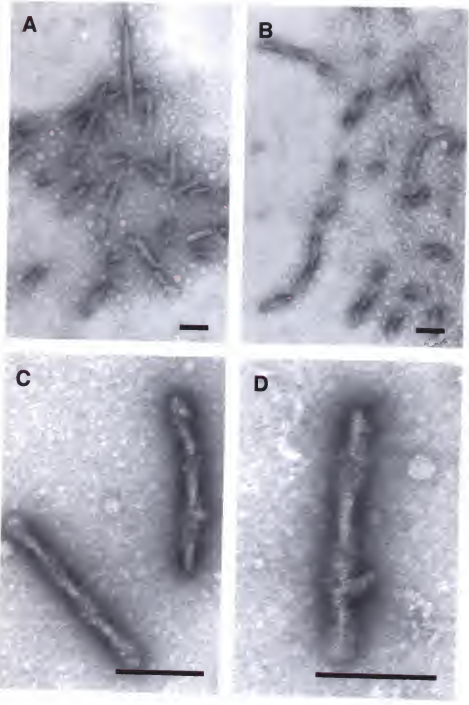
A
B
C
D

Figure 2-11. Elongation of MAP2 from Alzheimer Paired Helical Filaments. Panels a-d: MAP2-123 at 40 μM assembled from the ends of an Alzheimer paired helical filament 0.4 μM when incubated together under MAP2-123 assembly conditions. Panel e-f: MAP2-N123C assembled from Alzheimer seeds. Panel g: MAP2-NN123C assembled from Alzheimer seeds. The bars are 100 nm.

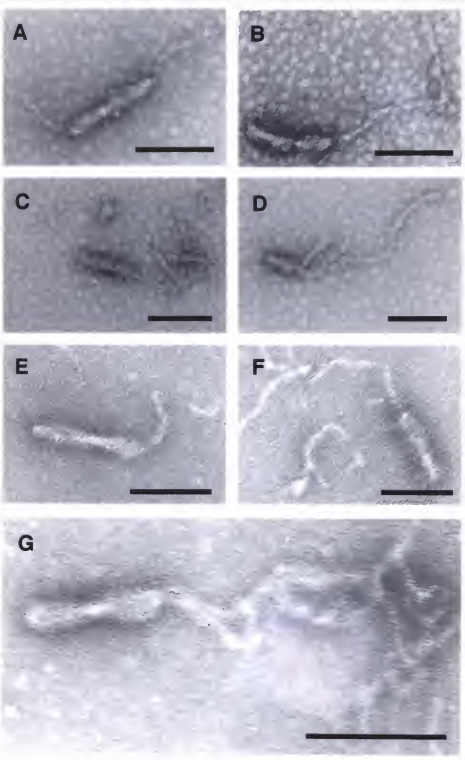
A
B
C
D
E
F
G

always emanated from the ends of the PHFs which suggests that MAP2 may modulate Alzheimer filament growth *in vivo*.

Assembly of Tau-123, Tau-K12 and Tau-N123C

Because neither the quantitation of the types of structures formed with recombinant Tau nor the rates that different Tau isoforms assemble have not been reported. Tau-123, Tau-K12 and Tau-N123C were cloned, expressed, purified and incubated under conditions known to stimulate assembly (Wille et al., 1992; Crowther et al., 1992; Schweers et al., 1995). This was done to obtain first hand knowledge of Tau assembly *in vitro*. The samples Tau-123, Tau-K12 and Tau-N123C each assembled at concentrations from 500 - 1000 μM, and they did form straight filaments, coiled filaments and some paired helical filaments (Figure 2-12 a-h). The samples tended to aggregate making visualization on the electron microscope difficult. The majority of the filaments formed and observed were of the straight filament type and their abundance may have obscured the identification of paired helical filaments. These Tau fragments do not polymerize as readily as MAP2-123, and this makes the absence of MAP2 in Alzheimer tangles more perplexing.

Discussion

These experiments demonstrated for the first time that full-length MA2C and fragments of MAP2 containing the microtubule-binding region assembled *in vitro* into filaments that share certain characteristics with filaments from Alzheimer neurofibrillary tangles. While the core structure clearly contains Tau protein (Wischik et al., 1988), there is no compelling evidence that Tau is the exclusive building block of paired helical filaments in Alzheimer disease. In fact, earlier researchers observed that antibodies directed against MAP2-specific epitopes bind to neurofibrillary tangles in autopsy brain tissue from Alzheimer patient (Nukina and Ihara, 1983), but cross-reactivity with Tau could not be definitively eliminated. One particular monoclonal antibody to MAP2 was especially effective in staining neurofibrillary tangles found in areas of Alzheimer disease brain

Figure 2-12. Filaments Assembled from Tau-123. Panel a-h: Various structures are observed by electron microscopy when Tau-123 is incubated at 500 - 1000 μM. Many straight filaments are observed as are coils and some twisting filaments resembling paired helical filaments. The bars are 100 nm.

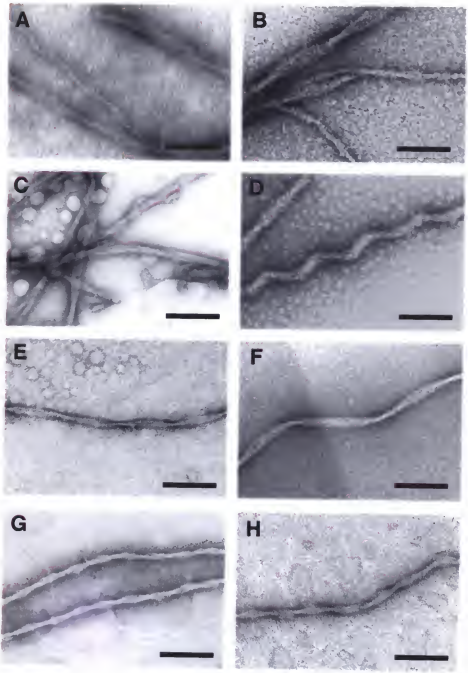
A
B
C
D
E
F
G
H

that tend to be most affected including the perihippocampal cortex and the CA1 region of the hippocampus (Kosik et al., 1984). In addition, polyclonal antibodies raised against MAP2 immunocytochemically stain abnormal, dystrophic neurites around senile plaques in Alzheimer brain (Dammerman et al., 1989). These findings showed that MAP2 is present in cell regions where neurofibrillary tangles accumulate. Now the demonstration that recombinant MAP2 fragments can assemble into Alzheimer-like filaments reproducibly raises the need for additional studies on the role of MAP2 in neurofibrillary tangle formation.

The ability of small Tau polypeptides corresponding to the repeat region to assemble into a myriad of structures suggests that all the information necessary for filament formation is available in the repeat region (Wille et el., 1992; Crowther et al., 1992; Schweers et al., 1995). This demonstration that the microtubule-binding region from MAP2 can assemble into straight filaments leads to the conclusion that the information needed to form straight filaments is found in the repeat sequences. Presumably sequence differences between MAP2 and Tau in this region account for the inability of MAP2-123 to form paired helical filaments *in vitro*. Of course, there may be many different reasons for the accumulation of predominantly paired helical filaments in Alzheimer disease, including factors that promote paired helical filament formation or those which facilitate straight filament degradation.

The assembly of Alzheimer-like straight filaments from full-length Tau purified from cycled microtubules (Wilson and Binder, 1995) and paired helical filaments from full-length recombinant four-repeat Tau (Crowther et al., 1994) has been demonstrated *in vitro*. It may have been expected from these results that features within full-length Tau permits its assembly into paired helical filaments and straight filaments whereas sequences in the projection arm of MAP2 may block the *in vitro* and/or intracellular formation of these types filaments with possible effects on the accumulation of intact MAP2 in such filaments found in Alzheimer disease. The work in this dissertation shows that full-length MAP2c with a

completely different projection arm from Tau assembles into straight filaments which share several characteristics with Alzheimer filaments. This clearly indicates that Tau is not the only naturally occurring MAP polymerized. The repeat region of MAP2, like Tau, contains all the information needed for assembly, and, MAP2c does not possess any assembly blocking region although it may be missing the structures that lead to paired helical filament formation.

Neurofibrillary tangles and amyloid plaques bind the dyes thioflavin S and Congo red, constituting a clinically useful set of markers in diagnosing Alzheimer disease (Inouye et al., 1993; LeVine, 1993). The Mandelkow lab demonstrated that paired helical filaments assembled from Tau-K12 also bind these aromatic dyes. Given the striking conservation of sequence between the Tau-K12 and MAP2-123, the Alzheimer-like filaments formed from MAP2 were also expected to bind these dyes. Binding of thioflavin S to filaments composed of MAP2-123, MAP2-N123C and MAP2c was attended by a characteristic fluorescence enhancement previously reported for thioflavin S interactions with Tau-K12 filaments and Alzheimer paired helical filaments (Schweers et el., 1995). Although this information along with the binding of MAP2 to Tau filaments implies certain structural similarities between Tau and MAP2 filaments, more work will have to be done to determine the motifs present in Tau and MAP2 that are responsible for thioflavin S binding.

The last remarks concern the type of filaments formed by recombinant MAP2 fragments and addresses several explanations for why MAP has not been found in filaments formed *in vivo*. All the MAP2 proteins expressed here polymerized into structures resembling straight filaments, and from the width measurements and experiments demonstrating assembly from an Alzheimer filament seed, it appears that these straight filaments correspond to one half of an Alzheimer straight filament or paired helical filament. The width of the MAP2 filaments agrees with this conclusion, and the seeding experiments clearly demonstrate that the stain exclusion of MAP2 filaments is different from the stain exclusion observed in Alzheimer filaments (Crowther, 1991). If the MAP2 filaments were

true paired straight filaments and not longitudinally split, then they should have the same stain exclusion properties as demonstrated with straight and paired helical filaments isolated from Alzheimer brain tissue (Crowther, 1991). This is not the case; and it would appear that although the repeat region of MAP2 does contain the information needed for filament assembly, it does not contain the primarysequence information necessary for paired helical filament formation.

CHAPTER 3
FORMATION OF AN OXIDIZED DIMER AS A REQUIRED STEP IN THE *IN VITRO* ASSEMBLY OF MAP2C AND MAP2 FRAGMENTS INTO FILAMENTS

Introduction

Early studies examining the *in vitro* polymerization of purified Tau with urea or transglutaminase (Montejo de Garcini et al., 1986; Montejo de Garcini and Avila, 1987; Dudek and Johnson; 1993) and more recent reports on the assembly of recombinant Tau (Wille et al., 1992; Crowther et al., 1992; Crowther et al. 1994; Schweers at. al. 1995) have employed assembly buffers lacking a reducing agent. The lack of reducing agents in assembly buffers presumably was based on the results from studies examining urea-induced polymerization of Tau purified from cycled microtubule preparations. This treatment of Tau presumably lead to assembly through deamination of glutamine residues, but they also speculated that thiol oxidation may be enhanced in the process. Later examination of pronase-treated Alzheimer paired helical filaments demonstrated that three and four-repeat fragments of Tau were in filaments (Jakes et al., 1991) and lead to the identification of fragments including a dimeric species at 27 kDa which could be reduced to a monomeric species at 13 kDa. That oxidizing conditions promoted the polymerization of Tau must have been apparent based on the lack of published results concerning assembly with reducing agents present. Still, it was not until 1993 that the Johnson lab proposed that oxidation *in vivo* may be a contributing factor in Alzheimer development (Troncoso et al., 1993). Since then, evidence suggesting that this may be true has grown significantly, and the polymerization of recombinant Tau has been shown to require intermolecular thiol oxidation (Schweers et al., 1995).

The only group of papers discussing Tau polymerization in the presence of reducing agents employed purified Tau (Wilson and Binder, 1995; Wilson and Binder, 1997). These reports addressed the issues concerning the use of physiologically relevant conditions for assembly. The authors argued that work with recombinant Tau utilizing buffers with acidic pHs, high salt and no reducing agents (Wille et al., 1992; Crowther et al., 1992; Crowther et al. 1994; Schweers at. al. 1995) were not physiologically relevant; and concerning the pH and salt concentration, they may be correct. Their conclusions about the relevant oxidation potential in a neuron were based on the report stating that intracellular reduced glutathione concentrations were between 1-10 mM (Hwang et al., 1992), and during normal times this probably is accurate. During the development of Alzheimer plaques and tangles, the neurons appear to be under oxidative stress (Smith et al., 1991; Benzi and Moretti, 1995; Smith et al., 1995; Pappolla et al., 1996), and cell culture experiments have demonstrated that β amyloid fibrils can cause oxidative stress (Goodman and Mattson, 1994; Mark et al., 1996; Mark et al., 1997). Oxidative stress promotes the formation of disulfide bonds in affected neurons, and presumably Tau-Tau dimerization is more likely than Tau-gluatathione dimerization which could sequester Tau preventing its incorporation into filaments. Oxidizing conditions are physiologically relevant during neurofibrillary tangle formation. The filaments formed in the Binder lab are not paired helical filaments. They are straight filaments with a diameter of 10 nm. These filaments assemble from Tau purified from cycled microtubules, but the do not assemble with Tau from whole brain extracts . The relevance of the conditions used to form these filaments is unclear. There does not seem to be any reason to discount work done under oxidizing conditions; and in fact, they may be more representative of neuronal conditions in tangle bearing neurodegenerative diseases.

The importance of dimerization for the *in vitro* polymerization of Tau K12 was suggested when Tau-K12 monomers were cross-linked with N, N'- p - phenylene - dimaleimide through the sole cysteine in the second repeat. These dimers, like Tau-K12

disulfide linked dimers, assembled into a variety of filamentous structure including paired helical filaments (Wille et al., 1992). The role of the unique cysteine in three-repeat Tau polymerization was further clarified when the reducing agent 2-mercaptoethanol was added to K12 samples for polymerization. Samples with 2-mercaptoethanol assembled eventually, but assembly took longer. The increased time for assembly in the presence of a reducing agent suggests that the reducing agent must be exhausted before assembly (Schweers et al., 1995). Assembly of the Tau-K12 with the cysteine mutated to alanine seemed to confirm the importance of the disulfide linked dimer as polymerization was greatly reduced with this mutant. No mention was made of the type of filaments formed by this mutant, but presumably no paired helical filaments were formed. Assembly of the four-repeat, two cysteine form of Tau-K12, Tau-K11, also did not assemble into filaments, and it was demonstrated by native gel electrophoresis that intramolecular disulfide linkages in addition to intermolecular linkages were formed (Schweers et al., 1995). These disulfide cross-linked monomers were of altered conformation and presumably blocked filament formation. The effects of intramolecular disulfide bond formation in four-repeat Tau was confirmed in experiments with a Tau-K11 mutant where the first cysteine was mutated to alanine. This mutated protein was only capable of forming intermolecular disulfide bonds, and it was assembly-competent forming polymers that resembled paired helical filaments. These experiments indicate that dimer formation is critical in the polymerization process.

Those experimental results lead to this investigation on the role of the disulfide cross-linked dimer in MAP2 assembly. Having demonstrated that the microtubule-binding region of MAP2 formed straight filaments and shared several similar thioflavin S and Alzheimer filaments binding surfaces with Tau, characterizing the role of the unique cysteine in three-repeat MAP2 provided an excellent means of comparing the assembly processes for MAP2 and Tau. In the initial experiments using MAP2-123 for assembly, the conditions used were based on those that stimulated assembly of Tau-K12 and Tau-123

(Schweers et al., 1995). Several solution conditions were varied over a small range to account for the sequence differences between MAP2-123 and Tau-123 and hopefully promote MAP2 polymerization. In these experiments, wells were prepared with and without dithiothreitol (DTT). Those without the reducing agent were found to polymerize in 5 days while those that were incubated with DTT took closer to 2 weeks. These results suggested that a disulfide cross-linked dimer was formed before assembly, and SDS-PAGE gels run in the absence of 2-mercaptoethanol provide evidence consistent with this conclusion. Additionally, experiments were carried out using three-repeat MAP2 where the cysteine was mutated to an alanine, the entire cysteine containing repeat was replaced with the cysteine lacking first repeat or the location of the cysteine-containing second repeat was shifted. The results from these experiments demonstrate the importance of the unique cysteine of MAP2 in filament assembly.

Materials and Methods

Materials

Synthetic single-stranded oligonucleotides for cloning and mutations were made by Genemed Synthesis Incorporated, and cDNA products were ligated into the pETh-3b vector for cloning and expression. This vector was a derivative of pBR-322 and was a gift from Dr. Donald McCarty at the University of Florida. Invitrogen One Shot competent cells or DM1 competent cells from Gibco-BRL were used for cloning, and E. coli BL21 (DE3) pLYS S competent cells from Novagen were used for protein expression. Agar, tryptone and yeast extract were obtained from DIFCO Laboratories. Tris base, sodium acetate, phenylmethylsulfonyl fluoride, dithiothreitol, sodium dodecylsulfate, ampicillin, magnesium chloride, 2- (N-morpholino) ethanesulfonic acid, DNase (#5025), sodium chloride, Folin reagent, thioflavin S and isopropyl-β-thiogalacto-pyranoside were from Sigma Chemical Company. DNA high melt agarose, Wizard Minipreps, dNTPs, Lambda DNA markers and certain restriction enzymes were obtained the bioproducts division of

Fisher Scientific. Most restriction enzymes were purchased from New England Biolabs while T4 DNA ligase, Taq DNA polymerase and chloramphenicol were purchased from Boehringer-Mannheim. FPLC materials including HiTrap SP disposable columns and Sephaglass Bandprep kits were obtained from Pharmacia. Microcon, Centricon and Centriprep devices for protein sample concentration were made by Amicon. Whatman Corporation provided the P11 phosphocellulose, and Coomassie Brilliant Blue R 250 was from Crescent Chemicals. Sitting bridge crystallization cells and ancillary material for polymerization experiments were obtained from Hampton Research.

The cDNA constructs for expressing MAP2-N123C and MAP2-N123C with the cysteine-to-alanine mutation at position 1709 in the second repeat were cloned by previous members of the Purich lab (Coffey et al., 1994) as were the plasmids containing cDNAs for MAP2-N133C and MAP2-N233C. MAP2-N133C has the entire second cysteine-containing 18 amino acid repeat replaced with an additional 18 amino acid cysteine-lacking third repeat at the second repeat position, and MAP2-N233C is the same construct with the cysteine-containing 18-amino acid second repeat reintroduced at the position of the first repeat. Additionally, the shorter analogues MAP2-123 with the cysteine to alanine mutation at position 1709 in the second and MAP2-133 with the second repeat replaced with a copy of the third repeat were made by cassette mutagenesis.

Briefly, the MAP2-123 containing plasmid had been engineered to contain a unique Afl II site at the 5' end of the second repeat and an unique Stu I site at the 3' end of the second repeat (Ainzstein and Purich, 1994). The MAP2-123 plasmid was digested with Afl II and Stu I releasing a small inserted that could be separated from the plasmid by gel electrophoresis. Synthetic oligonucleotides were designed which annealed to one another, coded for the mutations of interest and changed the Stu I site by silent mutation. These oligonucleotides when annealed had a single-stranded overhang on the 5' end which corresponded to the sticky end created by Afl II digestion and a blunt end on the 3' end corresponding to Stu I digestion. This insured the cassette was inserted in the correct

orientation when incubated with the digested and purified MAP2-123 plasmid. Ligations from the mix were transformed into a methylation negative strain of DM1 cells, and colonies were screened by the loss of the Stu I digestion site. Positive colonies were picked and sequenced by the ICBR DNA sequencing core at the University of Florida.

Dimerization of MAP2 Fragments Visualized by SDS-PAGE

Samples of MAP2-123 were incubated in crystallization cells under the conditions used for the filament assembly experiments. On days 1, 2 and 5 samples were removed and prepared for SDS-PAGE by adding sample buffer without reducing agents. The day 5 sample was prepared in duplicate with one sample being incubated with 4 mM dithiothreitol for 1 hour at 37 ° C to reduce disulfide before electrophoresis. The markers used were dye-labeled soybean trypsin inhibitor (27 kDa) and lysozyme (19 kDa), and the gel was 18% cross-linked acrylamide with 0.1% SDS.

Sedimentation Equilibrium Analysis of MAP2

Sedimentation equilibrium runs were performed in the Beckman XLA analytical centrifuge, and data were collected at 0.003 cm increments along the radial axis with UV-visible scans at 280 nm. Two samples were run at identical concentrations differing only that one contained dithiothreitol and one did not. The spectra were taken the first day and did not change over the course of 5 days implying equilibrium had been reached.

Results

The following experiments were performed to determine the role of the disulfide cross-linked dimer in the formation of MAP2 straight filaments. The role of the cysteine in the second repeat has been hinted at by the results of assembly experiments using MAP2-123 in the presence of the reducing agent dithiothreitol. Here straight filaments formed, but they took roughly twice the time to assemble. It was hypothesized that the filaments did not assemble until the reducing agent was exhausted, but the assembly reactions with dithiothreitol did not prove this. Possibly reduced dimers of MAP2-123 did assemble, and

the nucleation or elongation rates were simply diminished. These first experiments simply confirm that disulfide cross-linked dimers of MAP2-123 do form and that their time course of formation is consistent with dimerization being required for assembly.

Demonstration of Disulfide Cross-linked Dimer Formation

Samples of MAP2-123 were placed in sitting bridge crystallization wells under the conditions described previously for filament assembly. Samples were collected on various days until the fifth day when the samples were assembled as determined by electron microscopy of the samples. Two samples were collected on the fifth day and one was treated with 4 mM dithiothreitol for one hour at 37 ° C. All the samples were then mixed with nonreducing sample buffer and run on an 18 % acrylamide gel with 1 % SDS. As can be clearly observed on day 1, most of the sample has dimerized and by day 2 nearly all of the sample is dimeric (Figure 3-1). The dimer persists until day 5 when MAP2-123 filaments are abundant as judged by electron microscopy. Upon treatment with dithiothreitol, the day 5 sample returns to its monomeric form. With only one cysteine per MAP2-123 fragment, dimerization is required to form any disulfide linkage (DeTure et al., 1996). This dimerization was also confirmed for assembly of MAP2-N123C fragments (Zhang et al., 1996).

If dimerization is the only means for facilitating disulfide linkage to form, then analytical ultracentrifugation is a direct method to characterize the sedimentation behavior of MAP2-123 in the absence and presence of dithiothreitol. Equilibrium sedimentation offers the advantage that each protein species achieves its own exponential concentration gradient from the meniscus to the bottom of the sector; hence, the number of species and the amount of each can be estimated as the best fit of an arithmetic sum of exponentials to the observed protein concentration *versus* radial position. Equilibrium was attained in 1 day, and no change in the protein concentration gradient was subsequently detected over a 5 day run. This experiment showed that at a MAP2-123 concentration of 100 μM, nearly 36 % of the

Figure 3-1. Samples of MAP2-123 at Various Times of Assembly Were Run on a Nonreducing SDS-PAGE Gel. The sample is observed to form dimers during the first day of incubation, and these dimers persists through the period of filaments assembly. Treatment of the sample with dithiothreitol at day 5 confirms the formation of an intermolecular disulfide bond.

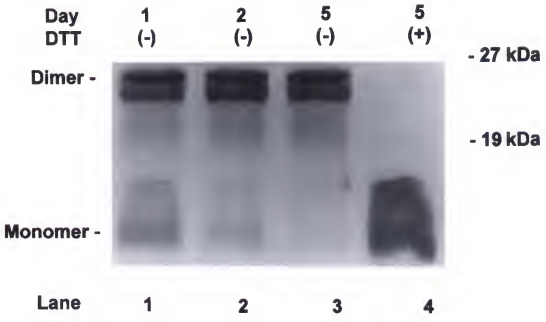
Day
DTT
1
(-)
2
(-)
5
(-)
5
(+)
- 27 kDa
Dimer -
- 19 kDa
Monomer -
Lane
1
2
3
4

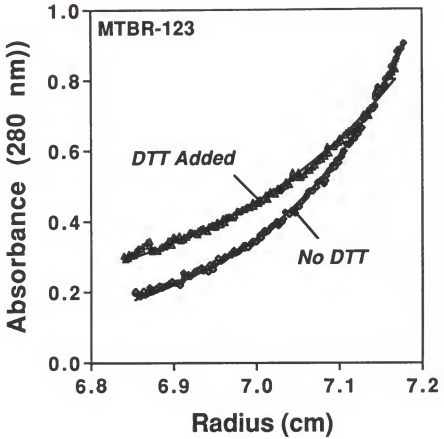

Figure 3-2. Formation of a MAP2-123 Disulfide Cross-linked Dimer is Confirmed by Analytical Ultracentrifugation. Sample of MAP2-123 at 100 μM were run in the presence and absence of dithiothreitol. The steeper curve in the absence of dithiothreitol demonstrates the formation of heavier species like dimers.

material was in the dimeric form in the absence of dithiothreitol (Figure 3-2). In contrast, no dimer could be detected in the presence of dithiothreitol. Dimer formation was confirmed for MAP2-N123C and MAP2c using equilibrium sedimentation, and again about one third of the material was found to be dimeric (DeTure et al., 1996; Zhang et al., 1996).

Assembly of MAP2-N123C (Cysteine1709Alanine) Mutant

Having demonstrated that dimers of MAP2-123 and MAP2-N123C form before filaments assemble, that the presence of dithiothreitol in the assembly reactions slows filament polymerization, that no dimers form in the presence of dithiothreitol and that material from filaments is all dimeric, the hypothesis was set forth that MAP2 fragments must form disulfide cross-linked dimers before they can be incorporated into straight filaments. To test this hypothesis, the MAP2-N123C (C1709A) mutant was expressed, purified and placed in crystallization wells as described earlier. This material became viscous after incubation in the sitting bridges for 3 weeks just as MAP2-N123C had, but examination of the material using electron microscopy showed that the material was different from the straight filaments formed by MAP2-N123C (Figure 3-3 a-b). Clumps of material were observed as were what is described here as coils of polymerized material. Occasionally, regions containing filaments with the same diameter as the MAP2-N123C were visible, but their persistence length was much less than that observed for the unmutated MAP2-N123C fragment. Examination of numerous micrographs of the samples confirmed that the curly masses were continuous and therefore filamentous, but the polymerized material was structurally different from paired helical filaments made with recombinant Tau fragments of straight filaments assembled from recombinant Tau or MAP2 fragments.

Assembly of MAP2-N133C and MAP2-N233C Mutants

Because the results using the MAP2-N123C (C1709A) mutant were unexpected and some of the polymers had small stretches resembling straight filaments, two more mutants made previously in the lab were expressed, purified and incubated under the same

Figure 3-3. Assembly of MAP2-N123C (C1709A), MAP2-N133C and MAP2-N233C. Panels a-b: MAP2-N123C polymerized into curly structures similar in diameter to MAP2-N123C. Panels c-d: Assembly of the MAP2-N133C mutant led to similar structures. Panels e-f: Reintroduction of the second repeat at a different location did not restore the ability to form straight filaments for MAP2-N233C. The bars are 100 nm.

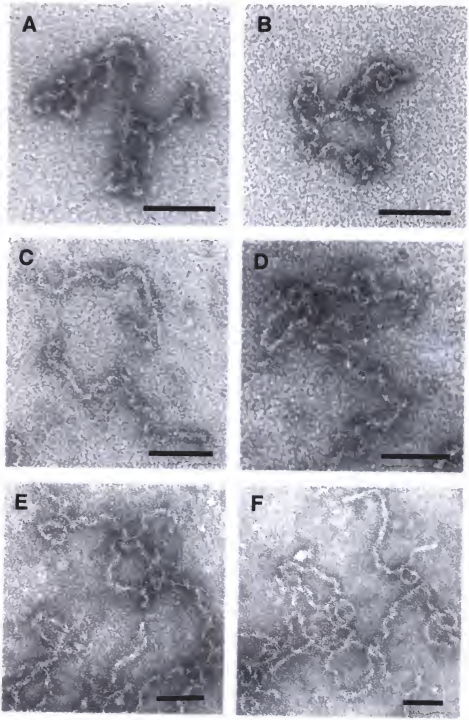
A
B
C
D
E
F

assembly conditions used for MAP2-N123C. MAP2-N133C had the entire cysteine-containing second repeat replaced with an additional copy of the cysteine-lacking third repeat. Unlike MAP2-N123C (C1709A), this mutant did not support microtubule assembly (Coffey, 1994). If the second repeat is as important in MAP2 assembly as it is in MAP2-promoted microtubule assembly, the results of these experiments with MAP2-N133C should be less ambiguous than those with MAP2-N123C (C1709A). These samples also became viscous when incubated, and electron microscopy showed that the structures formed were nearly identical to those observed with the cysteine to alanine mutant (Figure 3-3 c-d). Additionally, the mutant MAP2-N233C was expressed, purified and incubated under assembly conditions. This material also became viscous, but the electron micrographs showed the polymerized material to be nearly identical to structures formed with MAP2-N133C (Figure 3-3 e-f). These experiments confirmed the importance of the cysteine and its location in straight filament formation, but they also showed that the cysteine is not completely required for polymerization.

Assembly of the MAP2-123 (Cysteine1709Alanine) and MAP2-133 Mutants

Because MAP2-N123C does not polymerize as quickly as MAP2-123, and because the filaments of MAP2-N123C tend to aggregate more than those of MAP2-123, MAP2-123 was mutated forming MAP2-123 (C1709A) and MAP2-133. These mutants were expressed, purified and incubated concomitantly with MAP2-123, and they did not become viscous like the MAP2-123. At day five, the three samples were examined by electron microscopy. The MAP2-123 showed abundant filaments, but none were observed with either mutant. These samples were examined at day 8, week 2 and week 3 before any structures were observed. Both MAP2-123 (C1709A) and MAP2-133 formed some filaments by week 3 (Figure 3-4 a-d), but they were difficult to find on a grid. In fact most squares on the copper grids had no filaments, but they were consistently found with thorough investigation. The most interesting aspect of these assembly reactions was the

Figure 3-4. MAP2-123 without Cysteine 1709 and MAP2-133 Occasionally Formed Straight Filaments. Panels a-b: Replacement of cysteine 1709 with alanine greatly inhibited the polymerization process, but some straight filaments did form. Panels c-d: Replacement of the cysteine-containing second repeat with the third repeat sequence gave similar results. The bars are 100 nm.

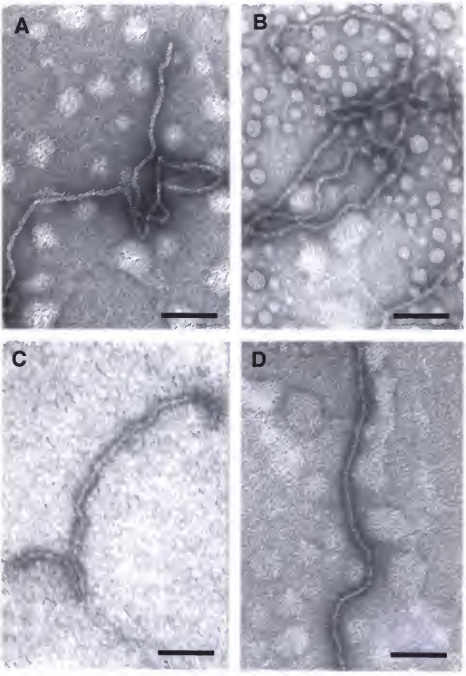
A
B
C
D

demonstration that the filaments formed were straight filaments with a diameter equal to filaments formed of MAP2-123. These results indicate that there is a polymerization pathway available to MAP2-123 under nondisulfide bond forming conditions, but the rate of formation is greatly inhibited compared to disulfide linked MAP2-123.

Discussion

These experiments suggest that the role of the disulfide cross-linked dimer in the filament assembly of recombinant Tau-K12 and MAP2-123 is probably similar. MAP2-123 has been shown to form a dimer before filaments are formed, and SDS-PAGE showed that these polymers mostly contain disulfide linked MAP2 dimers. Equilibrium sedimentation experiments also demonstrated that MAP2-123 does not form dimers in the presence of dithiothreitol. This would indicate that MAP2-123 has little propensity to dimerize in the absence of disulfide bond formation or that its association constant is very low. In agreement with this suggestion is the finding that MAP2-123 (C1709A) and MAP2-133 only form straight filaments at a significantly reduced rate compared to MAP2-123. These experiments were done at protein concentrations of 500 - 1000 μM; so it is possible that dimers did form from MAP2-123 (C1709A) and MAP2-133 at these high concentrations. This possibility remains to be confirmed. While disulfide cross-linked dimer formation is not required for MAP2-123 mutants to assemble, the oxidized dimer formation of MAP2-123 does appear to facilitate polymerization.

Interestingly, MAP2-N123C (C1709A), MAP2-N133C and MAP2-N233C polymerized, but different filamentous structures were formed. While changing the cysteine to an alanine or moving its location in MAP2-N123C did not noticeably affect the rate of polymer formation, these changes strongly influenced the types of filaments formed. These filaments were similar in width to the native MAP2-N123C filaments, but they were very curly in their appearance. In fact, small aggregates had to be examined closely to confirm the continuity of the polymers. For MAP2-N123C, changing the cysteine to

alanine did block the formation of straight filaments from disulfide cross-linked dimers, and it is not known how the assembled structures were related to those formed from MAP2-N123C. It would be useful to learn whether blocking disulfide cross-linked dimer formation with cysteine-to-alanine mutations affects the types of Tau-N123C structures formed.

Dimerization of MAP2-123 and the role of dimers in filament formation again underscores the similarities in the filaments formed from MAP2-123 and Tau-123. Both polymerize *in vitro*; both bind thioflavin S and assemble from Alzheimer filaments; both also form disulfide cross-linked dimers; and for both, dimer formation greatly increases the rate of filament formation. Thus it is surprising that Tau, but not MAP2, is found in Alzheimer filaments. These results also heighten interest regarding the role of the cysteine in the second repeat. In MAP2-N123C, replacing the cysteine with an alanine or serine did not affect the rate or extent of microtubule assembly *in vitro* (Coffey, 1994). One could speculate that this cysteinyl residue is preserved because it may be involved in a signaling event where nitrosylation would modify the thiol and affect MAP function (Tenneti et al., 1997). In fact, this lab has demonstrated that disulfide cross-linked dimers of Tau-N123C and MAP2-N123C are both capable of stimulating microtubule assembly *in vitro* at physiologically relevant concentrations and solution conditions (DeTure, DiNoto and Purich, 1998). The cysteines responsible for cross-linking MAP dimers may be conserved so that cross-linked dimers can stabilize the cytoskeletal network during times of lowered membrane integrity or oxidative stress. This could explain why the cells risk maintaining the unique cysteine in three-repeat adult MAP2 and why four-repeat Tau is the predominant adult Tau. If MAP2 does not form stabile filaments, then there is no risk from three-repeat MAP2, and if four-repeat Tau forms mostly intramolecular disulfide bonds, then it does not dimerize as much. So perhaps four-repeat Tau is a means of allowing some disulfide cross-linked dimers to form under emergency conditions while lowering the chances of massive Tau dimerization occurring when it is not wanted.

CHAPTER 4
IDENTIFICATION OF AMINO ACID MUTATIONS PERMITTING FORMATION OF PAIRED HELICAL FILAMENTS FROM MAP2-123

Introduction

The work up to this point has demonstrated that MAP2 fragments containing the microtubule-binding region are capable of polymerizing *in vitro* into straight filaments at concentrations that are an order of magnitude lower than those needed with recombinant Tau. Like purified Tau (Binder and Wilson, 1997), MAP2 fragments can assemble from the ends of Alzheimer paired helical filaments without forming paired helical filaments. This demonstrates that MAP2 fragments and Tau share some similar binding surfaces. That thioflavin S binds Alzheimer paired helical filaments as well as filaments formed with Tau-K12 or MAP2-123 suggests that all of these filaments share a similar thioflavin S binding pocket. Additionally, the polymerization of Tau-K12 and MAP2-123 proceeds through the formation of a disulfide cross-linked dimer, and blocking disulfide linked dimer formation greatly lowered the rate of filament formation. These experimental results along with the fact that MAP2 is present in the cell body where Alzheimer neurofibrillary tangles form suggests that the factors which permit Tau, but not MAP2, filaments to form and accumulate should be determined.

Recently certain polyglycosaminoglycans were shown to stimulate the assembly of recombinant Tau (Goedert et al., 1996 and Perez et al., 1996). One study showed that three- and four-repeat Tau both assembled into a variety of structures. These structures including some paired helical filaments when three-repeat isoforms were incubated in the presence of 0.05 - 0.50 mg/mL polyglycosaminoglycans (Goedert et al., 1996). Polyglycosaminoglycans with the highest linear charge density were the most effective, and

the stimulation was polyanion-specific such that polyglutamic acid was ineffective. This study also demonstrated that heparin bound to Tau and competed with microtubules for Tau binding, thereby resulting in microtubule depolymerization. They showed that heparan sulfate and hyperphosphorylated Tau were present in the same neurons at the earliest stages of neurofibrillary tangle pathology. During the same period, other related studies suggested that the effect was not polyanion specific, because polyglutamic acid produced similar effects (Perez et al., 1996). The latter workers demonstrated that a synthetic polypeptide equivalent to the third 18-amino acid repeat of four-repeat Tau (i.e. the second repeat in three-repeat Tau) assembled in the presence of heparin forming filaments 12 nm wide.

The Mandelkow lab later demonstrated that RNA from 0.05 - 0.50 mg/mL stimulated the *in vitro* polymerization of recombinant Tau (Kampers et al., 1996). As was true in the polyglycosaminoglycans studies, RNA promoted the assembly of Tau at lower concentrations in one day, as compared to a month. The filaments closely resembled those formed in the absence of RNA at higher concentrations over longer times and included paired helical filaments from full-length three-repeat Tau. Using the Tau-K12 with the cysteine mutated to alanine, they also showed the process is still dependent on the formation of a disulfide linked dimer; however RNA stimulated polymerization of Tau-1234 which has two cysteines and can form intramolecular disulfide bonds. They suggested that cytosolic RNA is more pertinent than the polyglycosaminoglycans which are normally part of the extracellular matrix. Finally, they proposed polyanions may facilitate Tau assembly in two ways. First polyanions may act to concentrate Tau allowing polymerization at lower concentrations; and second, polyanions may bind Tau exposing the repeat region which is very assembly competent. Now it would be interesting to determine if any Alzheimer risk factors lead to increased concentrations of these polyanions, but currently they can be used as a tool in achieving assembly at lower concentrations over shorter periods of time.

To better understand the process, several Tau constructs were employed corresponding to Tau-123, Tau-K12 and Tau-N123C. These polypeptides were used to reproduce some of the experimental results for Tau, and they allowed the personal examination of Tau filaments to better assess the range of structures Tau could form *in vitro*. Conditions were then replicated using recombinant MAP2-123 and MAP2-N123C to study the effects of heparin and tRNA on polymerization. These agents did affect MAP2 assembly, but they were incapable of inducing paired helical filament formation. Tau-123 forms paired helical filaments whereas MAP2-123 cannot; a finding that led to the hypothesis that regions of MAP2 may prevent paired helical filament formation. Furthermore, if these areas were altered to resemble Tau, then paired helical filaments would form from these mutated MAP2 proteins. Examination of the sequences of Tau-123 and MAP2-123 allowed me to identify two regions termed Module-A and Module-B which were thought to control filament morphology (Figure 4-1). The work in this chapter details the effects of certain polyanions on MAP2-123 assembly, and these experiments show that subtle differences in the primary sequences of Tau and MAP2 control the ability of MAP2-123 to form paired helical filaments *in vitro*.

Materials and Methods

Materials

Synthetic single-stranded oligonucleotides for cloning and mutations were made by Genemed Synthesis Incorporated, and cDNA products were ligated into the pETh-3b vector for cloning and expression. This vector was a derivative of pBR-322 and was a gift from Dr. Donald McCarty at the University of Florida. Invitrogen One Shot competent cells and DM1 competent cells from Gibco-BRL were used for cloning, and E. coli BL21 (DE3) pLYS S competent cells from Novagen were used for protein expression. Agar, tryptone and yeast extract were obtained from DIFCO Laboratories. Tris base, sodium acetate, phenylmethylsulfonyl fluoride, dithiothreitol, sodium dodecylsulfate, ampicillin,

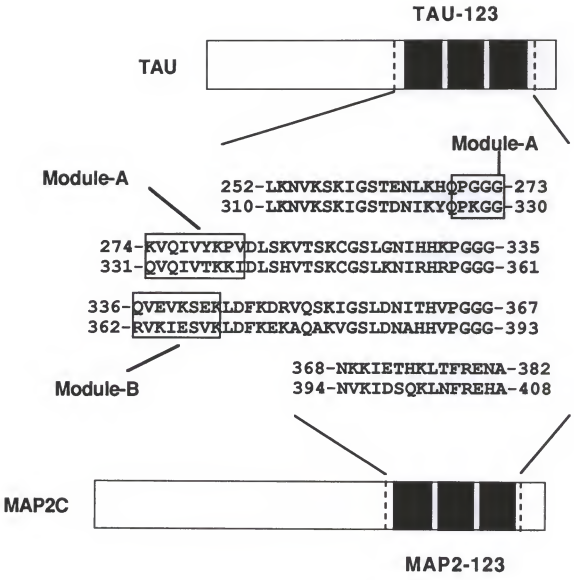

Figure 4-1. Sequence Comparison of MAP2-123 and Tau-123 and the Identification of Module-A and Module-B. Close examination of the MAP2-123 and Tau-123 sequences shows they are 70 % identical with most of the significant differences in Module-A after the first repeat and Module-B after the second repeat.

magnesium chloride, 2- (N-morpholino) ethanesulfonic acid, DNase (#5025), sodium chloride, Folin reagent, thioflavin S, heparin, heparan sulfate , tRNA and isopropyl-β-thiogalacto-pyranoside were from Sigma Chemical Company. DNA high melt agarose, Wizard Minipreps, dNTPs, Lambda DNA markers and certain restriction enzymes were obtained from the bioproducts division of Fisher Scientific. Most restriction enzymes were purchased from New England Biolabs while T4 DNA ligase, Taq DNA polymerase and chloramphenicol were purchased from Boehringer-Mannheim. FPLC materials including HiTrap SP disposable columns and Sephaglass Bandprep kits were obtained from Pharmacia. Microcon, Centricon and Centriprep devices for protein sample concentration were made by Amicon. Whatman Corporation provided the P11 phosphocellulose, and Coomassie Brilliant Blue R 250 was from Crescent Chemicals. Sitting bridge crystallization cells and ancillary material for polymerization experiments were obtained from Hampton Research. Purified paired helical filament preparations from Alzheimer brain tissue were a generous gift from Dr. Peter Davies at Albert Einstein University.

MAP2-123 was mutated so that the non-Tau Module-A residues were converted by cassette mutagenesis to those found in wild type Tau. The mutations in Module-A are at the end of the first repeat and the inter-repeat before the start of the second repeat. These mutations in MAP2-123 are flanked by a Bam HI site on the 5' side of the mutations and an Afl II site on the 3' side of the mutations. Oligonucleotides were designed that annealed to one another, coded for the mutations of interest, created overhangs which complemented the Bam HI and Afl II sticky ends and destroyed the Bam HI and Afl II sites when inserted into the cDNA sequence. Cloning simply involved digesting MAP2-123 with Bam HI and Afl II, purifying the released fragment from the plasmid by gel electrophoresis and ligating the annealed oligonucleotides into the plasmid. Transformed Invitrogen One Shot competent cells were plated and colonies were collected for screening of their plasmids. Plasmids which had lost both their Bam HI and Afl II sites were grown in quantity and sequenced by the ICBR DNA sequencing core at the University of Florida.

MAP2-123 with Module-B of the inter-repeat between the second and third repeats was mutated to match the Tau sequence using four primer PCR. This technique is analogous to the method used for deleting the extra repeat from the four-repeat Tau clone above, but no sequences were removed. Internal primers were designed that complemented one another, contained the mutations and coded for a silent mutation that created a Hind III site on the 3' side of the mutations for screening. These primers were used individually with primers for the ends of the clone that contained restriction sites for cloning. The PCR products for the front and back of the molecule were purified by gel electrophoresis and used as template in a second reaction with the primers for the ends of the molecule. The product from this PCR reaction was digested with Nde I and Eco RI and cloned into the pETh-3b plasmid that had been digested with the same restriction enzymes and purified. Plasmids from colonies were screened for the addition of the Hind III site, and positives were grown in quantity for sequencing by the ICBR DNA sequencing core at the University of Florida.

Individual point mutations in Module-B were generated using cassette mutagenesis. Module-B is flanked on the 5' side by the Stu I site and on the 3' side by the Hind III site introduced for screening in the MAP2-123 Module-B mutant. Oligonucleotides were designed that annealed to one another, coded for the mutation of interest, had a blunt 5' end, created a 3' overhang which complemented the Hind III sticky end and destroyed the Hind III site when inserted into the MAP2-123 cDNA sequence. Plasmid containing MAP2-123 [Module-B] digested with Stu I and Hind III was gel purified to remove the small released fragment and incubated with the annealed oligonucleotides. The mixture was then ligated and transformed into Invitrogen One Shot competent cells. Plasmids were purified from different colonies and screened for the loss of the Hind III site. Positives for each point mutation were identified, and sequencing by the ICBR DNA sequencing core at the University of Florida confirmed each point mutation was generated.

In Vitro Assembly of Filaments with tRNA or Heparin

Studies demonstrating the efficiency of Tau polymerization in the presence of polyanions, such as polyglycosaminoglycans or RNA, prompted the use of similar conditions to determine which MAP2 mutants assembled more like Tau does. If the sample behaved like Tau, then assembly with these agents permitted polymerization in a single day using concentrations below 1 mg/mL. Like the conditions for MAP2 fragment assembly, purified recombinant material is dialyzed into 100 mM Tris at pH 6.8 until the salt is removed. The samples are typically 2 mg/mL, and the protein concentration was determined using the method of Lowry. Samples at 50 - 200 μM were placed in 1.5 mL Eppendorf tubes with between 0.01 and 0.50 mg/mL tRNA or heparin. The concentrations of polyanion that worked best were between 0.01 and 0.10 mg/mL which were lower than those reportedly used for Tau polymerization (Goedert et al., 1996; Perez et al., 1996 and Kampers et al., 1996). These samples were then incubated overnight at 37 °C and examined by electron microscope for filament assembly as described below.

Results

Several reports have documented that certain polyanions like, glycosaminoglycans and RNA, enhance the *in vitro* polymerization of recombinant Tau (Goedert et al., 1996; Perez et al., 1996; Kampers et al., 1996). These substances lower the concentrations of Tau-123 needed for assembly to below the 100 μM, and these agents also accelerate assembly so polymerization only takes one day, not one month. Full-length three- and four-repeat Tau that failed to assemble *in vitro* polymerized in one day when 0.05 to 0.50 mg/mL tRNA or heparin was present. Tau assembled in the presence of these agents still formed a variety of structures including paired helical filaments, straight filaments and others. These results suggested that heparin or RNA may increase the rate of MAP2 assembly and could possibly induce the formation of paired helical filaments from the microtubule-binding region of MAP2. Because this study is focused on identifying factors

which allow MAP2 fragments to form paired helical filaments, experiments were first carried out to determine the effects of RNA and polyglycosaminoglycans on assembly of MAP2 fragments of the microtubule-binding region.

Assembly of MAP2-123 in the Presence of Heparin or Heparan Sulfate

Experiments for the polymerization of Tau in the presence of heparin were carried out in a number of different buffers including: 1 x MEM (pH 6.4) with 50 mM NaCl; 30 mM MOPS (pH 7.4) and 100 mM Tris (pH 6.8) (Goedert et al., 1996; Perez et al., 1996; Kampers et al., 1996). The experiments with MAP2-123 were carried out at different concentrations of protein (50 - 800 μM) and of heparin or heparan sulfate (0.01 - 0.50 mg/mL). These experiments were carried out in all the buffers used above and also in the MAP2 assembly buffer described earlier. No polymers could be detected at high polyanion concentrations. Heparin and heparan sulfate both seemed to inhibit the assembly of MAP2-123, and when filaments did form, they were straight filaments. No paired helical filament-like structure formed under any of the conditions tested. MAP2-123 (800 μM) assembled normally in the absence of heparin (Figure 4-2 a-d); but as heparin was added, the filaments appear to condense or stop forming (Figure 4-2 e-p). The same was true at 200 μM and 500 μM MAP2-123 (data not shown). These results indicated that heparin interacts with MAP2-123 differently than with Tau, but no studies have been published on the effects of higher concentrations of polyglycosaminoglycans on Tau assembly.

Assembly of MAP2-123 in the Presence of tRNA

Since Tau polymerization was also facilitated by the addition of RNA, assembly reactions with MAP2-123 were prepared to determine the effects of RNA on polymerization. MAP2-123 concentrations were varied from 50 - 500 μM and total RNA, ribosomal RNA and transfer RNA were used at concentrations from 0.01 - 0.50 mg/mL. None of the conditions tested stimulated MAP2-123 polymerization; nor did they induce the formation of paired helical filaments (Figure 4-3 a-b). In fact, increasing tRNA concentration decreased the amount of filaments that formed with MAP2-123. Finally,

Figure 4-2. Assembly of MAP2-123 in the Presence of Heparin. Panels a-b: MAP2-123 at 800 mM assembled for 5 days without heparin added. Panels c-d: MAP2-123 at 800 mM assembled for 5 days with 80 μM (monomeric concentration) heparin added. Panels e-f: MAP2-123 at 800 mM assembled for 5 days with 160 μM heparin added. Panels g-h: MAP2-123 at 800 mM assembled for 5 days with 400 μM heparin added. The MAP2-123 filaments seem to condense and form less frequently as heparin is increased. The bars are 100 nm.

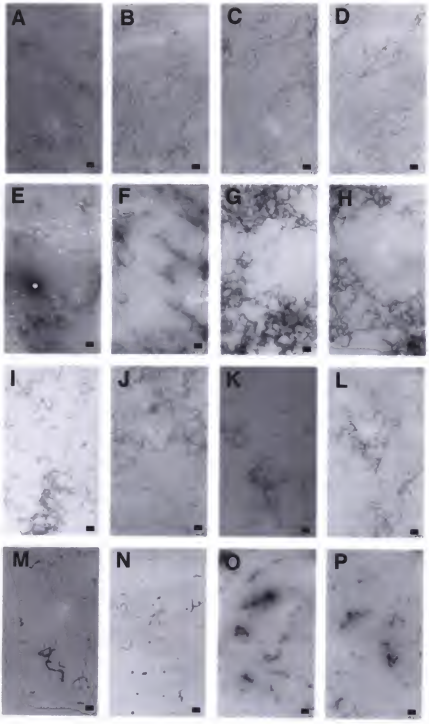
A
B
C
D
E
F
G
H
I
J
K
L
M
N
O
P

control experiments were done using Tau-N123C, Tau-K12 and Tau-123 to confirm the RNA effect and to see the types of structures formed by Tau. Mostly straight filaments were observed with the Tau samples in the presence of tRNA, but paired helical filaments were forming although their abundance was limited (Figure 4-3 c-f). The use of tRNA did not appear to shift the equilibrium towards paired helical filament formation. It only increased the rate of assembly.

Assembly of MAP2-123 [Module-A] Mutants

Mutations of MAP2-123 were chosen to identify those residues that block paired helical filament formation (i.e. these mutations should make MAP2-123 display assembly properties of Tau-123). The rationale is that if a mutation allows MAP2-123 filament assembly to resemble that of Tau-123, then incubation in the presence of tRNA should permit filament assembly at lower protein concentrations, and polymerization should be observed after incubation for about one day. Samples were also prepared without RNA, and typically the results were the same. Mutations in Module-A involved five amino acid residues within a stretch of 14 residues at the end of the first repeat. One of these five mutations was a lysine-to-glycine mutation at position 1689, the only MAP repeated sequence to end in PKGG rather than PGGG. Unlike Tau, the synthetic polypeptides of the first repeat in MAP2 cannot stimulate microtubule assembly, and these sequence differences may lead to different polymerization behavior of Tau-123 and MAP2-123. Samples (50 - 200 μM) were incubated with tRNA (0.01 to 0.20 mg/mL) in sealed Eppendorf tubes overnight at 37 ° C. When examined by electron microscopy, the first difference between MAP2-123 and MAP2-123 [Module-A] was the formation of numerous filaments. These filaments resembled those formed from MAP2-123 with respect to filament width, but they aggregated in a manner unlike MAP2-123 samples (Figure 4-4 a-d). Upon closer examination, these filaments exhibited modulations in width from 8 - 18 nm (Figure 4-4 e-h). Broadly speaking, these filaments resembled Tau-123 paired helical filaments, but the filaments lacked the periodicity observed in true Alzheimer paired helical

Figure 4-3. MAP2-123 Assembly was Inhibited by tRNA while Tau-123 Assembled Readily into Paired helical Filaments when tRNA was added. Panel a: MAP2-123 at 400 μM assembled without tRNA. Panel b: MAP2-123 at 400 μM assembled with 0.05 mg/mL tRNA. Panels c-f: Tau-123 at 200 μM assembled with 0.05 mg/mL tRNA. The bars are 100 nm.

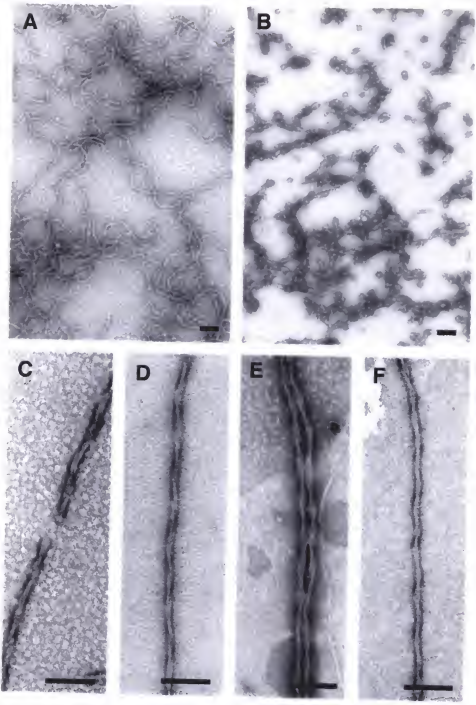
A
B
C
D
E
F

filaments. Clearly, the MAP2-123 [Module-A] mutants had become more similar to Tau-123, because they assembled into a variety of filamentous structures like Tau.

Assembly of MAP2-123 [Module-B] Mutants

MAP2-123 [Module-B] involved four mutations in a seven amino acid run immediately following the cysteine-containing second repeat in MAP2. Each of the mutations involved a charged residue in the region where each MAP is most divergent in primary sequence. Experiments were prepared under a variety of conditions with tRNA, as was the case for MAP2-123 [Module-A] mutants. Examination of the sample under the electron microscope revealed the formation of numerous filaments (Figure 4-5 a-e), of which many were paired helical filament-like structures (Figure 4-5 f). The filaments had a very regular modulation in width from 8 - 18 nm with a crossover distance of 55 - 60 nm. They were in fact more twisted than Alzheimer paired helical filaments, but this type of filaments is observed when recombinant Tau is assembled with RNA or heparin (Kampers et al., 1996). The formation of a variety of structures is the hallmark of Tau, and the fact that MAP2-123 [Module-B] forms paired helical filaments was a promising finding. Clearly, both Module-A and Module-B mutants formed different types of paired helical filament-like structures, suggesting that perhaps separate modules in Tau were responsible for Tau forming paired helical filaments. This hypothesis has not been tested as a concentrated effort was begun to determine the fewest amino acid mutations needed to convert MAP2-123 into a paired helical filament forming protein.

Assembly of MAP2-123 [Module-B] Point Mutants R1723Q, K1725E and E1727K

In MAP2-123 [Module-B] four mutations were made simultaneously. Point mutations were introduced individually in MAP2-123 to determine the minimum number of changes needed for paired helical filaments formation. These single mutations in the region of MAP2 called Module-B are at R1723Q designated MAP2-123-MBP1; K1725E designated MAP2-123-MBP2; E1727K designated MAP2-123-MBP3 and V1729E designated MAP2-123-MBP4. Because these mutants may have the capacity to form

Figure 4-4. Assembly of MAP2-123 [Module-A] into Filaments which Formed Lateral Associations. Panels a-d: MAP2-123 [Module-A] assembled at 200 μM in the presence of 0.05 mg/mL tRNA formed filaments that tended to form lateral associations with one another. Panels e-h: MAP2-123 [Module-A] assembled at 200 μM in the presence of 0.05 mg/mL tRNA formed some filaments that twisted with modulations in width from 8 - 18 nm, but they did not exhibit a regular crossover distance. The bars are 100 nm.

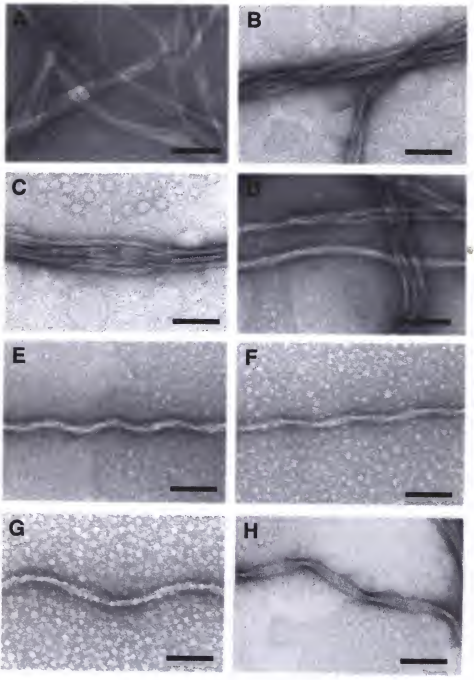
A
B
C
D
E
F
G
H

Figure 4-5. Assembly of MAP2-123 [Module-B] into Paired Helical Filaments. Panels a-f: MAP2-123 [Module-B] assembled at 200 μM in the presence of 0.05 mg/mL tRNA formed filaments that were easily recognized as paired helical filaments when examined individually. They had modulations in width from 8 - 18 nm with a regular crossover distance of 55 - 60 nm. The bars are 100 nm.

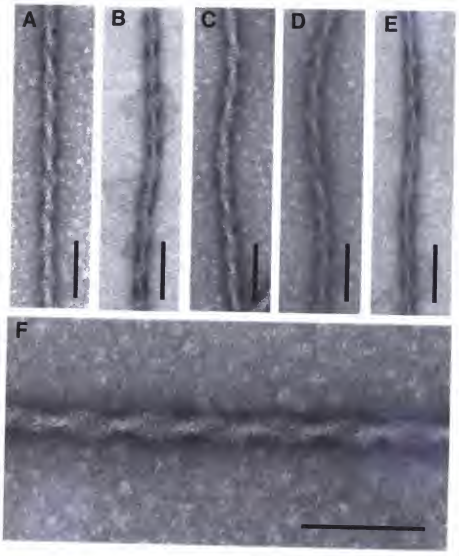
A
B
C
D
E
F

paired helical filaments, samples were prepared under the conditions used with Tau that included tRNA, and samples were also prepared in sitting bridge cells for the assembly reactions without tRNA were they to behave like MAP2-123. In fact, most of the point mutants exhibited assembly properties that were intermediate in nature.

At concentrations of 50 - 200 μM, MAP2-123-MBP1, MAP2-123-MBP2 and MAP2-123-MBP3 all assembled in the presence of tRNA (0.01 - 0.20 mg/mL), but the number of filaments formed was substantially below that observed with MAP2-123 [Module-A] or MAP2-123 [Module-B]. Additionally, these point mutants formed aggregates that resembled sheets and were not filamentous. These three mutants did not polymerize as well as Tau-123 in the presence of tRNA or heparin, and they assembled poorly in the absence of polyanions. The filaments of MAP2-123-MBP1 (Figure 4-6 a-h), MAP2-123-MBP2 (Figure 4-7 a-f) and MAP2-123-MBP3 (Figure 4-8 a-i) all exhibited various types of structures including two classes of straight filaments with diameters of 8 - 10 nm or 16 - 18 nm. The MAP2-123-MBP1 and MAP2-123-MBP2 formed mostly straight filament 8 - 10 nm wide with some crumpled sheet structures. The MAP2-123-MBP2 and MAP2-123-MBP3 each formed some miniature paired helical filament structures 6 - 10 nm wide. Without tRNA, the MAP2-123-MBP3 formed many short filaments of 8 - 10 nm in width with several longer filaments resembling braided filaments approximately 20 nm in diameter. With tRNA, this sample polymerized readily into longer 6 - 10 nm paired helical filaments that resembled the dashed miniature filaments described for Tau-123 (Crowther et al., 1992). Although these mutants exhibited some assembly properties comparable to Tau, they did not polymerize to the extent of MAP2-123 [Module-B] in the presence of polyanions, and they did not form Alzheimer-like PHFs.

Assembly of MAP2-123 [Module-B] Point Mutant V1729E

Although this mutant was constructed and tested with the other Module-B point mutants, its polymerization behavior was noticeably different from the others. Protein samples (50 - 200 μM) were prepared with tRNA (0.01 - 0.20 mg/mL) and incubated

Figure 4-6. Assembly of MAP2-123-MBP1 into Various Structures. Panels a-h: MAP2-123-MBP1 at 200 μM was assembled with 0.05 mg/mL tRNA and different types of straight filaments and paired helical filaments were observed to form. The bars are 100 nm.

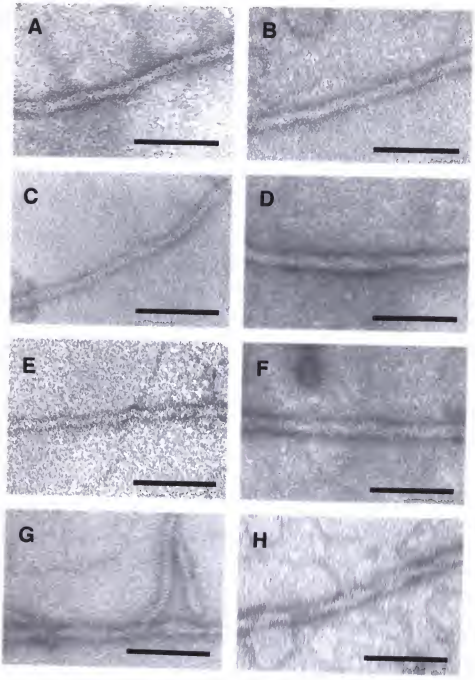
A
B
C
D
E
F
G
H

Figure 4-7. Assembly of MAP2-123-MBP2 into Various Structures. Panels a-f: MAP2-123-MBP2 at 200 μM was assembled with 0.05 mg/mL tRNA and different types of straight filaments and paired helical filaments were observed to form. The bars are 100 nm.

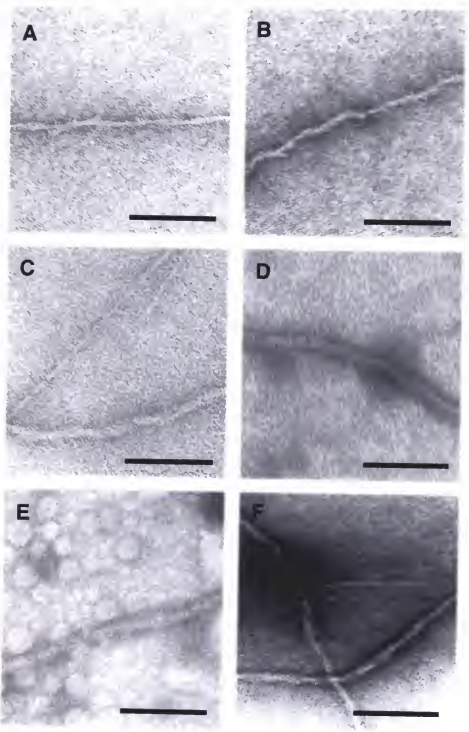
A
B
C
D
E
F

Figure 4-8. Assembly of MAP2-123-MBP3 into Various Structures. Panels a-i: MAP2-123-MBP3 at 200 μM was assembled with 0.05 mg/mL tRNA and different types of straight filaments and paired helical filaments were observed to form. The bars are 100 nm.

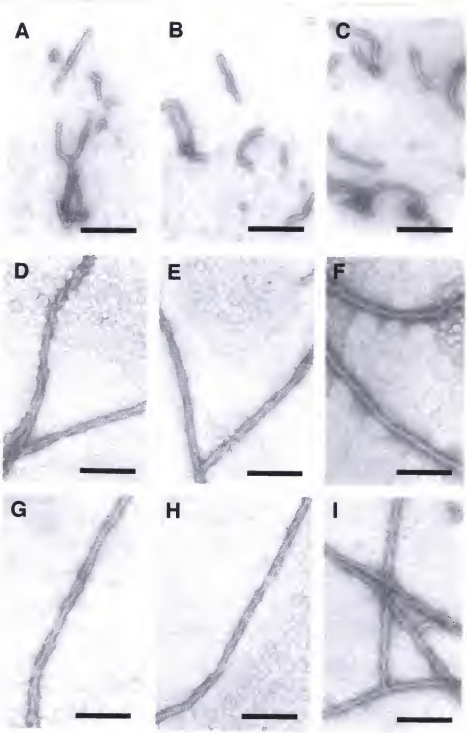
A
B
C
D
E
F
G
H
I

overnight at 37 ° C. Upon examination by electron microscopy, numerous filaments were observed, and many resembled paired helical filaments with obvious similarities to the MAP2-123 [Module-B] filaments (Figure 4-9 a-h). In fact, those assembled at 100 μM with 0.05 mg/mL tRNA formed paired helical filaments almost entirely. These filaments had modulations in diameter from 8 - 18 nm with a regular crossover distance of 55 - 65 nm. The MAP2-123-MBP4 sample also formed paired helical filaments in the presence of 0.01 - 0.20 mg/mL heparin, and these filaments were indistinguishable from filaments formed with full-length four-repeat Tau in the presence of heparin (Kampers et al., 1996). Straight filaments with a diameter of 8 - 10 nm or 16 - 18 nm were also observed, and this variety of filamentous structures is reminiscent of the structures formed from Tau. Because MAP2-123-MBP4 formed mostly paired helical filaments in the presence of tRNA or heparin, protein samples were prepared without these agents present. Samples (100 - 800 μM) were prepared in the sitting bridge cells at room temperature and in sealed 1.5 mL Eppendorf tubes at 37 ° C. Samples were examined at day-2, day-5, day-8, week-2 and week-3. Filaments formed readily by week 2, and many had widths in the 8 - 10 nm and 16 - 18 nm range (Figure 4-10 a-d). These types of filaments accounted for most of the structures observed by electron microscopy. In addition to the straight filaments, there were many twisted filaments, including paired helical filament-like structures resembling those observed with tRNA or heparin (Figure 4-10 e-h). Somewhat suprisingly, this mutant MAP2-123 was found to polymerize into filaments more rapidly than does Tau-123 in the absence of tRNA or heparin. However, a larger proportion of paired helical filaments formed when these polymerization-enhancing agents were included in the assembly reactions. These experiments demonstrated that very subtle changes in the sequence can make MAP2-123 behave like Tau-123, and it is likely that the glutamate 342 in human Tau may be important in paired helical filament assembly.

Figure 4-9. Assembly of MAP2-123-MBP4 into Paired Helical Filaments. Panels a-h: MAP2-123-MBP4 at 200 μM was assembled with 0.05 mg/mL tRNA and mostly paired helical filaments were observed to form. These filaments resembled those formed from MAP2-123 [Module-B] with modulations in width from 8 - 18 nm and a regular crossover distance of 55 - 60 nm. The bars are 100 nm.

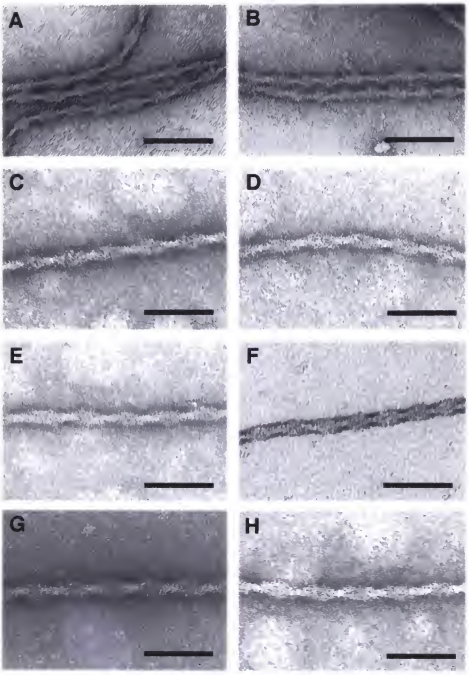
A
B
C
D
E
F
G
H

Figure 4-10. Assembly of MAP2-123-MBP4 into Various Structures when tRNA is Excluded. Panels a-d: MAP2-123-MBP4 at 200 μM was assembled in the absence of tRNA and different types of straight filaments were observed. Panel e-h: Paired helical filaments were also observed to form, but less than 10 % of the filaments were paired helical filaments. The bars are 100 nm.

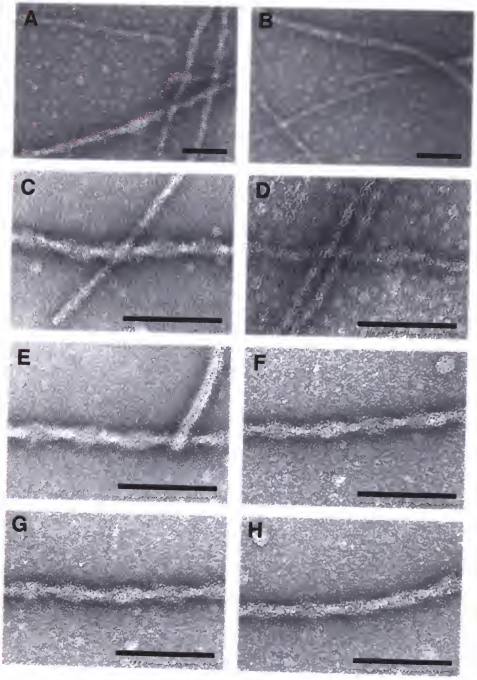
A
B
C
D
E
F
G
H

Discussion

To better understand the factors that control Tau polymerization in Alzheimer disease and the other diseases characterized by neurofibrillary tangles, I undertook this work on the assembly behavior of MAP2. It now appears that small changes in primary sequence can confer upon MAP2-123 the ability to form paired helical filament-like structures. At the same time, several differences in the assembly properties of MAP2-123 and Tau-123 were also observed. These differential effects were most prominent in the assembly reactions containing heparin and tRNA. The presence of heparin or tRNA inhibited the MAP2-123 assembly process, and these agents never induced the formation of any paired helical filament-like structures with MAP2-123. They were employed as a tool in the experiments with the MAP2-123 mutants. The use of tRNA and heparin allowed for assembly reactions with lower protein concentrations and shorter incubation times.

Tau-123 polymerized in the absence of polyanions at concentration from 500 - 1000 μM when incubated for 3 - 4 weeks, and a variety of structures formed including straight filaments, coils and paired helical filaments. The Tau-123 filaments aggregated; they were difficult to observe individually on the electron microscope, and they did not polymerize to the extent observed with MAP2-123. Incubation of the Tau-123 samples with the heparin or tRNA did decrease the amount of time or lower the protein concentration needed to form filaments. However, the filaments never formed in abundance. In fact, the proportion of true paired helical filament-like structures that form with Tau-123 is quite low. Although recent papers have shown Tau polymerizes *in vitro* into a variety of structures including paired helical filaments, these results suggest that there are differences between Alzheimer paired helical filaments and those formed *in vitro*. Most obvious is that Alzheimer tangles are almost entirely paired helical filaments, whereas those formed *in vitro* are almost entirely straight filaments. This may arise from a preferential degradation of straight filaments as compared to paired helical filaments that form in Alzheimer disease.

The MAP2-123 [Module-A] was polymerized in the presence of tRNA at low protein concentration after an overnight incubation at 37 ° C. Like Tau-123, the structures formed were mostly straight filaments that formed lateral associations and assembled into aggregates. Additionally, the MAP2-123 [Module-A] formed some filaments which modulated in width from 8 - 18 nm. MAP2-123 [Module-A], like Tau, formed more than one type of filamentous structure and polymerized in the presence of tRNA. The MAP2-123 [Module-B] mutants formed mostly paired helical filament-like structures with numerous straight filaments. This mutant actually formed a larger proportion of paired helical filament-like structures than Tau-123; and they resembled the Tau-123 paired helical filaments made with heparin (Kampers et al., 1996). These results indicated that individual amino acid residues in the Module-B region of MAP2-123 may control paired helical filament formation.

None of the individual point mutants in Module-B of MAP2-123 turned out to behave like MAP2-123. MAP2-123-MBP3 was the only mutant that polymerized well at low concentrations without tRNA or heparin. This was similar to the MAP2-123 assembly behavior, but MAP2-123-MBP3 differed from MAP2-123 in its ability to form multiple type of filaments. The structures formed included straight filaments 8 - 10 nm wide and miniature paired helical filaments with modulations in width of 6 - 10 nm. MAP2-123-MBP1 and MAP2-123-MBP2 did not assemble well without tRNA or heparin; but in the presence of these polyanions, they were assembled into several types of filaments like Tau-123. These structures included straight filaments 8 - 10 nm wide, straight filaments 16 - 18 nm wide and some paired helical filament-like structures although none exhibited the regular periodicity and characteristic width modulations observed in Alzheimer filaments. Some MAP2-123-MBP1 filaments modulated in width from 8 - 18 nm, but they formed infrequently. The MAP2-123-MBP2 formed miniature paired helical filaments 6 - 10 nm in diameter resembling those formed by Tau-123 (Crowther et al., 1992) or MAP2-123-MBP3, but they formed less frequently than the straight filaments.

Moreover, MAP2-123-MBP4 did not polymerize as well as MAP2-123 in the absence of tRNA or heparin, but in the presence of these polyanions it appeared to polymerize more extensively than Tau-123. The use of tRNA or heparin resulted in the formation of numerous paired helical filaments with a diameter of 8 - 18 nm and a regular crossover distance of 55 - 60 nm. Straight filaments of 8 - 10 nm and 16 - 18 nm were also observed, but their abundance was less than that of the paired helical filaments. In the assembly reactions without polyanions, these same structures were observed, but the straight filaments accounted for most of the filaments observed. Still, MAP2-123-MBP4 formed a variety of filamentous structures as does Tau-123 when incubated without polyanions, and it assembled more quickly and at lower concentrations than Tau-123. In the presence of tRNA, it assembled more quickly than Tau-123, and the proportion of paired helical filaments formed was much larger than that observed with Tau-123.

These experiments demonstrate that the *in vitro* polymerization properties of MAP2-123 are very susceptible to small changes in the primary sequence around the second repeat. This second repeat contains the lone cysteine in the microtubule-binding region, and it has been demonstrated that the second repeat sequence stimulated microtubule assembly (Joly et al., 1989; Coffey et al., 1994). Additionally, phosphorylation sites which control MAP2-stimulated microtubule assembly are localized in and around this repeat (Ainzstein et al., 1994) further emphasizing the importance of the second repeat in MAP2 interactions with microtubules. Because small changes in the primary sequence in and around the second repeat of MAP2 generated an assembly competent protein that forms paired helical filament-like structures *in vitro*, it is possible these changes have been selected against so that MAP2 fragments do not assemble *in vivo*. If this were true, then using this information may lead to the identification of regions in Tau which could be targeted to prevent Tau assembly and the formation of neurofibrillary tangles.

CHAPTER 5
CONCLUSIONS AND FUTURE DIRECTIONS

Conclusions

Microtubule-associated protein Tau is the major component of the pronase-resistant core of paired helical filaments from Alzheimer neurofibrillary tangles (Wischik et al., 1988), and nearly one dozen other neurodegenerative diseases have neuropathology characterized by the presence of structures resembling neurofibrillary tangles (Wisniewski et al., 1978; Jellinger, 1996; Spillantini et al., 1997). This dissertation research examined the *in vitro* assembly properties of the microtubule-binding region of another neuronal microtubule-associated protein designated MAP2. The findings presented here in conjunction with the results from earlier studies suggest that MAP2 may also be a component of filaments in these other diseases because : (a) The microtubule-binding region of Tau is known to polymerize into a variety of filaments including some that resemble Alzheimer filaments (Crowther, 1992; Schweers et al., 1995). (b) MAP2 and Tau share a microtubule-binding region that is 70% identical in primary sequence. (c) Neurofibrillary tangles form in the cell bodies of neurons in Alzheimer disease where MAP2 is predominant while Tau is an axonal protein. (d) Neither MAP2 or Tau from Alzheimer brain stimulate tubulin assembly (Iqbal et al., 1986) suggesting that MAP2 and Tau are exposed to similar regulatory events in Alzheimer disease and may be located in the same cellular regions. Together, these findings suggest that if MAP2 can polymerize, then its presence should be sought in the filaments of all the neurofibrillary containing diseases. If it does not polymerize, then it should be studied to learn how Tau assembly might be prevented. The purpose of this study was to determine whether the microtubule-binding

region of MAP2 could assemble *in vitro* into filaments resembling Alzheimer paired helical filaments, and to learn what factors control MAP2 polymerization.

Using conditions known to promote the assembly of Tau-K12 and Tau-123, components that contain the repeat region of the microtubule-binding region (Schweers et al., 1995), recombinant MAP2-123 was tested to determine whether it contained sequences which prevented its assembly. The results clearly demonstrated that MAP2-123 could assemble into structures resembling Alzheimer straight filaments. Additionally, fragments of MAP2 containing the projection arm in addition to the microtubule-binding region were incubated under similar conditions to determine if sequences outside the repeat region of MAP2-123 which are absent in Tau prevented the polymerization of MAP2. These fragments, MAP2-N123C and MAP2-NN123C, and full-length MAP2c all assembled into polymers resembling Alzheimer straight filaments. These straight filaments had a diameter of 8 - 12 nm depending on the fragment, and comparison of electron micrographs of Alzheimer paired helical filaments and MAP2 filaments suggested that the MAP2 straight filaments correspond to half of an Alzheimer paired helical filament.

Additional studies demonstrated that MAP2-123, MAP2-N123C and MAP2-NN123C polymerized from the ends of Alzheimer paired helical filament seeds in an assembly reaction that did not induce the formation of paired helical filaments. These experiments confirmed that the MAP2 straight filaments correspond to half of a paired helical filament. Even more significantly, they suggested that MAP2 may modulate Tau filament assembly in Alzheimer disease. This would occur if the MAP2 could add onto the ends of Alzheimer filaments as a competitive binding inhibitor thereby preventing Tau addition until the MAP2 was removed. These results also suggested that MAP2 and Tau share certain structurally similar surfaces since they both can bind and elongate from Alzheimer filaments (Wilson and Binder, 1997). Binding studies with the Alzheimer diagnostic dye thioflavin S and MAP2 filaments demonstrated that the interaction leads to characteristic fluorescence similar to that observed with thioflavin S binding to Alzheimer

filaments (Schweers et al., 1995). This was a second line of evidence for a structurally similar element in MAP2 and Tau, and it further demonstrated that MAP2 filaments share structural features with Alzheimer filaments.

After demonstrating that the microtubule-binding region of MAP2 polymerized into filaments resembling Alzheimer filaments, experiments were conducted to evaluate the role of the second repeat cysteine in the polymerization process. The analogous cysteine in three-repeat Tau was shown to form an intermolecular disulfide linkage which resulted in the formation of a dimer, and the assembly of Tau-K12 containing the three repeats was shown to be greatly inhibited when formation of this disulfide cross-linked dimer was blocked by mutating the cysteine to an alanine (Schweers et al., 1995). The SDS-PAGE data presented here demonstrated that a disulfide cross-linked dimer does form before MAP2 filaments are formed, and these results were confirmed by analytical ultracentrifugation. The role of this dimer in the assembly process was studied using MAP2-123 (C1709A), a protein that could not form disulfide cross-linked dimers. The assembly reaction with this mutant was greatly retarded, but the formation of filaments was observed upon incubation at high concentrations for 3 - 4 weeks. This lag behavior suggests that disulfide cross-linked dimer formation is not required for polymerization, but disulfide cross-linked dimer formation does increase the rate of reaction and lower the concentration of MAP2-123 needed for assembly. These results are in agreement with those for Tau-K12 (Schweers et al., 1995) and suggest that filaments can form before the neurons of Alzheimer patients are under oxidative stress. Again, our findings enforce the idea that Tau and MAP2 filaments are very similar emphasizing the importance of finding the factors which permit Tau and not MAP2 polymerization and accumulation *in vivo*.

Several notable differences in the polymerization behavior of MAP2 and Tau were revealed in the course of these studies. Because the Tau-123 and MAP2-123 constructs containing the repeat region polymerized better than longer forms (Crowther et al., 1992; Wille et al., 1992; DeTure et al., 1996), these proteins were used to examine the effects of

various polyanionic components and solution conditions on filament formation. Interestingly, MAP2-123 (500 - 1000 μM) polymerized within 5 days, compared to 4 weeks required by Tau-123. MAP2-123 assembled at concentrations below 50 μM, whereas assembly of Tau-123 required concentrations greater than 500 μM. The other major difference between Tau and MAP2 filaments was the ability of Tau-123 to form many different structures including two classes of straight filaments (8 - 10 nm and 16 -18 nm), coils, ribbons and some filaments resembling true paired helical filaments. MAP2-123 only formed 8 - 10 nm straight filaments. This versatility in forming many different structures appears to be a hallmark of Tau. It is possible that paired helical filaments are more stable *in vivo*, and this is why Tau paired helical filaments are predominant in Alzheimer brain.

Because MAP2 only forms straight filaments, efforts to identify factors and conditions that promote paired helical filament formation were undertaken. Recent studies on the assembly of Tau in the presence of certain polyanions, like heparin and tRNA, have demonstrated that these factors promote Tau assembly (Perez et al., 1996; Goedert et al., 1996; Kampers et al., 1996). These agents lower the concentration of Tau needed for assembly to below 100 μM, and they decrease the assembly time to under 24 hours. These findings were useful, because these polyanionic agents can be used as a tool in the *in vitro* assembly reactions with Tau. These polyanions do not force the formation of more paired helical filaments. They simply decrease the reaction times and concentrations of Tau-123 needed for assembly. Because the tRNA and polyglycosaminoglycans are candidates for stimulating Tau polymerization in Alzheimer tangles, their effects on MAP2-123 assembly were tested. The ratio of Tau:heparin for paired helical filament formation was optimal at 4:1 (Goedert et al., 1996), and MAP2-123:heparin ratios from 1:1 - 10:1 were tested. Neither heparin, heparan sulfate or tRNA stimulated assembly of MAP2-123 nor did any of them induce the formation of paired helical filaments. In fact, these polyanions all interfered with MAP2-123 assembly and inhibited MAP2-123 assembly in a concentration

dependent manner. These results, and the MAP2 assembly from Alzheimer filaments, suggested that the ability to form paired helical filaments was intrinsic to Tau-123, and outside factors did not cause paired helical filaments formation *in vitro*. In the Alzheimer neuron, this may or may not be true, and cellular factors may be involved in the selective formation and/or accumulation of paired helical filaments.

If all the information needed to form paired helical filaments is contained in the primary sequence of Tau-123, then motifs in MAP2-123 that promote paired helical filament formation must be absent or motifs that block paired helical filament formation must be present. The goal of the last set of experiments was to identify amino acids mutations in MAP2-123 which would permit and enhance the formation of paired helical filaments *in vitro*. When the sequences of Tau-123 and MAP2-123 were aligned, two regions were identified that differed most in amino acid composition. Module-A is located at the end of the first repeat, and Module-B is located after the end of the second repeat. The MAP2-123 [Module-A] mutants assembled into a number of structures including straight filaments which bundled and some twisting filament with modulations in width from 10 - 20 nm that resembled paired helical filaments. This suggested that amino acids in Module-A of MAP2-123 do help control the formation of only straight filaments of 8 - 10 nm. The MAP2-123 [Module-B] mutants formed numerous paired helical filaments of 8 - 18 nm which easily outnumbered the straight filaments. This suggested that amino acids in Module-B were extremely important in controlling the filament morphology of MAP2-123 structures. The final experiments were done to identify which specific amino acids controlled paired helical filament formation in MAP2-123.

The four mutations in Module-B of MAP2-123 were made individually, and they were incubated with tRNA under conditions that facilitated Tau-123 assembly or without tRNA under conditions that favored MAP2-123 assembly. The MAP2-123 point mutants R1723Q, K1725E, E1727K and V1729E each acquired certain assembly characteristics similar to Tau. They all polymerized in the presence of tRNA at concentrations below 100

μM, but only MAP2-123-MBP3, the E1727K mutant, polymerized well at concentrations of 200 - 400 μM without tRNA in 5 days like MAP2-123. Each of these mutants acquired the ability to assemble into a variety of structures including straight filaments, coils, ribbons, braided filaments and most notably paired helical filaments. The mutants MBP2 (K1725E) and MBP3 (E1727K) each formed miniature paired helical filaments while MBP4 (V1729E) formed true paired helical filament-like structures with modulations in width from 8 - 18 nm. The MAP2-123-MBP4 (V1729E) almost entirely formed paired helical filaments under certain MAP2:tRNA ratios; and in the absence of tRNA, it formed a larger proportion of paired helical filaments than was observed in the Tau-123 control experiments. These results demonstrated that individual point mutations in the Module-B sequence could convey many characteristics of Tau-123 to MAP2-123 suggesting that these amino acids in Tau must be important for proper function since they are conserved in mammals.

In summary, MAP2 fragments and full-length MAP2c assembled readily into straight filaments 8 - 12 nm in diameter. At physiological pH, these filaments formed at concentrations that were one order of magnitude lower than required for Tau assembly. The MAP2 filaments bound thioflavin S in a manner resembling Alzheimer filaments, and MAP2 fragments assembled from the ends of Alzheimer filaments. The results of these experiments demonstrated that the microtubule-binding regions of Tau and MAP2 may share tertiary structural features. Additionally, the polymerization process for MAP2 and Tau fragments proceeded more readily after disulfide cross-linked dimer formation occurred; however, some filaments formed when disulfide formation was inhibited. MAP2 and Tau were shown to behave differently in the presence of heparin or tRNA. These agents promoted Tau assembly but inhibited MAP2 polymerization. Finally, amino acids in Module-B of MAP2 were identified that prevented paired helical filament formation.

A summary of the assembly characteristics of the fragments used in this study can be found in Table 5-1. Taken together, these results suggest that the microtubule-binding

Table 5-1. Summary of Assembly Characteristics of MAP2 Recombinant Proteins.

Protein	Filament Types	Comments
MAP2-123	Straight Filaments	8.7 ± 1.0 nm
MAP2-N123C	Straight Filaments	10.6 ± 1.0 nm
MAP2-NN123C	Straight Filaments	11.8 ± 1.4 nm
MAP2c	Straight Filaments	12.4 ± 1.2 nm
MAP2-123 [Module-A]	Two Straight Filaments >> Paired Helical Filaments	8 - 10 nm / 16 - 18 nm 8 - 18 nm / no regular helix RNA promotes assembly
MAP2-123 [Module-B]	Paired Helical Filaments >> Two Straight Filaments	8 - 18 nm / regular helix 8 - 10 nm / 16 - 18 nm RNA promotes assembly
MAP2-123-MBP1	Two Straight Filaments	8 - 10 nm / 16 - 18 nm RNA promotes assembly
MAP2-123-MBP2	Straight Filaments > Mini Paired Helical Filaments	8 - 10 nm / 6 - 10 nm RNA promotes assembly
MAP2-123-MBP3	Straight Filaments > Mini Paired Helical Filaments	8 - 10 nm / 6 - 10 nm RNA promotes assembly
MAP2-123-MBP4	Paired Helical Filaments > Two Straight Filaments	8 - 18 nm / regular helix 8 - 10 nm / 16 - 18 nm RNA promotes assembly
Tau-123	Two Straight Filaments >> Paired Helical Filaments Mini PHFs, Coils, Ribbons	8 - 10 nm / 12 - 15 nm 8 - 18 nm / regular helix RNA promotes assembly

regions of Tau and MAP2 are extremely similar; and if the factors which block MAP2 assembly in Alzheimer disease can be identified, then methods for preventing Tau polymerization might be developed from this information.

Future Directions

The results on MAP2 polymerization presented in this dissertation clearly indicate that the microtubule-binding regions of Tau and MAP2 are highly related, yet only Tau has

been identified biochemically as a component of the pronase-resistant core of Alzheimer paired helical filaments (Wischik et a., 1988). Other proteins like MAP2 may be minor components of the Alzheimer filaments, or MAP2 may never be incorporated into Alzheimer filaments. Understanding the factors which prevent MAP2 assembly and/or accumulation into Alzheimer filaments may explain why Tau is incorporated into filaments selectively. This information could lead to the development of methods for inhibiting Tau assembly in Alzheimer disease. About a dozen neurodegenerative diseases exhibit neurofibrillary tangle pathology (Wisniewski et al., 1978; Jellinger, 1996; Spillantini et al., 1997), but only the filaments from Alzheimer brain have been purified and analyzed biochemically. Since MAP2 assembles quite well *in vitro*, MAP2 may prove to be a component in tangles formed during the progression of these diseases. Examining brain tissue from patients affected with these disorders may lead to the discovery of filaments containing MAP2. The majority of antibodies against MAP2 have epitopes in the projection arm of MAP2, but this region of MAP2 may be removed during NFT formation as levels of certain proteases appear to be elevated. Generating an antibody to the MTBR of MAP2 outside the core fragment which assembles would increase the probability of identifying MAP2 in the tangles of these diseases if it is a component of the filaments.

One poorly understood aspect of Alzheimer filament formation is the paradox that neurofibrillary tangles contain mainly paired helical filaments whereas those formed *in vitro* with recombinant Tau are predominantly straight filaments (Crowther et al, 1994; Schweers et al., 1995; Wilson and Binder, 1995). Presumably, paired helical filaments form more rapidly than straight filaments, and their different rates of formation leads to the preponderance of paired helical filaments. However, Tau may assemble into straight filaments more rapidly than it forms paired helical filaments *in vivo*, but the straight filaments may be more susceptible to degradation. This would also lead a majority of paired heilcal filaments in Alzheimer neurofibrillary tangles. This hypothesis could be tested with Tau filaments *in vitro* to determine which Tau structures are the most stable,

protease resistant or susceptible to depolymerizing agents. Such experiments could lead to an explanation of why MAP2 straight filaments are not found in Alzheimer disease. A comparison of the stability of Alzheimer paired helical filaments and straight filaments to filaments composed of recombinant Tau or MAP2 may explain the preponderance of certain filament types in the different diseases with neurofibrillary tangles. If MAP2 did assemble into straight filaments in Alzheimer tangles and if paired helical filaments predominate due to their stability, it would be expected that MAP2 might never be identified as a component of pronase-treated Alzheimer filaments. Additionally if this scenario were correct, the components in the straight filaments may have been missed in the biochemical characterization of the Alzheimer tangles which contain mostly paired helical filaments (Wischik et al., 1988). No one has examined the proteolysis of MAP2 filaments or compared the relative stability of Tau paired helical filaments and straight filaments.

High-molecular-weight MAP2 is highly susceptible to proteolysis in the hinge region which connects the microtubule-binding region to the projection arm of the molecule. The microtubule-binding domain of MAP2 can be generated by cleavage with thrombin, chymotrypsin, trypsin or calpain (Vallee and Borisy, 1977; Joly et al., 1989; Johnson et al., 1991a), and work presented in this dissertation demonstrates fragments of MAP2 corresponding to MAP2 cleavage by these proteases can assemble into Alzheimer-like filaments. Any aberrant action of these proteases and related proteases within the neuron could generate proteolytic cleavage products capable of forming straight Alzheimer-like filaments or fragments that could be incorporated into Tau straight filaments. For example, calpain and cathepsin D which both cleave MAP2 (Johnson et al., 1991a; Johnson et al., 1991b) are also thought to be activated in Alzheimer disease (Cataldo and Nixon, 1990; Saito et al., 1993). The ability of the microtubule-binding regions of Tau or MAP2 from Alzheimer brain to assemble *in vitro* remains to be determined. These proteins can be purified, and the microtubule-binding region can be generated by protease cleavage. The ability of these proteins to polymerize could be compared to the assembly of

corresponding recombinant proteins. Perhaps the rate of assembly is not as important as the stability of the filament that forms. Maybe most of the filaments from Alzheimer Tau form paired helical filaments while recombinant Tau forms mostly straight filaments. This knowledge could then be used to screen agents that modify Tau and force its assembly into paired helical filaments not straight filaments. If one believes that recombinant Tau assembly is an important model system, then understanding how it relates to the assembly of purified Alzheimer Tau is even more important.

Familial multiple system tauopathy, progressive supranuclear palsy and corticobasal degeneration are three disease in which the filaments in the neurofibrillary tangles do not resemble Alzheimer filaments. Possibly factors found in Alzheimer brain are absent in these diseases. Investigations on the relative concentrations of kinases, phosphatases, calcium ions, AGEs, polyglycosaminoglycans or other cellular compounds could lead to the identification of which components are acting abnormally in these neurodegenerative diseases. Were MAP2 never to be found as a component of the neurofibrillary tangles from any of these disorders, neurofibrillary tangles still form in the cell body where MAP2 is located. This implies that factors which alter Tau function may also affect MAP2. The work showing that microtubule-associated proteins from Alzheimer brain could not promote tubulin assembly (Iqbal et al., 1986) suggests that MAP2 and Tau must both be affected. These experiments showed the Tau to be hyperphosphorylated, but microtubule assembly should have been stimulated if the MAP2 was normal. No one has closely examined the MAP2 from Alzheimer brain or the brains from individuals with the other neurofibrillary diseases to see how MAP2 promotes microtubule assembly or functions in stabilizing microtubules. This should be done because dendritic changes in Alzheimer disease are extensive, and they are thought to reflect abnormal MAP2 behavior (McKee et al., 1989; Irving et al., 1996; Anderton et al., 1998). Because it is not known what kills the afflicted neurons in Alzheimer disease, the loss of cytoskeletal structure due to abnormal Tau and/or MAP2 function may be responsible. Clearly, axons and dendrites are

needed for proper neuronal function, and the loss of either of these structures may trigger neuronal death.

Identifying the factors that precipitate in neuronal degeneration and death in Alzheimer disease is hampered by the fact that brain tissue from these patients cannot be analyzed until death. This means decades of time pass between onset of the disease and the biochemical sampling of tissue. At this time, there is no suitable animal or cellular model exhibiting both senile plaques and neurofibrillary tangles characteristic of Alzheimer disease. Transgenic mice have been generated with mutant amyloid precursor protein or presenilin transgenes (Sturchler-Pierrat et al., 1997; Oyama et al., 1998; Price and Sisodia, 1998). These mice exhibit increased concentrations of β-amyloid peptides, dystrophic neurites, oxidative stress and amyloid deposits, but the formation of neurofibrillary tangles do not accompany the plaques. This is true even for mice carrying both mutated amyloid precursor protein and presenilin 1 transgenes (Holcomb et al., 1998). Additionally, no animal models have been developed which exhibit neurofibrillary tangles. This may change soon as genes carrying Tau mutations have been identified in Pick's disease or multiple system tauopathy with presenile dementia (Hutton et al., 1998; Spillantini et al., 1998; Poorkaj et al., 1998). It would be beneficial to generate mice carrying transgenes with the mutations found in Tau that are linked to Pick's disease. These mice could then be examined for neurofibrillary tangles formation and factors which leads to the onset of this disease might be easier to identify as mice could be sacrificed at different stages in the development of the disease. Additionally, transgenic animals closer to humans than mice could be generated which carry the familial Alzheimer mutations. These animals may then form senile plaques and neurofibrillary tangles due to differences in neuronal composition.

Another limiting factor in the study of paired helical filament and straight filament formation *in vitro* is the lack of a truly quantitative assay for following filament formation. Centrifugation techniques often lack the ability to discern between precipitation, aggregation and filaments formation while quantitation on the basis of electron micrographs

is susceptible to clumping distortions and unequal adsorption rates. The use of fluorescent probes to measure filament assembly might prove to be quite useful. During the writing of this dissertation, the use of thioflavin S as a quantitative measure of filament polymerization was reported (Friedhoff et al., 1998). This workers demonstrated the potential of this assay and described some of the limitations. The greatest problem was that the assay is only linear from 0.1 - 4.0 μM of monomeric Tau in filaments, but it was routinely used at monomeric protein concentrations as high as 100 μM. There is also the concern that disulfide cross-linked dimers fluoresce when bound to thioflavin S (personal communication, Kampers). Finally, the study never proves that structures other than paired helical filaments cause thioflavin S fluorescence, although they show electron micrographs of samples containing straight filaments and paired helical filaments which lead to thioflavin S fluorescence. The study does demonstrate that under the right conditions fluorescence may be viable, and more work should be done to define the conditions where this assay operates accurately.

No one has looked at the differences in binding affinity for AD-Tau binding to itself, normal Tau or MAP2 although AD-Tau binds to each of these species (Alonso et al., 1994; Alonso et al., 1996; Alonso et al., 1997). The rapid formation of specific dimeric species may prevent certain Tau or MAP2 isoforms from forming dimers that can be incorporated into filaments. This incorporation of certain isoforms of Tau into filaments certainly is observed in the neurofibrillary tangle bearing diseases which do not form paired helical filaments (Spillantini et al., 1997). Quantitation of the rate of dimerization or the equilibrium constant for dimerization may be more convenient than measuring filament assembly, but there still are several obstacles. Non-reducing SDS-PAGE can be used to follow homodimerization if the time-course of dimer formation is long enough, but the technique cannot be used if the samples that are the same size. Better techniques should be developed for quantifying dimerization. Currently, techniques are being developed in the Purich lab to label MAP2 or Tau so that filament assembly is not affected. Then

dimerization in the presence and absence of reducing agents can be followed continuously in the analytical ultracentrifuge. This would permit quantitation of the equilibrium constant for dimer formation of different species. These constructs should also allow filament formation to be directly observed using fluorescence microscopy, and this would allow the direct quantitation of filaments. In fact, if filaments form *in vivo* which are polar due to the selective incorporation of particular heterodimers, this could be visualized with fluorescence microscopy by quantifying the rate of growth from each end of an unlabeled Alzheimer filament with labeled protein.

Under normal conditions, Tau should be absent from the neuronal cell body where neurofibrillary tangles are most frequently observed to accumulate in affected neurons (Anderton et al., 1993; Trojanowski and Lee, 1994). Incorrect targeting of Tau to the neuronal cell body where proteolysis may generate fragments of the microtubule-binding region from both Tau and the normally resident MAP2 could be a factor in neurofibrillary tangle formation. In this regard, studies of Tau and MAP2 copolymerization *in vitro* may reveal whether their combined presence promotes or inhibits the polymerization process. MAP2 fragments may affect nucleation by altering the minimum concentration of Tau required for paired helical filament assembly. Indeed, the experiments presented here suggest that MAP2 fragments containing the repeat region are capable of binding Tau paired helical filaments and have the potential to modulate the addition of Tau subunits onto the ends of these filaments. Regardless of whether MAP2 fragments become incorporated into Alzheimer filaments, the demonstration that they bind and assemble from the ends of these filaments implies that if this occurs *in vivo* MAP2 fragments can act to mediate Tau elongation from paired helical filaments. In this scenario, higher concentrations of MAP2 would decrease the rate of Tau addition onto filaments while lower concentration of MAP2 would lead to increased rates of Tau addition. These experiments revealed a potentially important role for MAP2 during Alzheimer neurofibrillary tangle formation, and experiments need to be done to determine how MAP2 affects Tau assembly.

Currently, no reports have been published on the assembly of recombinant Tau and MAP2 heterodimers. Alzheimer Tau is know to bind normal Tau and MAP2 presumably by forming a disulfide linkage, and it is known that the AD-Tau assembles into 2.5 - 3.3 nm filaments in the presence of normal Tau but not normal MAP2 (Alonso et al., 1996; Alonso et al., 1997). These filaments resemble those formed when Alzheimer paired helical filaments are deglycosylated (Wang et al. 1996). This suggests that the MAP2 interaction somehow blocks assembly. By using the recombinant microtubule-binding domain of Tau or MAP2 with AD-Tau to form heterodimers, it could be determined if the ability of MAP2 to interfere with AD-Tau assembly was an inherent property of the microtubule-binding region of MAP2 or whether cellular modifications or perhaps the projection arm interfered with AD-Tau assembly. This would lend support to the hypothesis that MAP2 could modulate Alzheimer filament assembly by adding to the ends of Alzheimer filaments and preventing Tau elongation. Looking at the addition of MAP2 homodimers, Tau homodimers or Tau and MAP2 heterodimers to purified filaments from Alzheimer brain tissue or brain tissue from the other neurodegenerative disease might suggest how these filaments form in each specific disease.

Filaments from Alzheimer patients are extremely insoluble and contain a pronase-resistant core (Wischik et el., 1988), but little work has been done to describe the factors which stabilize the filaments. The development of methodology for generating filaments from Tau and MAP2 *in vitro*, permits the differential disassembly properties of these filaments to be investigated. These experiments could explain why certain Tau isoforms are selectively incorporated into the filaments from different diseases (Spillantini et al., 1997). Additionally, cellular components could be screened for their ability to preferentially stabilize straight and paired helical filaments. The identification of a kinase which confers stability to these filaments or the identification of a protease which only digests unpolymerized Tau may indicate which factors should be examined for their role in tangle formation and disease development. These studies could also lead to the discovery

of cellular agents which can disassemble Tau filaments. If these agents are not active in Alzheimer development, restoring their activity might be therapeutic.

Specific amino acids in MAP2-123 have been identified that prevent the formation of paired helical filaments, but it is not known if these residues (a) were inhibiting a paired helical filament promoting motif elsewhere in MAP2-123 or (b) did not constitute a paired-helical-filament-promoting motif. If MAP2-123 already contains a paired-helical-filament-promoting motif, then disruption of the Module-B sequence by deletion or replacement should still allow the formation of paired helical filaments. If the Module-B region of Tau-123 actually coded for a paired-helical-filaments-promoting motif, then the substitutions allowable in MAP2-123 [Module -B] should be limited as the motif itself must be conserved. Additionally, the requirements on the location of the paired-helical-filament-promoting motif could be determined. Presumably, Tau-123 does not contain any paired-helical-filament-inhibiting motifs so random mutations in Module-B should disrupt the ability of Tau-123 to form paired helical filaments unless there are other paired-helical-filament-promoting sequences in Tau-123. However, replacement of the Tau-123 Module-B sequence with that of MAP2-123 [Module-B] sequence should interfere with paired helical filament formation if the MAP2-123 [Module-B] sequence actually does inhibit paired helical filament formation. These experiments where Tau-123 [Module-B] are mutated to the sequences in MAP2-123 [Module-B] should help determine how these Module-B sequences are functioning, and if they are paired-helical-filament-promoting sequences, they might be attractive targets for disrupting paired helical filament formation *in vivo*.

The experimental results presented in this dissertation should aid in the design of further experiments to determine how neurofibrillary tangles, and specifically paired helical filaments, form. Tau, the major component of Alzheimer filaments, is a potentially harmful MAP, but mice lacking Tau have been made and appear healthy (Brandt, 1996). Apparently, some of the roles of these microtubule-associated proteins remain unknown.

LIST OF REFERENCES

Ainzstein, A. M. and Purich, D. L. (1994) Stimulation of Tubulin Polymerization by MAP2: Control by Protein Kinase C Phosphorylation at Specific Sites in the MT Binding Region. *J. Biol. Chem.* 269: 28465-28471.

Alberts, B., Bray, D., Lewis, J., Raff, M., Roberts, K. and Watson, J. D. (1994) Molecular Biology of the Cell. 788-847, Garland Publishing Inc. New York, NY.

Alonso, A. C., Grundke-Iqbal, I., Barra, H. S., and Iqbal, K. (1997) Abnormal Phosphorylation of Tau and the Mechanism of Alzheimer Neurofibrillary Degeneration: Sequestration of Microtubule-associated Proteins 1 and 2 and the disassembly of Microtubules by the Abnormal Tau. *Proc. Natl. Acad. Sci U.S.A.* 94: 298-303.

Alonso, A. C., Grundke-Iqbal, I., and Iqbal, K. (1996) Alzheimer's Disease Hyperphosphorylated Tau Sequesters Normal Tau into Tangles of Filaments and Disassembles Microtubules. *Nat. Med.* 2: 783-787.

Alonso, A. C., Zaidi, T., Grundke-Iqbal, I. and Iqbal, K (1994) Role of Abnormally Phosphorylated Tau in the Breakdown of Microtubules in Alzheimer Disease. *Proc. Natl. Acad. Sci. U.S.A.* 91: 5562-5566.

Anderton, B. H. (1993) Expression and Processing of Pathologic Proteins in Alzheimer's Disease. *Hippocampus* 3: 227-237.

Anderton, B. H., Breinberg, D., Downes, M. J., Green, P. J., Tomlinson, B. E., Ulrich, J., Wood, J. N. and Kahn, J. (1982) Monoclonal Antibodies Show that Neurofibrillary Tangles and Neurofilaments Share Antigenic Determinants. *Nature* 298: 84-86.

Anderton, B. H., Callahan, L., Coleman, P., Davies, P., Flood, D., Jicha, G. A., Ohm, T. and Weaver, C. (1998) Dendritic Changes in Alzheimer's Disease and Factors that May Underlie These Changes. *Prog. Neurobiol.* 55: 595-609.

Angelastro, J. M. and Purich, D. L. (1992) 2'-Deoxy-GTP in the Microtubule Cytoskeleton of Neuronal Cells Cultured with Nerve Growth Factor. *J. Biol. Chem.* 267: 25685-25689.

Angelastro, J. M. and Purich, D. L., (1994) Microtubule Dynamics: Bioenergetics and Control. *Adv. Enzymol. Relat. Areas Mol. Biol.* 69: 121-154.

Baas, P. W. and Ahmad, F. J. (1992) The Plus Ends of Microtubules are the Exclusive Nucleating Structures for Microtubules in the Axon. *J. Cell Biol.* 116: 1231-1241.

Baudier, J. and Cole, R. D. (1987) Phosphorylation of Tau Proteins to a State Like that in Alzheimer's Brain Is Catalyzed by a Calcium/Calmodulin-dependent Kinase and Modulated by Phospholipids. *J. Biol. Chem.* 262: 17577-17583.

Benzi, G. and Moretti, A. (1995) Are Reactive Oxygen Species Involved in Alzheimer's Disease? *Neurobiol. Aging* 16: 661-674.

Berling, B., Wille, H., Roll, B., Mandelkow, E., Garner, C. and Mandelkow, E. (1994) Phosphorylation of Microtubule-associated Protein 2C at Ser136 by Proline-directed Kinases. *Eur. J. Cell Biol.* 64: 120-130.

Billingsley, M. L. and Kincaid, R. L. (1997) Regulated Phosphorylation and Dephosphorylation of Tau Protein: Effects on Microtubule Interaction, Intracellular Trafficking and Neurodegeneration. *Biochem. J.* 323: 577-591.

Blanks, J. C., Schmidt, S. Y., Torigoe, Y., Porrello, K. V., Hinton, D. R. and Blanks, H. I. (1996) Retinal Pathology in Alzheimer's Disease: Regional Neuron Loss and Glial Changes in GCL. *Neurobiol. Aging* 17: 385-395.

Bloom, G., Wagner, M., Pfister, K. and Brady, S. (1988) Native Structure and Physical Properties of Bovine Brain Kinesin and Identification of the ATP-binding Subunit Polypeptide. *Biochemistry* 27: 3409-3416.

Bray, D, and Bunge, M. B. (1981) Serial Analysis of Microtubules in Cultured Rat Sensory Axons. *J. Neurocytol.* 10: 589-605.

Brinkley, B. R. (1985) Microtubule Organizing Centers. *Ann. Rev. Cell Biol.* 1: 145-172.

Brion, J. P., Couck, A. M., Passareiro, E. and Flament-Durand, J. (1985) Neurofibrillary Tangles of Alzheimer's Disease: An Immunohistochemical Study. *J. Submicrosc. Cytol.* 17: 89-96.

Cai, X., Golde, T. E. and Younkin, G. S. (1993) Release of Excess Amyloid β Protein from a Mutant Amyloid A Precursor. *Science* 259: 514-160.

Campion, D., Flaman, J. M., Brice, A., Hannequin, D., Martin, C., Moreau, V., Charbonnier, F., Didierjean, O. and Tardieu, S. (1995) Mutations of the Presenilin I Gene in Families with Early-onset Alzheimer's Disease. *Human Mol. Genet* 4: 2373-2377.

Cataldo, A. M. and Nixon, R. A. (1990) Enzymatically Active Lysosomal Proteases Are Associated with Amyloid Deposits in Alzheimer Brain. *Proc. Natl. Acad. Sci. U.S.A.* 87: 3861-3865.

Chen, W. J., Goldstein, J. L. and Brown, M. S. (1990) NPXY, a Sequence often Found in Cytoplasmic Tails, Is Required for Coated-pit Mediated Internalization of the Low Density Lipoprotein Receptor. *J. Biol. Chem.* 265: 3116-3123.

Chin, S. and Goldman J. E. (1996) Glial Inclusions in CNS Degenerative Diseases. *J. Neuropathol. Exp. Neurol.* 55: 499-508.

Citron, M., Oltersdorf, T., Haass, C., McConlogue, L., Hung, A. Y., Seubert, P., Vigo-Pelfrey, C., Lieberburg, I. and Selkoe, D. J. (1992) Mutation of the β-amyloid Precursor Protein in Familial Alzheimer's Disease Increases β-protein Production. *Nature* 360: 672-674.

Coffey, R. L. (1994) The Microtubule-binding Region of Microtubule-associated Protein 2: Investigations with Site-Directed Mutagenesis, Ph.D. Dissertation, University of Florida.

Coffey, R. L., Joly, J. C., Cain, B. D., and Purich, D. L. (1994) Exploring the Microtubule-binding Region of Bovine Microtubule-associated Protein-2 (MAP2): cDNA Sequencing, Bacterial Expression, and Site-directed Mutagenesis. *Biochemistry* 33: 13199-13207.

Coffey, R. L., and Purich, D. L. (1994) Non-cooperative Binding of the MAP2 Microtubule-binding Region to Microtubules. *J. Biol. Chem.* 270: 1035-1040.

Cork, L. C. (1990) Neuropathology of Down Syndrome and Alzheimer Disease. *Am. J. Med. Genet Suppl.* 7: 282-286.

Cork, L. C., Sternberger, L. A., Casanova, M. F., Struble, R. G. and Price, D. L. (1986) Phosphorylated Neurofilament Antigens in Neurofibrillary Tangles in Alzheimer's Disease. *J. Neuropathol. Exp. Neurol.* 45: 56-64.

Cressman, C. M. and Shea, T. B. (1995) Hyperphosphorylation of Tau and Filopodial Retraction Following Microinjection of Protein Kinase C Catalytic Subunits. *J Neurosci. Res.* 42: 648-656.

Crowther, R. A. (1991) Straight and Paired Helical Filaments in Alzheimer Disease Have a Common Structural Unit. *Proc. Natl. Acad. Sci. U.S.A.* 88: 2288-2292.

Crowther, R. A., Olesen, O. F., Jakes, R., and Goedert, M. (1992) The Microtubule Binding Repeats of Tau Protein Assemble into Filaments Like those Found in Alzheimer's Disease. *FEBS Lett.* 309: 199-202.

Crowther, R. A., Olesen, O. F., Smith, M. J., Jakes, R., and Goedert, M. (1994) Assembly of Alzheimer-like Filaments from Full-length Tau Protein. *FEBS Lett.* 337: 135-138.

Dammerman, M., Yen, S. H., and Shafit-Zagardo, B. (1989) Sequence of a Human MAP2 Region Sharing Epitopes with Alzheimer Neurofibrillary Tangles. *J. Neurosci. Res.* 24: 487-495.

DeTure, M. A., Zhang, E. Y., Bubb, M. R., and Purich D. L. (1996) *In Vitro* Polymerization of Embryonic MAP2c and Fragments of the MAP2 Microtubule Binding Region into Structures Resembling Paired Helical Filaments. *J. Biol. Chem.* 271: 32702-32706.

DeTure, M. A. DiNoto, L. and Purich, D. L. (1998) unpublished findings.

Dickson, D. W., Feany, M. B., Yen, S., Mattiace, L. A. and Davies, P. (1996) Cytoskeletal Pathology in Non-Alzheimer Degenerative Dementia: New Lesions in Diffuse Lewy Body Disease, Pick's Disease and Corticobasal Degeneration. *J. Neural Transm.* 47: 31-46.

Dillman, J. F., Dabney, L. P. and Pfister, K. K. (1996) Cytoplasmic Dynein Is Associated with Slow Axonal Transport. *Proc. Natl. Acad. Sci. U.S.A.* 93: 141-144.

Doll, T., Meichsner, M., Riederer, B. M., Honneger, P. and Matus, A (1993) An Isoform of Microtubule-associated Protein 2 (MAP2) Containing Four Repeats of the Tubulin-binding Motif. *J. Cell Sci.* 106: 633-639.

Dudek, S. M. and Johnson, G. V. (1993) Transglutaminase Catalyzes the Formation of Sodium Dodecyl Sulfate-insoluble, Alz-50-reactive Polymers of Tau.*Neurochem.* 61:1159-1162.

Ennulat, D., Liem, R., Hashim, G., and Shelanski, M. L. (1989) Two Separate 18-amino Acid Domains of Tau Promote Polymerization of Tubulin. *J. Biol. Chem.* 264: 5327-5330.

Feany, M. B. and Dickson, D. W. (1995) Widespread Cytoskeletal Pathology Characterizes Corticobasal Degeneration. *Am. J. Pathol.* 146: 1388-1396.

Feany, M. B. and Dickson, D. W. (1996) Neurodegenerative Disorders with Extensive Tau Pathology: A Comparative Study and Review. *Ann. Neurol.* 40: 139-148.

Flament, S., Delacourte, A., Verny, M., Hauw, J. J. and Javoy-Agid, F. (1991) Abnormal Tau Proteins in Progressive Supranuclear Palsy. Similarities and Differences with the Neurofibrillary Degeneration of the Alzheimer Type. *Acta Neuropathol.* 81: 591-596.

Flynn, G., Joly, J. C., and Purich, D. L. (1987a) The 28,000 kDa Microtubule-binding Domain of Microtubule-associated Protein-2 also Contains a Neurofilament-binding Site. *Biochem. Biophys. Res. Comm.* 148: 1453-1459.

Flynn, G., and Purich, D. L. (1987b) GTP Regeneration Influences Interactions of Microtubules, Neurofilaments, and Microtubule-associated Proteins *in Vitro*. *J. Biol. Chem.* 262: 15443-15447.

Friedhoff, P., Schneider, A., Mandelkoe, E. M. and Mandelkow, E. (1998) Rapid Assembly of Alzheimer-like Paired Helical Filaments from Microtubule-associated Protein Tau Monitored by Fluorescence in Solution. *Biochem.* 37: 10223-10230.

Gaelen, R. C. and Haley, B. E. (1977) Interactions of a Photoaffinity Analog of GTP with the Proteins of Microtubules. *Proc Natl. Acad. Sci. U.S.A.* 74: 4375-4377.

Gaelen, R. C. and Haley, B. E. (1979) Use of a GTP Photoaffinity Probe to Resolve Aspects of the Mechanism of Tubulin Polymerization. *J. Biol. Chem.* 254: 11982-11987.

Garner, C. C., Bruggs, B. and Matus, A. (1988) A 70-kilodalton Microtubule-associated Protein (MAP2c), Related to MAP2. *J. Neurochem.* 50: 609-615.

Ghetti, B., Tagliavini, F., Giaconne, G., Bugiani, O., Frangione, B., Farlow, M. R. and Dlouhy, S. R. (1994) Familial Gerstmann-Straussler-Scheinker Disease with Neurofibrillary Tangles. *Mol. Neurobiol.* 8: 41-48.

Gibb, W. R., Esiri, M. M. and Lees, A. J. (1987) Clinical and Pathological Features of Diffuse Cortical Lewy Body Disease. *Brain* 110: 1131-1153.

Glenner, G. G. and Wong, C. W. (1984) Alzheimer's Disease: Initial Report on the Purification and Characterization of a Novel Cerebrovascular Amyloid Protein. *Biochem. Biophys. Res. Comm.* 120: 885-890.

Goedert, M., Crowther, R. A. and Garner, C. C. (1991) Molecular Characterization of Microtubule-associated Proteins Tau and MAP2. *TINS* 14: 193-199.

Goedert, M., Jakes, R., Spillantini, M. G., Hasegawa, M., Smith, M. J., and Crowther, R. A. (1996) Assembly of Microtubule-associated Protein Tau into Alzheimer-like Filaments Induced by Sulfated Glycosaminoglycans. *Nature* 383: 550-553.

Goedert, M., Spillantini, M. G., Cairns, N. J. and Crowther, R. A. (1992) Tau Proteins of Alzheimer Paired Helical Filaments: Abnormal Phosphorylation of all Six Brain Isoforms. *Neuron* 8: 159-168.

Goedert, M., Spillantini, M. G., Jakes, R., Rutherford, D. and Crowther, R. A. (1989) Multiple Isoforms of Human Microtubule-associated Protein Tau: Sequences and Localization in Neurofibrillary Tangles of Alzheimer's Disease. *Neuron* 3: 519-526.

Goedert, M., Wischik, C. M., Crowther, R. A., Walker, J. E. and Klug, A. (1988) Cloning and Sequencing of the cDNA Encoding a Core Protein of the Paired Helical Filament of Alzheimer Disease: Identification as the Microtubule-associated Protein Tau. *Proc. Natl. Acad. Sci. U.S.A.* 85: 4051-4055.

Goode, B. L. and Feinstein, S. C. (1994) Identification of a Novel Microtubule Binding and Assembly Domain in the Developmentally Regulated Inter-Repeat Domain of Tau. *J. Cell Biol.* 124: 769-782.

Goodman, Y. and Mattson, M. P. (1994) Secreted forms of β-amyloid Precursor Protein Protect Hippocampal Neurons Against Amyloid β-peptide-induced Oxidative Injury. *Exp. Neurol.* 128: 1-12.

Greenberg, S. M., Koo, E. H., Selko, D. J., Qiu, W. Q. and Kosik, K. S. (1994) Secreted β-amyloid Precursor Protein Stimulates Mitogen Activated Protein Kinase and Enhances Tau Phosphorylation. *Proc. Natl. Acad. Sci. U.S.A* 91: 7104-7108.

Grundke-Iqbal, I., Iqbal, K., Tung, Y. C., Quinlan, M., Wisniewski, H. M., and Binder, L. I. (1986) Abnormal Phosphorylation of the Microtubule-associated Protein Tau in Alzheimer Cytoskeletal Pathology. *Proc. Natl. Acad. Sci. U.S.A.* 83: 4913-4917.

Hagiwara, H., Yorifuji, H., Sato-Yoshitake, R. and Hirokawa, N. (1994) Competition between Motor Proteins (Kinesin and Cytoplasmic Dynein) and Fibrous Microtubule-associated Proteins to Microtubules. *J. Biol. Chem.* 269: 3581-3589.

Hall, Z. (1994) An Introduction to Molecular Neurobiology. 1-555, Sinauer Associates, Sunderland MA.

Hardy, J. (1992) Framing Beta-amyloid, *Nat Genet* 1: 233-234.

Heins, S., Wong, P. C., Muller, S., Goldie, K., Cleveland, D. W. and Aebi, U. (1993) The Rod Domain of NF-L Determines Neurofilament Architecture, Whereas the End Domains Specify Filament Assembly and Network Formation. *J Cell Biol.* 123: 1517-1533.

Hirano, A., Dembitzer, H. M., Kurland, L. T. and Zimmerman, H. M. (1968) The Fine Structure of some Intraganglionic Alterations: Neurofibrillary Tangles, Granulovacuolar Bodies and Rod-like Structures as Seen in Guam Amyotrophic Lateral Sclerosis and Parkinsonism-dementia Complex. *J. Neuropathol. Exp. Neurol.* 27: 167-182.

Hirano, A., Malamud, N. and Kurland, L. T. (1961) Parkinsonism-dementia Complex, an Endemic Disease on the Island of Guam. *Brain* 84: 662-679.

Hirokawa, M. (1982) Cross-linker System Between Neurofilaments, Microtubules, and Membranous Organelles in Frog Axons Revealed by Quick-freeze, Deep-etching Method. *J. Cell Biol.* 94, 129-142.

Hirokawa, N., Hisanaga, S., and Shiomura, Y. (1988) MAP2 is a Component of Crossbridges Between Microtubules and Neurofilaments in the Neuronal Cytoskeleton: Quick-freeze, Deep-etch Immunoelectron Microscopy and Reconstitution Studies. *J. Neurosci.* 8: 2769-2779

Holcomb, L., Gordon, M. N., McGowan, E., Yu, X., Benkovic, S., Jantzen, P., Wright, K., Saad, I., Mueller, R., Morgan, D., Sanders, S., Zehr, C., O'Campo, K., Hardy, J., Prada, C. M., Eckman, C., Younkin, S., Hsiao, K. and Duff, K. (1998) Accelerated Alzheimer-type Phenotype in Transgenic Mice Carrying both Mutant Amyloid Precursor Protein and Presenilin 1 Transgenes. *Nat. Med.* 4: 97-100.

Hoshi, M., Nishida, E., Miyata, Y., Sakai, H., Miyoshi, T., Ogawara, H. and Akiyama, T. (1997) Protein Kinase C Phosphorylates Tau and Induces its Functional Alterations. *FEBS Lett.* 217: 237-241.

Hsiao, K., Dlouhy, S. R., Farlow, M. R., Cass, C. Da Costa, M., Conneally, P. M. Hodes, M. E., Ghetti, B. and Prusiner, S. B. (1992) Mutant Prion Proteins in Gerstmann-Straussler-Scheinker Disease with Neurofibrillary Tangles. *Nat. Genet* 1: 68-71.

Hutton, M., Lendon, C. L., Rizzu, P., Baker, M., Froelich, S., Houlden. H., Pickering-Brown, S., Chakaverty, S., Isaacs, A., Grover, A., Hackett, J., Adamson, J., Lincoln, S., Dickson, D. W., Mann, D., Lynch, T. and Heutink, P. (1998) Association of Misense and 5' Splice-site Mutations in Tau with the Inherited Dementia FTDP-17. *Nature* 393: 702-705.

Hwang, C., Sinskey, A. J. and Lodish, H. F. (1992) Oxidized Redox State of Glutathione in the Endoplasmic Reticulum. *Science* 257: 1496-1502.

Inouye, H., Fraser, P. E., and Kirschner, D. A. (1993) Structure of Beta-crystallite Assemblies Formed by Alzheimer Beta-amyloid Protein Analogues: Analysis by X-ray Diffraction. *Biophys. J.* 64: 502-519.

Iqbal, K., Grunde-Iqbal, I., Zaidi, T., Merz, P. A., Wen, G. W., Shaikh, S. S., Wisniewski, H. M., Alafuzoff, I. and Winblad, B. (1986) Defective Brain Microtubule Assembly in Alzheimer's Disease. *Lancet* 2: 421-426.

Irving, E. A., McCulloch, J. and Dewar, D. (1996) Intracortical Perfusion of Glutamate *in Vivo* Induces Alterations of Tau and Microtubule-associated Protein 2 Immunoreactivity in the Rat. *Acta Neuropathol.* 92: 186-196.

Jakes, R., Novak, M., Davison, M. and Wischik, C. M. (1991) Identification of 3- and 4-repeat Tau Isoforms within the PHF in Alzheimer's Disease. *E.M.B.O. J.* 10: 2715-2729.

Jayaram, G. and Haley, B. E. (1994) Identification of Peptides within the Base Binding Domains of the GTP- and ATP-specific Binding Sites of Tubulin. *J. Biol. Chem.* 269: 3233-3242.

Jellinger, K. A. (1996) Structural Basis of Dementia in Neurodegenerative Disorders. *J. Neural Transm.* 47: 1-29.

Johnson, G. V., Litersky, J. M. and Jope, R. S. (1991a) Degradation of Microtubule-associated Protein 2 and Brain Spectrin by Calpain: A Comparative Study. *J. Neurochem.* 56: 1630-1638.

Johnson, G. V., Litersky, J. M. and Whitaker, J. N. (1991b) Proteolysis of Microtubule-associated Protein 2 and Tubulin by Cathepsin D. *J. Neurochem.* 57: 1577-1583.

Joly, J. C., Flynn, G., and Purich, D. L. (1989) The Microtubule-binding Fragment of Microtubule-associated Protein-2: Location of the Protease-accessible Site and Identification of an Assembly-promoting Peptide. *J. Cell Biol.* 109: 2289-2294.

Joly, J. C. and Purich, D. L. (1990) Peptides Corresponding to the Second Repeated Sequence in MAP2 Inhibit MAP Binding to Microtubules. *Biochemistry* 29: 8916-8920.

Kalcheva, N., Albala, J., O'Guin, K., Rubino, H., Garner, C., and Shafit-Zagardo, B. (1995) Genomic Structure of Human Microtubule-associated Protein 2 (MAP2) and Characterization of Additional MAP2 Isoforms. *Proc. Natl. Acad. Sci. U.S.A.* 92: 10894-10898.

Kampers, T., Fridhoff, P., Biernat, J., Mandelkow, E. and Mandelkow, E. (1996) RNA Stimulates Aggregation of Microtubule-Associated Protein Tau into Alzheimer-like Paired Helical Filaments. *FEBS Letts.* 399: 344-349.

Kang, J., Lemaire, H. G., Unterbeck, A., Salbaum, J. M., Masters, C. L., Grzeschik, K. H., Multhaup, G., Beyreuther, K. and Muller-Hill, B. (1987) The Precursor of Alzheimer's Disease Amyloid A4 Protein Resembles a Cell-surface Receptor. *Nature* 325: 733-736.

Karr, T. L., Podrasky, A. E., and Purich, D. L. (1979) Participation of Guanine Nucleotides in Nucleation and Elongation Steps of Microtubule Assembly. *Proc. Natl. Acad. Sci. U.S.A.* 76: 5475-5479.

Kidd M. (1963) Paired Helical Filaments in Electron Microscopy of Alzheimer's Disease. *Nature* 197: 192-193.

Kobayashi, T. (1975) Dephosphorylation of Tubulin-bound Guanosine Triphosphate During Microtubule Assembly. *J. Biochem.* 77: 1193-1197.

Kosik, K. S., Duffy, L. K., Dowling, M. M., Abraham, C., McCluskey, A. and Selkoe, D. J. (1984) Microtubule-associated Protein 2: Monoclonal Antibodies Demonstrate the Selective Incorporation of Certain Epitopes into Alzheimer Neurofibrillary Tangles. *Proc. Natl. Acad. Sci. U.S.A.* 81: 7941-7945.

Kosik, K. S., Joachim, C. L. and Selkoe, D. J. (1986) Microtubule-associated Protein Tau is a Major Antigenic Component of Paired Helical Filaments in Alzheimer Disease. *Proc. Natl. Acad. Sci. U.S.A.* 83: 4044-4048.

Kosik, K. S., Orecchio, L. D., Bakalis, S., Duffy, L. and Neve, R. L. (1988) Partial Sequence of MAP2 in the Region of a Shared Epitope with Alzheimer Neurofibrillary Tangles. *J. Neurochem.* 51: 587-598.

Kowalski, R. J. and Williams, R. C. (1993) Microtubule-associated Protein 2 Alters the Dynamic Properties of Microtubule Assembly and Disassembly. *J. Biol. Chem.* 268: 9847-9855.

Ksiezak-Reding, H., Morgan, K., Mattiace, L. A., Davies, P., Liu, W. K., Yen, S. H., Weidenheim, K. and Dickson, D. W. (1994) Ultrastructure and Biochemical Composition of Paired Helical Filaments in Corticobasal Degeneration. *Am. J. Pathol.* 145: 1496-1508.

Lee, G., Neve, R. L. and Kosik, K. S. (1989) The microtubule-binding Domain of Tau. *Neuron* 2: 1615-1624.

Lee, M. K., Xu, Z., Wong, P. C. and Cleveland, D. W. (1993) Neurofilaments are Obligate Heteropolymers in Vivo. *J. Cell Biol.* 122: 1337-1350.

LeVine, H. (1993) Thioflavine T Interaction with Synthetic Alzheimer's Disease Beta-amyloid Peptides: Detection of Amyloid Aggregation in Solution. *Protein Sci.* 2: 404-410.

Litersky, J. M. and Johnson, G. V. (1993) Phosphorylation by cAMP-dependent Protein Kinase Inhibits the Degradation of Tau by Calpain. *J. Biol. Chem.* 267: 1563-1568.

Litersky, J. M., Johnson, G. V. W., Jakes, R., Goedert, M., Lee. M and Seubert, P. (1996) Tau Protein is Phosphorylated by Cyclic AMP-dependent Protein Kinase and Calcium/Calmodulin-dependent Protein Kinase II within its Microtubule-binding Domain at Ser-262 and Ser-356. *Biochem. J.* 316: 655-660.

Littauer, U. Z., Giveon, D., Thierauf, M., Ginzburg, I., and Ponstingl, H. (1986) Common and Distinct Tubulin Binding Sites for Microtubule-Associated Proteins. *Proc. Natl. Acad. Sci. U.S.A.* 83: 7162-7166.

Lopata, M. A. and Cleveland, D. W. (1987) In Vivo Microtubules are Copolymers of Available Beta-tubulin Isotypes: Localization of Each of Six Vertebrate Beta-tubulin Isotypes Using Polyclonal Antibodies Elicited by Synthetic Peptide Antigens. *J. Cell Biol.* 105: 1707-1720.

Lopez A. L. and Sheetz, M. P. (1995) A Microtubule-associated Protein (MAP2) Kinase Restores Microtubule Motility in Embryonic Brain. *J. Biol. Chem.* 270: 12511-12517.

Love, S., Bridges, L. R. and Case, C. P. (1995) Neurofibrillary Tangles in Niemann-Pick Disease Type C. *Brain* 118: 119-129.

MacNeal, R.K. and Purich, D.L. (1978) Stoichiometry and Role of GTP Hydrolysis in Bovine Neurotubule Assembly. *J Biol Chem.* 253: 4683-4687.

Malik, F., Brillinger, D. and Vale, R. D. (1994) High-resolution Tracking of Microtubule Motility Driven by a Single Kinesin Motor. *Proc. Natl. Acad. Sci. U.S.A.* 91: 4584-4588.

Mandelkow, E. M., Biernat, J., Drewes, G., Gustke, B., Trinczek, B. and Mandelkow, E. (1995) Tau Domains, Phosphorylation, and Interactions with Microtubules. *Neurobiol. Aging* 16: 355-363.

Manetto, V., Perry, G., Tabaton, M., Mulvihill, P., Fried, V. A., Smith, H. T., Gambetti, P. and Autilio-Gambetti, L. (1988) Ubiquitin is Associated with Abnormal Cytoplasmic Filaments Characteristic of Neurodegenerative Diseases. *Proc. Natl. Acad. Sci. U.S.A.* 85: 4501-4505.

Mark, R. J., Blanc, E. M. and Mattson, M. P. (1996) Amyloid β-peptide and Oxidative Cellular Injury in Alzheimer's Disease. *Mol. Neurobiol.* 12: 211-224.

Mark, R. J., Keller, J. N., Kruman, I. and Mattson, M/ P. (1997) Basic FCF Attenuates Amyloid β-peptide-induced Oxidative Stress, Mitochondrial Dysfunction, and Impairment of Na+/K+ ATPase Activity in Hippocampal Neurons. *Brain Res.* 756: 205-214.

McDonald, H. B., Stewart, R. J. and Goldstein, L. S.(1990) The kinesin-like NCD Protein of Drosophila Is a Minus End-directed Microtubule Motor. *Cell* 63:1159-65.

McKee, A. C., Kowall, N. W. and Kosik, K. S. (1989) Microtubular Reorganization and Dendritic Growth Response in Alzheimer's Disease. *Ann. Neurol.* 26: 652-659.

Miller, C. C., Brion, J. P., Calvert, R., Chin, T. K., Eagles, P. A., Downes, M. J., Flament-Durand, J., Haugh, M., Kahn, J. and Probst, A. (1986) Alzheimer's Paired Helical Filaments Share Epitopes with Neurofilament Side Arms. *EMBO J.* 5: 269-276.

Mitchison, T. and Kirschner, M. (1984) Dynamic Instability of Microtubule Growth. *Nature* 312: 237-242.

Montejo de Garcini, E, and Avila, J. (1987) In Vitro Conditions for the Self-polymerization of the Microtubule-associated Protein, Tau Factor. *J. Biochem.* 102: 1415-1421.

Montejo de Garcini, E., Carrascosa, J. L., Correas, I., Nieto, A. and Avila, J. (1988) Tau Factor Polymers are Similar to Paired Helical Filaments of Alzheimer's Disease. *FEBS Lett.* 236:150-154.

Montejo de Garcini, E., Serrano, L. and Avila, J. (1986) Self Assembly of Microtubule-associated Protein Tau into Filaments Resembling Those Found in Alzheimer Disease. *Biochem. Biophys. Res. Comm.*141: 790-796.

Mulvihill, P. and Perry, G. (1989) Immunoaffinity Demonstration that Paired Helical Filaments of Alzheimer Disease Share Epitopes with Neurofilaments, MAP2 and Tau. *Brain Res.* 484: 150-156.

Murayama, S., Mori, H., Ihara, Y. and Tomonaga, M. (1990) Immunocytochemical and Ultrastructural Studies of Pick's Disease. *Ann. Neurol.* 27: 394-405.

Nangaku, M., Sato-Yoshitake, R., Okada, Y., Noda, Y., Takemura, R., Yamazaki, H and Hirokawa, N. (1994) KIF1B, a Novel Microtubule Plus End-directed Monomeric Motor Protein for Transport of Mitochondria. *Cell* 79: 1209-1220.

Neve, R. L., Selkoe, D. J., Kurnit, D. M. and Kosik, K. S. (1986) A cDNA for a Human Microtubule-associated Protein 2 Epitope in the Alzheimer Neurofibrillary Tangle. *Brain Res.* 387: 193-196.

Nukina, N. and Ihara, Y. (1983) One of the Antigenic Determinants of Paired Helical Filaments is Related to MAP protein. *Proc. Japan Acad.* 59: 284-292.

Olson, M. I. and Shaw, C. M. (1969) Presenile Dementia and Alzheimer's Disease in Mongolism. *Brain* 92: 147-156.

Oltersdorf, T., Ward, P. J., Henriksson, T., Beattie, E. C., Neve, R., Lieberburg, I. and Fritz, L. C. (1990) The Alzheimer Amyloid Precursor Protein: Identification of a Stable Intermediate in the Biosynthetic/Degradative Pathway. *J. Biol. Chem.* 265: 4492-4497.

Oyama, F., Sawamura, N., Kobayashi, K., Kawashima, M. M., Kuramochi, T., Ito, M., Tomita, T., Marayama, K., Saido, T. C., Iwatsubo, T., Capell, A., Walter, J., Grunberg, J., Ueyama, Y., Haass, C. and Ihara, Y. (1998) Mutant Presenilin 2 Transgenic Mouse: Effect on an Age-dependent Increase of Amyloid Beta-protein 42 in the Brain. *J. Neurochem.* 71: 313-322.

Paudel, H. K. (1997) Phosphorylation by Neuronal CDC2-like Protein Kinase Promotes Dimerization of Tau Protein *in Vitro*. *J, Biol. Chem.* 272: 28328-28334.

Paulus, W. and Selim, M. (1990) Corticonigral Degeneration with Neuronal Achromasia and Basal Neurofibrillary Tangles. *Acta Neuropathol.* 88: 113-121.

Pappolla, M. A., Sos, M., Omar, R. A. and Sambamurti, K. (1996) The Heat Shock/Oxidative Stress Connection. Relevance to Alzheimer Disease. *Mol. Chem. Neuropathol.* 28: 21-34.

Paschal, B. M., Obar, R. A. and Vallee, R. B. (1989) Interaction of Brain Cytoplasmic Dynein and MAP2 with a Common Sequence at the C-terminus of Tubulin. *Nature* 342: 569-572.

Perez, M., Valpuesta, J. M., Medina, M., Montejo de Garcini, E., and Avila, J. (1996) Polymerization of Tau into Filaments in the Presence of Heparin: The Minimal Sequence Required for Tau-Tau Interaction. *J. Neurochem.* 67: 1183-1190.

Perry, G., Richey, P. L., Siedlak, S. L., DeWitt, D. A., Barnett, J., Greenberg, B. D. and Kalaria, N. (1993) Immunocytochemical Evidence that the β-protein Precursor is an Integral Component of Neurofibrillary Tangles of Alzheimer's Disease. *Am. J. Path.* 143: 1586-1592.

Perry, G., Siedlak, S. L., Richey, P., Kawai, M., Cras, P., Kalaria, R. N., Galloway, P. G., Scardina, J. M., Cordell, B., Greenberg, B. D., Ledbetter, S. R. and Ganbetti, P. (1991) Association of Heparan Sulfate Proteoglycan with the Neurofibrillary Tangles of Alzheimer's Disease. *J. Neurosci.* 11: 3679-3683.

Pollanen, M. S., Bergeron, C. and Weyer, L. (1992) Detergent-insoluble Cortical Lewy Body Fibrils Share Epitopes with Neurofilament and Tau. *J. Neurochem.* 58: 1953-1956.

Poorkaj, P., Bird, T. D., Wijsman, E., Nemens, E., Garruto, R. M., Anderson, L., Andreadis, A., Wiederholt, W. C., Raskind, M. and Schellenberg, G. D. (1998) Tau is a Candidate Gene for Chromosome 17 Frontotemporal Dementia. *Ann. Neurol.* 43: 815-825.

Ponte, P., Gonzalez-DeWhitt, P., Schilling, J., Miller, J., Hsu, D., Greenberg, B., Davis, K., Wallace, W., Lieberburg, I. and Fuller, F. A. (1988) New A4 Amyloid mRNA Contains a Domain Homologous to Serine Proteinase Inhibitors. *Nature* 331: 525-527.

Price, D. L. and Sisodia, S. S. (1998) Mutant Genes in Familial Alzheimer's Disease and Transgenic Models. *Ann. Rev. Neurosci.* 21: 479-505.

Purich, D. L., and Kristofferson, D. (1984) Microtubule Assembly: A Review of Progress, Principles, and Perspectives. *Adv. Protein Chem.* 36: 133-212.

Rubino, H. M., Dammerman, M., Shafit-Zagardo, B. and Erlichman, J. (1989) Localization and Characterization of the Binding Site for the Regulatory Subunit of Type II cAMP-dependent Protein Kinase on MAP2. *Neuron* 3: 631-638.

Saito, K. I., Elce, J. S., Hamos, J. E. and Nixon, R. A. (1993) Widespread Activation of Calcium-activated Neutral Proteinase (Calpain) in the Brain of Alzheimer Disease: A potential Molecular Basis for Neuronal Degeneration. *Neurobiol.* 90: 26-28-2632.

Scaife, R. M., Wilson, L. and Purich, D. L. (1992) Microtubule Protein ADP-ribosylation In Vitro Leads to Assembly Inhibition and Rapid Depolymerization. *Biochemistry* 31: 310-316.

Schweers, O., Mandelkow, E. M., Biernat, J., and Mandelkow, E. (1995) Oxidation of Cysteine-322 in the Repeat Domain of Microtubule-associated Protein Tau Controls the in Vitro Assembly of Paired Helical Filaments. *Proc. Natl. Acad. Sci. U.S.A.* 92: 8463-8467.

Selkoe, D. (1994) Normal and Abnormal Biology of the Beta-amyloid Precursor Protein. *Ann. Rev. Neurosci.* 17: 489-517.

Shaw, G (1998) Neurofilaments. 1-192, Verlager, New York, NY.

Shaw, G. and Chau, V. (1988) Ubiquitin and Microtubule-associated Protein Tau Immunoreactivity Each Define Distinct Structures with Differing Distributions and Solubility Properties in Alzheimer Brain. *Proc. Natl. Acad. Sci. U.S.A.* 85:2854-2858.

Shioi, J., Anderson, J. P., Ripellino, J. A. and Robakis, N. K. (1992) Chondroitin Sulfate Proteoglycan Form of the Alzheimer's β-amyloid Precursor. *J. Biol. Chem.* 267: 13819-13822.

Shivanna, B. D., Mejillano, M. R., Williams, T. D. and Himes, R. H. (1993) Exchangeable GTP Binding Site of Beta-tubulin. Identification of Cysteine 12 as the Major Site of Cross-linking by Direct Photoaffinity Labeling. *J. Biol. Chem.* 268: 127-132.

Smith, C. D., Carney, J. M., Starke-Reed, P. E., Oliver, C. N., Stadtman, E. R., Floyd, R. A. and Markesbery, W. R. (1991) Excess Brain Protein Oxidation and Enzyme Dysfunction in Normal Aging and Alzheimer Disease. *Proc. Natl. Acad. Sci. U.S.A.* 88: 10540-10543.

Smith, M. A., Sayre, L. M., Monnier, V. M. and Perry, G. (1995) Radical AGEing in Alzheimer's Disease. *Trends Neurosci.* 18: 172-176.

Snow, A. D., Henderson, M., Nochlin, D. Kresse, H. and Wight, T. N. (1992) Peripheral Distribution of Dermatan Sulfate Proteoglycans in Amyloid-containing Plaques and their Presence in Neurofibrillary Tangles of Alzheimer's Disease. *J. Histochem. Cytochem.* 40: 105-113.

Sontag, E., Nunbhakdi-Craig, V., Lee, G., Bloom, G. S. and Mumby, M. C. (1996) Regulation of the Phosphorylation State and Microtubule-binding Activity of Tau by Protein Phosphatase 2A. *Neuron* 17: 1201-1207.

Spiegelman, B. M., Pennington, S. M. and Kirschner, M. W. (1977) Turnover of Tubulin and the N-site GTP in Chinese Hamster Ovary Cells. *Cell* 12: 587-600.

Spillantini, M. G., Goedert, M., Jakes, R. and Klug, A. (1990) Topographical Relationship between β-amyloid and Tau Protein Epitopes in Tangle-bearing Cells in Alzheimer's Disease. *Proc. Natl. Acad. Sci. U.S.A.* 87: 3952-3956.

Spillantini, M. G., Crowther, R. A. and Goedert, M. (1992) Comparison of the Neurofibrillary Pathology in Alzheimer's Disease and Familial Presenile Dementia with Tangles. *Acta Neuropathol.* 92: 42-48.

Spillantini, M. G., Crowther, R. A. and Goedert, M. (1996) Comparison of the Neurofibrillary Pathology in Alzheimer's Disease and Familial Presenile Dementia with Tangles. *Acta. Neuropathol* .92: 42-48.

Spillantini, M. G., Goedert, M., Crowther, R. A., Murrell, J. R., Farlow, M. R. and Ghetti, B. (1997) Familial Multiple System Tauopathy with Presenile Dementia: a Disease with Abundant Neuronal and Glial Tau Filaments. *Proc. Natl. Acad. Sci. U.S.A.* 94: 4113-4118.

Spillantini, M. G., Murrell, J. R., Goedert, M., Farlow, M. R., Klug, A. and Ghetti, B. (1998) Mutation in the Tau Gene in Familial Multiple System Tauopathy with Presenile Dementia. *Proc. Natl. Acad. Sci. U.S.A.* 95: 7737-7741.

Strittmatter, W. J., Saunders, A. M., Schmechel, D., Pericak-Vance, M., Enghild, J., Salvesen, G. S. and Roses, A. D. (1993) Apolipoprotein E: High-affinity Binding to Beta-amyloid and Increased Frequency of Type 4 Allele in Late-onset Familial Alzheimer Disease. *Proc. Natl. Acad. Sci. U.S.A.* 90: 1977-1981.

Sturchler-Pierrat, C., Abramowski, D., Duke, M., Wiederhold, K. H., Mistl, C., Rothacher, S., Ledermann, B., Burki, K., Frey, P., Paganetti, P. A., Waridel, C., Calhoun, M. E., Jucker, M., Probst, A., Staufenbiel, M. and Sommer, B. (1997) Two Amyloid Precursor Transgeninc Mouse Models with Alzheimer Disease-like Pathology. *Proc. Natl. Acad. Sci. U.S.A.* 94: 13287-13292.

Sumi, S. M., Bird, T. D., Nochlin, D. and Raskind, M. A. (1992) Familial Presenile Dementia with Psychosis Associated with Cortical Neurofibrillary Tangles and Degeneration of the Amygdala. *Neurol.* 42: 120-127.

Tagliavini, F., Giaconne, G., Frangione, B. and Bugiani, O. (1988) Preamyloid Deposits in the Cerebral Cortex of Patients with Alzheimer's Disease and Nondemented Individuals. *Neurosci. Lett.* 93: 191-196.

Tagliavini, F., Giaconne, G., Prelli, F., Verga, L., Porro, m., Trojanowski, J. Q., Farlow, M. R., Frangione B., Ghetti, B. and Bugiani, O. (1993) A68 is a Component of Paired Helical Filaments of Gerstmann-Straussler-Scheinker Disease, Indiana Kindred. *Brain Res.* 616: 325-329.

Talamo, B. R., Rudel, R. A., Kosik, K. S., Lee, V. M., Neff, S., Adelman, L. and Kauer, J. S. (1989) Pathological Changes in Olfactory Neurons in Patients with Alzheimer's Disease. *Nature* 337: 736-739.

Tanzi, R. E., McClatchey, A. I., Lamperti, E. D., Villa-Komaroff, L., Gusella, J. F. and Neve, R. L. (1988) Protease Inhibitor Domain Encoded by an Amyloid Protein Precursor mRNA Associated with Alzheimer's Disease. *Nature* 331: 528-532.

Tenneti, L., D'Emilia, D. M. and Lipton, S. A. (1997) Suppression of Neuronal Apoptosis by S-nitrosylation of Caspases. *Neusci. Lett.* 236: 139-142.

Terry, R. D. (1963) The Fine Structure of Neurofibrillary Tangles in Alzheimer's Disease. *J. Neuropath. Exp. Neurol.* 22: 629-642.

Theurkauf, W. E. and Vallee, R. B. (1982) Molecular Characterization of the cAMP-dependent Kinase Bound to Microtubule-associated Protein 2. *J. Biol. Chem.* 257: 3284-3290.

Tranchant, C., Sergeant, N., Wattez, A., Mohr, M., Warter, J. M. and Delacourte, A. (1997) Neurofibrillary Tangles in Gerstmann-Straussler-Scheinker Syndrome with the A117V Prion Mutation. *J. Neurol. Neurosurg. Psychiatry* 63: 240-246.

Trojanowski, J. Q. and Lee, V. M. (1994) Paired Helical Filament Tau in Alzheimer's Disease. The Kinase Connection. *Am. J. Pathol.* 144: 449-453.

Troncoso, J. C., Costello, A., Watson, A. L. and Johnson, G. W. (1993) In Vitro Polymerization of Oxidized Tau into Filaments *Brain Res.* 613: 313-316.

Tsuyama, S., Terayama, Y. Matsuyama, S. (1987) Numerous Phosphates of Microtubule-associated Protein 2 in Living Rat Brain. *J. Biol. Chem.* 262: 10886-10892.

Tucker, R. P., Binder, L. I., Viereck, C., Hemmings, B. A. and Matus, A. I. (1988) The Sequential Appearance of Low- and High-molecular-weight Forms of MAP2 in the Developing Cerebellum. *J. Neurosci.* 8: 4503-4512.

Ugolini, G., Cattaneo, A. and Novak, M. (1997) Co-localization of Truncated Tau and DNA Fragmentation in Alzheimer's Disease Neurons. *Neuroreport* 8: 3709-3712.

Utton, M. A., Vandecandelaere, A., Wagner, U., Reynolds, C. H., Gibb, G. M., Miller, C. C. J., Bayley, P. M. and Anderton, B. H. (1997) Phosphorylation of Tau by Glycogen Synthase Kinase 3β Affects the Ability of Tau to Promote Microtubule self-assembly. *Biochem. J.* 323: 741-747.

Vale, R. D. (1992) Microtubule Motors: Many New Models off the Assembly Line. *TIBS* 17: 300-303.

Vallee, R. B. and Borisy, G. G. (1977) Removal of the Projections from Cytoplasmic Microtubules *in Vitro* by Digestion with Trypsin. *J. Biol. Chem.* 255: 10532-10536.

Vallee, R. B. (1980) Structure and Phosphorylation of Microtubule-associated Protein 2 (MAP2). *Proc. Natl. Acad. Sci. U.S.A.* 77: 3206-3210.

Vermersch, P., Robitaille, Y., Bernier, L., Wattez, A., Gauvreau, D. and Delacourte, A. (1994) Biochemical Mapping of Neurofibrillary Degeneration in a Case of Progressive Supranuclear Palsy: Evidence for General Cortical Involvement. *Acta Neuropathol.* 87: 572-577.

Viereck, C., Tucker, R. P. and Matus, A. (1989) The Adult Rat Olfactory System Expresses Microtubule-associated Proteins Found in the Developing Brain. *J. Neurosci.* 9: 3547-3557.

Villasante, A., Wang, D., Dobner, P., Dolph, P., Lewis, S. A. and Cowan, N. J. (1986) Six Mouse Alpha-tubulin mRNAs Encode Five Distinct Isotypes: Testis-specific Expression of Two Sister Genes. *Mol. Cell. Biol.* 6: 2409-2419.

Wang, D. W., Villasante, E., Lewis, S. A. and Cowan, N. J. (1986) The Mammalian Beta-tubulin Repertoire: Hematopoietic Expression of a Novel, Heterologous Beta-tubulin Isotype. *J. Cell Biol.* 103: 1903-1910.

Wang, J. Z., Grundke-Iqbal, I. and Iqbal, K. (1996) Glycosylation of Microtubule-associated Protein Tau: An Abnormal Posttranslational Modification in Alzheimer's Disease. *Nat. Med.* 2: 871-875.

Waterman-Storer, C. M., Karki, S. B., Kuznetsov, S. A., Tabb, J. S., Weiss, D. G., Langford, G. M. and Holzbaur, E. L. (1997) The Interaction Between Cytoplasmic Dynein and Dynactin Is Required for Fast Axonal Transport. *Proc. Natl. Acad. Sci. U.S.A.* 94: 12180-12185.

Wiche, G. (1989) High Molecular Weight Microtubule-associated Proteins: Properties and Functions. *Biochem J.* 259: 1-12.

Weidemann, A., Konig, G., Bunke, D., Fischer, P., Salbaum, J. M., Masters, C. L. and Beyreuther, K. (1989) Identification, Biogenesis, and Localization of Precursors of Alzheimer's Disease A4 Amyloid Protein. *Cell* 57: 115-126.

Wilcock G. K. and Esiri, M. M. (1982) Plaques, Tangles and Dementia: A Quantitative Study. *J Neurol. Sci.* 56: 343-356.

Wille, H., Drewes, G., Biernat, J., Mandelkow, E. M., and Mandelkow, E. (1992) Alzheimer-like Paired Helical Filaments and Antiparallel Dimers Formed from Microtubule-associated Protein Tau in Vitro. *J. Cell Biol.* 118: 573-584.

Wilson, D. M., and Binder, L. I. (1995) Polymerization of Microtubule-associated Protein Tau Under Near-physiological Conditions. *J. Biol. Chem.* 270: 24306-24314.

Wilson, D. M. and Binder, L.I. (1997) Free Fatty Acids Stimulate the Polymerization of Tau and Amyloid Beta Peptides. In Vitro Evidence for a Common Effector of Pathogenesis in Alzheimer's Disease. *Am. J. Pathol.* 150: 2181-2195.

Wischik, C. M., Crowther, R. A., Stewart, M. and Roth, M. (1985) Subunit Structure of Paired Helical Filaments in Alzheimer's Disease. *J. Cell Biol.* 100: 1905-1912.

Wischik C. M., Novak M., Thogersen H. C., Edwards P. C., Runswick M. J., Jakes R., Walker J. E., Milstein C., Roth M., and Klug A. (1988) Isolation of a Fragment of Tau Derived from the Core of the Paired Helical Filament of Alzheimer Disease. *Proc. Natl. Acad. Sci. U.S.A.* 85: 4506-4510.

Wisniewski, H. M., Narang, H. K. and Corsellis, J. A. N. (1976a) Ultrastructural Studies of the Neuropil and Neurofibrillary Tangles in Alzheimer's Disease and Post-tramatic Dementia. *J. Neuropathol. Exp. Neurol.* 35: 367-373.

Wisniewski, H. M., Narang, H. K. and Terry, R. D. (1976b) Neurofibrillary Tangles of Paired Helical Filaments. *J. Neurol. Sci.* 27: 173-181.

Wisniewski, H. M., Wegiel, J., Wang, K. C., Kujawa, M. and Lach, B. (1989) Ultrastructural Studies of the Cells Forming Amyloid Fibers in Classical Plaques. *Can. J. Neurol. Sci.* 16: 535-542.

Wisniewski, K., Jervis, G. A., Moretz, R. C. and Wisniewski, H. M. (1978) Alzheimer Neurofibrillary Tangles in Diseases Other than Senile and Presenile Dementia. *Ann. Neurol.* 5: 288-294.

Yang, S., Song, J., Yu, J. and Shiah, S. (1993) Protein Kinase FA/GSK3 Phosphorylates Tau on Ser-235-Pro and Ser-404-Pro that are Abnormally Phosphorylated in Alzheimer's Disease Brain. *J. Neurochem.* 61: 1742-1747.

Yen, S. H., Dickson, D. W., Crowe, A., Butler, M. and Shelanski, M. L. (1987) Alzheimer's Neurofibrillary Tangles Contain Unique Epitopes and Epitopes in Common with the Heat-stable Microtubule-associated Proteins Tan and MAP2. *Am. J. Pathol.* 126: 81-91.

Zeeberg, B. and Caplow, M. (1979) Determination of Free and Bound Microtubular Protein and Guanine Nucleotide Under Equilibrium Conditions. (1979) *Biochemistry*. 18: 3880-3886.

Zhang, E. Y., DeTure, M. A., Bubb, M. R., Caviston, T. L., Erdos, G. W., Whittaker, S. D., and Purich, D. L. (1996) Self-assembly of the Brain MAP2 Microtubule-binding Region into Polymeric Structures Resembling Alzheimer Filaments. *Biochem. Biophys. Res. Commun.* 229: 176-181

Zhang, E. Y. (1997) MAP2c and MAP2d: *In Vitro* Interaction with Microtubules and Localization of Protein Kinase C Phosphorylation Site, Ph.D. Dissertation, University of Florida.

BIOGRAPHICAL SKETCH

Michael Anthony Deture was born on January 27, 1966, in Tallahassee, Florida. He attended Davidson College in North Carolina and was awarded a Bachelor of Science degree in 1988. He continued his education at Clemson University in South Carolina where he studied physical chemistry and received his Master of Science degree. After spending one year in Charleston, South Carolina, where he met and married Monica Jenkins, he entered graduate school in the Department of Biochemistry and Molecular Biology at the University of Florida during 1992. His studies have been carried out under Dr. Daniel L Purich and are concerned with elucidating the factors which contribute to neurofibrillary tangle formation in Alzheimer Disease. After graduating in 1998 with his doctorate degree and two young children, Skylar and Haley, in hand Michael hopes to continue studying neurofibrillary tangle containing Neurodegenerative Diseases at the Mayo Clinic in Jacksonville, Florida.

I certify that I have read this study and that in my opinion it conforms to acceptable standards of scholarly presentation and is fully adequate, in scope and quality, as a dissertation for the degree of Doctor of Philosophy.

Daniel L. Purich
Professor of Biochemistry and
Molecular Biology

I certify that I have read this study and that in my opinion it conforms to acceptable standards of scholarly presentation and is fully adequate, in scope and quality, as a dissertation for the degree of Doctor of Philosophy.

Robert J. Cohen
Associate Professor of Biochemistry
and Molecular Biology

I certify that I have read this study and that in my opinion it conforms to acceptable standards of scholarly presentation and is fully adequate, in scope and quality, as a dissertation for the degree of Doctor of Philosophy.

Ben M. Dunn
Distinguished Professor of Biochemistry
and Molecular Biology

I certify that I have read this study and that in my opinion it conforms to acceptable standards of scholarly presentation and is fully adequate, in scope and quality, as a dissertation for the degree of Doctor of Philosophy.

Thomas H. Mareci
Associate Professor of Biochemistry
and Molecular Biology

I certify that I have read this study and that in my opinion it conforms to acceptable standards of scholarly presentation and is fully adequate, in scope and quality, as a dissertation for the degree of Doctor of Philosophy.

Gerard P. J. Shaw
Professor of Neuroscience

This dissertation was submitted to the Graduate Faculty of the College of Medicine and to the Graduate School and was accepted as partial fulfillment of the requirements for the degree of Doctor of Philosophy.

December, 1998

Robert D. Watson

Dean, College of Medicine

Dean, Graduate School